I. THE RELATIONSHIP OF THE PYRIDINE NUCLEOTIDE

CYCLE TO RICININE BIOSYNTHESIS

IN RICINUS COMMUNIS L.

II. BIOCHEMISTRY OF METHYLCYCLOPENTANE

MONOTERPENOIDS

By

RONALD DOYLE JOHNSON

Bachelor of Science

Oklahoma State University

Stillwater, Oklahoma

1967

Submitted to the Faculty of the Graduate College
of the Oklahoma State University
in partial fulfillment of the requirements
for the degree of
DOCTOR OF PHILOSOPHY
May, 1972

I. THE RELATIONSHIP OF THE PYRIDINE NUCLEOTIDE

CYCLE TO RICININE BIOSYNTHESIS

IN RICINUS COMMUNIS L.

II. BIOCHEMISTRY OF METHYLCYCLOPENTANE

MONOTERPENOIDS

Thesis Approved:

_____
George R. Waller
Thesis Adviser

_____
K. D. Berlin

_____
H. Olin Spivey

_____
Eddie Basler

_____
George V. Odell

_____
N. Durham
Dean of the Graduate College

ACKNOWLEDGEMENTS

TABLE OF CONTENTS

PART TWO

LIST OF TABLES

. . .

LIST OF FIGURES

LIST OF SCHEMES

PART ONE

THE RELATIONSHIP OF THE PYRIDINE NUCLEOTIDE CYCLE

TO RICININE BIOSYNTHESIS IN <u>RICINUS</u> <u>COMMUNIS</u> L.

CHAPTER I

INTRODUCTION

A biogenetic relationship between the pyridine nucleotide cycle
and certain pyridine alkaloids was suggested by Leete and Leitz in 1956
(1). Waller and Gholson later conducted the first definitive experi-
ments which indicated that the pyridinium moiety of nicotinamide adenine
dinucleotide (NAD) and other compounds of the pyridine nucleotide cycle
were precursors of the alkaloid ricinine (3). Other results supported
this relationship for nicotine in tobacco plants (4). In a more recent
paper, data concerning the level of incorporation of label from quino-
linic acid into ricinine in the presence and absence of excess exogenous
NAD led the authors to postulate that the pathways of biosynthesis of
ricinine and NAD were independent and that ricinine biosynthesis was
separate and independent of the cycle (5).

The experiments described herein were designed to help clarify the
relationship of the pyridine nucleotide cycle to ricinine biosynthesis
by inhibiting the cycle with certain compounds and then observing the
effect on ricinine biosynthesis. The objective of this research was to
determine whether or not the pyridine nucleotide cycle was an obligatory
pathway in the biosynthesis of ricinine.

CHAPTER II

LITERATURE REVIEW

A. Structure and Properties

Ricinine, N-methyl-4-methoxy-3-cyano-2-pyridone, was first discov-
ered in castor bean seeds by Tuson (6), in 1864, and its structure
elucidated by Maqueune and Philippe in 1904 (7). Ricinine was shown to
be optically inactive (8), to melt at 201.5°C (corrected) and to sublime
at 170-180°/20 mm. It is sparingly soluble in water, alcohol, chloro-
form and pyridine and insoluble in ether.

Skursky et al. (9) have reported ultraviolet absorption maxima in
water at 307 and 255 nm of highly purified ricinine with molar extinc-
tion coefficients of 8.77×10^3 and 4.29×10^3 liters M^{-1} cm^{-1}, respec-
tively.

B. Biosynthesis of Ricinine

Ricinine biosynthesis in the castor bean plant was first studied
using radioisotopes by Dubeck and Kirkwood (10). They fed L-methionine-
methyl-^{14}C, choline-methyl-^{14}C and sodium formate-^{14}C to germinating
castor seeds and found that only the carbon-14 labeled methyl group of
methionine was incorporated into the methyl groups of ricinine to a
significant level.

Waller and Henderson (11) found that succinic acid or a related
four-carbon dicarboxylic acid from the citric acid cycle was a direct

precursor of ricinine. This four-carbon dicarboxylic acid was incorpor-
ated so that one of the carboxyl groups became the nitrile group of
ricinine and the methylene groups became carbons 2 and 3 of the pyridine
ring of ricinine, while the other carboxyl group was lost through de-
carboxylation. Using succinic acid-1,4-^{14}C, Waller and Henderson also
found 85% of the label in the nitrile group and 15% in the α-pyridone ring
of ricinine. Juby and Marion (12), using succinic acid-2,3-^{14}C, found 38.9%
of the label in carbon 2, 38.3% in carbon 3 and 20.8% in the nitrile
carbon.

Glycerol-^{14}C was shown to be incorporated into the pyridine ring of
ricinine (11,12,13,14). Glycerol was shown to serve as a source of
carbon atoms 4, 5 and 6 of ricinine (14). Using glycerol-1,3-^{14}C and
glycerol-2-^{14}C, it was shown that no randomization of label occurred upon
incorporation into ricinine (14). Chandler has shown that 3-phospho-
glyceraldehyde and fructose-1-6-diphosphate were converted to quinolinic
acid to a greater extent than glycerol, indicating that 3-phosphoglycer-
aldehyde combines directly with aspartic acid to form quinolinic acid
(15). Suzuki and Gholson have recently shown that in the presence of a
triose phosphate isomerase inhibitor only dihydroxyacetone-phosphate was
converted to quinolinic acid (16).

1. The Pyridine Nucleotide Cycle and Its Relationship to Ricinine Bio-
synthesis

Leete and Leitz (1) first suggested that ricinine might be formed
from NAD or related substituted pyridine compounds.

Nicotinic acid-7-^{14}C was shown to be incorporated into ricinine (1,
17,18), with the label appearing in the nitrile group. Nicotinamide-7-
^{14}C and ^{15}N-amide labeled nicotinamide also were incorporated into the

nitrile group (19). Ring-labeled nicotinamide-^{3}H was also incorporated

into ricinine (19). Quinolinic acid-2,3,7,8-^{14}C was found to be incor-

porated into ricinine at a rate equal to or better than either nicotinic

acid-7-^{14}C or nicotinamide-7-^{14}C (3,20) and it has also been shown that

quinolinic acid can be converted to nicotinic acid mononucleotide in

vitro in plants (20), as well as microorganisms (21,22) and animals (23,

24). This was further proof that quinolinic acid served as a key inter-

mediate in the formation of pyridine compounds in plants. The discovery

that the pyridine moiety entered the NAD biosynthesis pathway de novo as

nicotinic acid mononucleotide, which was formed from quinolinic acid and

5-phosphoribosyl pyrophosphate (25,26,27), provided the basis for the

formulation by Waller et al. (1) of the pyridine nucleotide cycle as

shown in Figure 1. In this scheme quinolinic acid was converted to

nicotinic acid mononucleotide by quinolinic acid decarboxylase; nicotinic

acid mononucleotide was then converted to desamido-NAD by nicotinic acid

mononucleotide adenyl transferase; desamido-NAD was converted to NAD by

NAD synthetase; NAD was converted to nicotinamide by NAD glycohydrolase;

nicotinamide was converted to nicotinic acid by nicotinamide deamidase

and nicotinic acid was converted to nicotinic acid mononucleotide by

nicotinic acid phosphoribosyl transferase (28). Keller et al. (29),

using perfusion techniques in rat liver, have shown that in vivo, nico-

tinamide was converted to nicotinamide mononucleotide which was conver-

ted to NAD which was converted back to nicotinamide. Figure 2 illustra-

tes this nicotinamide to NAD shunt. It has been postulated that this

shunt exists in plants (30).

Several studies (1,2,3) have been conducted which indicated that

the pyridine nucleotide cycle served an obligatory role in the
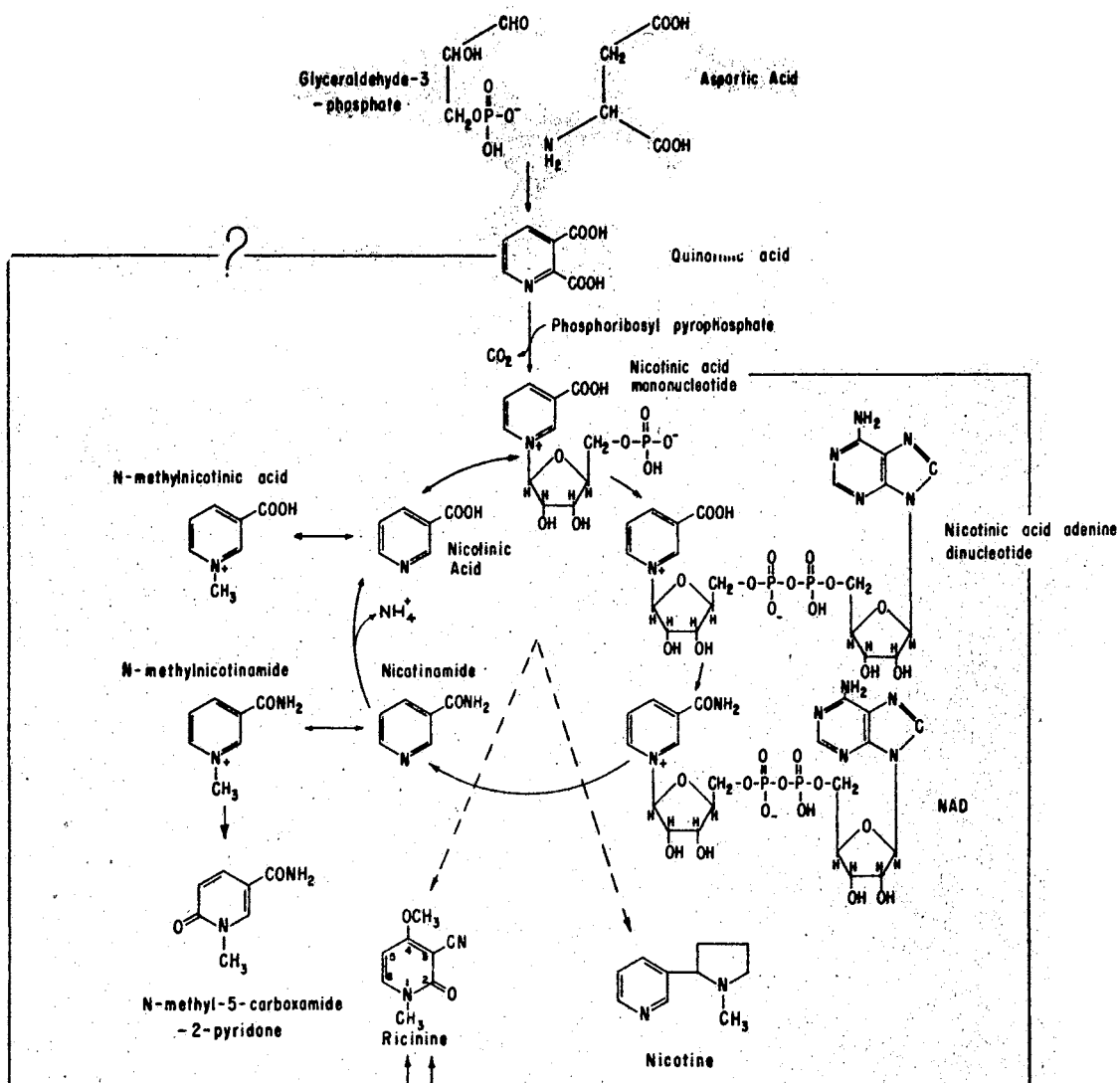
Figure 1. The Pyridine Nucleotide Cycle (2)
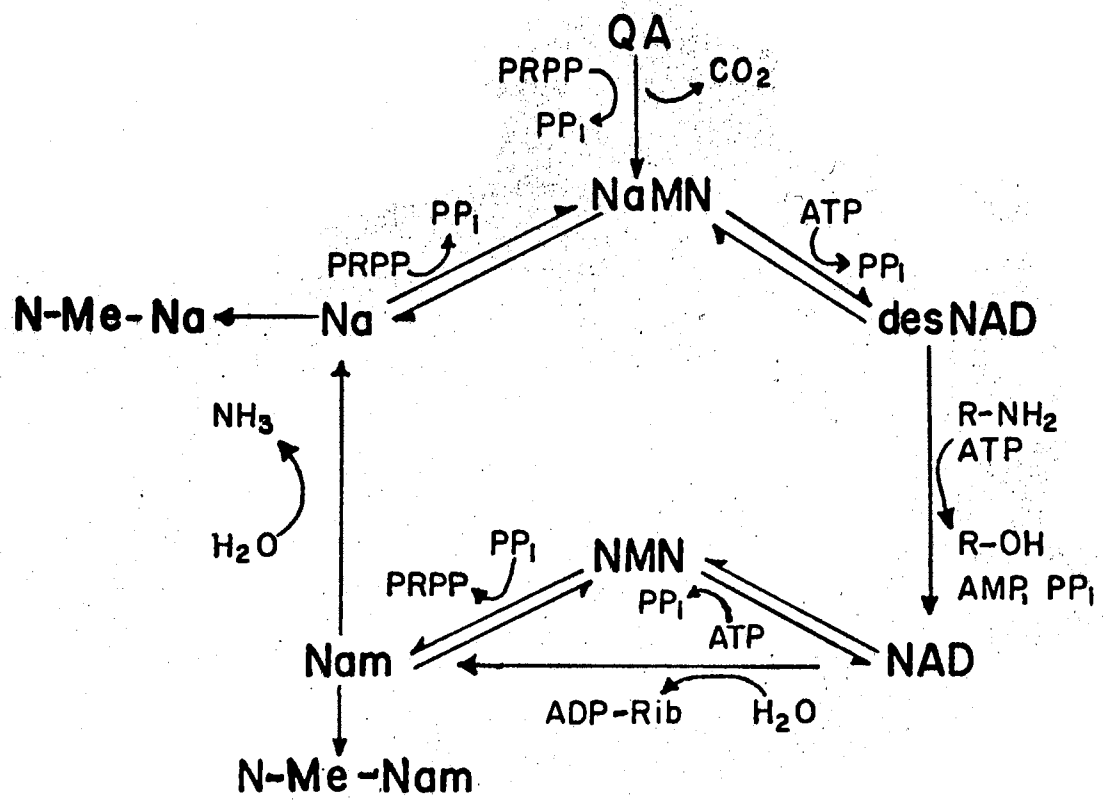
Figure 2. Biosynthesis of NAD in Rat Liver (29)

QA	= Quinolinic Acid
NaMN	= Nicotinic acid Mononucleotide
desNAD	= Nicotinic acid Adenine Dinucleotide
NAD	= Nicotinamide Adenine Dinucleotide
Nam	= Nicotinamide
N-Me-Nam	= N-Methyl Nicotinamide
Na	= Nicotinic acid
N-Me-Na	= N-Methyl Nicotinic acid

biosynthesis of ricinine in the castor bean plant from quinolinic acid.
Hiles and Byerrum, however, have suggested that the biosynthesis of
ricinine from quinolinic acid occurs by a separate pathway, independent
of the cycle (5). This conclusion was based on evidence indicating an
increase in incorporation of label into ricinine from labeled quinolinic
acid in the presence of excess exogenous NAD. However, this conclusion
can be valid only if one assumes NAD is an obligatory intermediate in
the biosynthesis of ricinine from quinolinic acid and that exogenous
NAD can be transported across the cellular membrane intact. Figure 3
describes their postulated schemes for NAD and ricinine biosynthesis.
Another explanation of their results is that ricinine was biosynthesized
from an intermediate before NAD in the cycle, such as desamido-NAD or,
more likely, nicotinic acid mononucleotide. However, the labeling ex-
periments of Waller and Henderson (19) indicated that the amide nitro-
gen of nicotinamide was incorporated directly into the nitrile group of
nitrogen. If ricinine were to arise from nicotinic acid mononucleotide,
a direct incorporation of the amide nitrogen of nicotinamide into
ricinine would not be expected, but rather an incorporation from a ni-
trogen pool such as ammonia or glutamate. Such seemingly conflicting
results have cast little light on the mystery of ricinine biosynthesis
in relation to the cycle.

2. Pyridine Nucleotide Cycle Inhibitors

Several compounds have been found to inhibit the pyridine nucleo-
tide cycle in animals at various points. Alazopeptin and 6-diazo-5-oxo-
norleucine, (DON), two potent glutamine antagonists and azaserine, a
less potent glutamine antagonist, have been shown to inhibit the pyridine
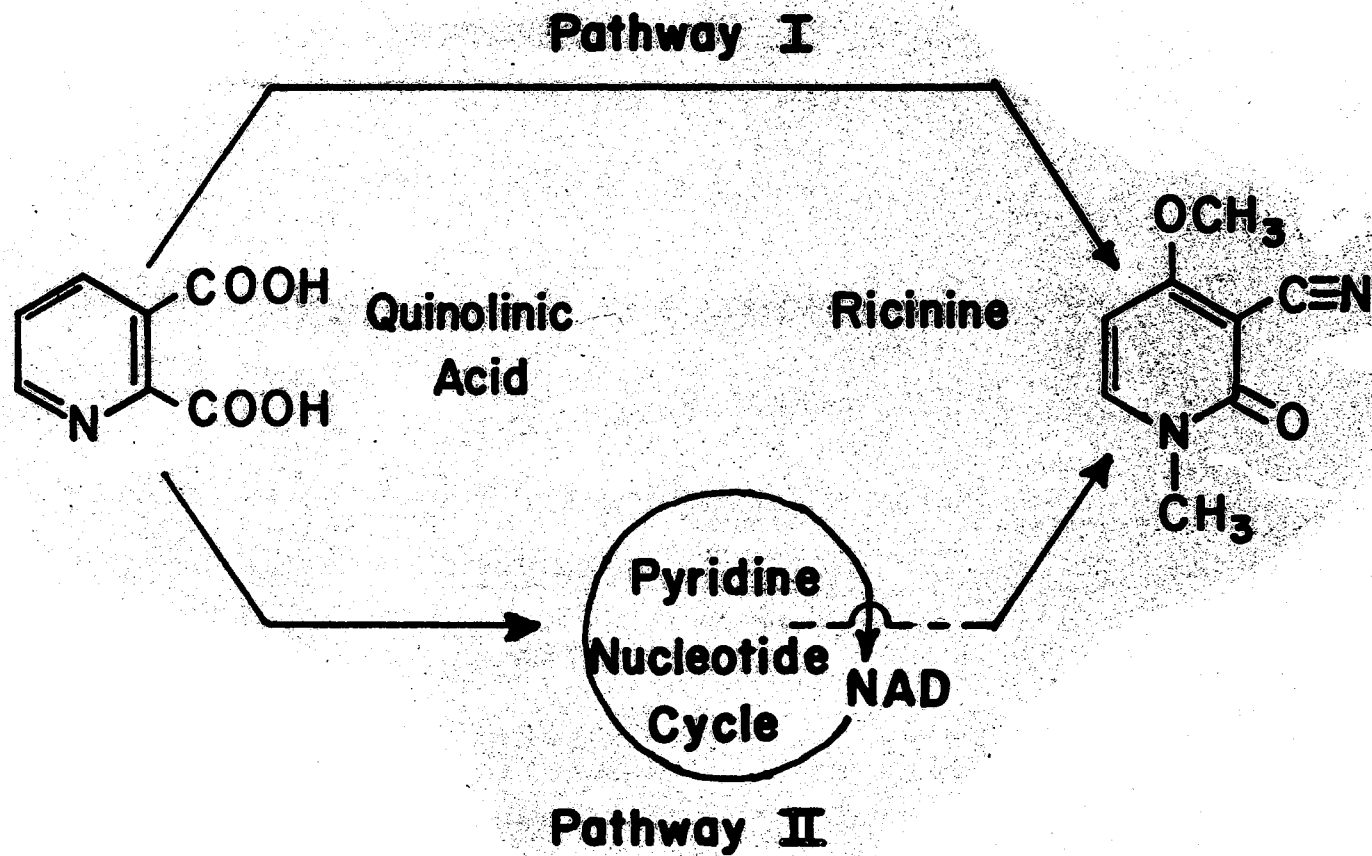
Figure 3. Postulated Pathways of Ricinine Biosynthesis from Quinolinic Acid (5).

nucleotide cycle (31,38,40). Two other azo-compounds, azaleucine and azauracil, were also considered as possible inhibitors.

Azaserine has been shown to be a glutamine antagonist (31) and has been shown by several workers to inhibit the NAD synthetase reaction in which desamido-NAD is converted to NAD with glutamine or ammonia as the nitrogen donor in liver (32-36), as well as in brain (37). Addition of excess nicotinamide just before adding azaserine or DON seemed to counteract this inhibition (35), however addition of glutamine after addition of azaserine or DON did not counteract this inhibition (35). This probably was because azaserine and DON are irreversible inhibitors (31,38). DON has been shown to be forty times more potent a glutamine antagonist than azaserine (31). This might explain the lack of any significant accumulation of desamido-NAD in the presence of azaserine (35,39), yet a definite accumulation was noted in the presence of DON in mouse liver and mouse tumor cells (39). Another explanation for this result could be that in mouse liver an enzyme was present which destroyed azaserine but not DON (40,41). DON also inhibited the re-action of phosphoribosyl pyrophosphate plus glutamine yielding glutamate plus 5-phosphoribosyl amine (42), which was catalyzed by phosphoribosyl pyrophate amido transferase. DON probably acted as a glutamine antagon-ist in this case also.

Alazopeptin has also been shown to cause inhibition of NAD synthe-sis in mouse liver and mouse tumor cells (39). It was shown to be about as potent an inhibitor as DON and since its structure is similar to that of DON it probably inhibited at the NAD synthetase reaction as does DON.

4-Azaleucine, an amino acid found in cultures of Streptomyces neocaliberis, has a structure similar to that of glutamine, DON and

INHIBITOR STRUCTURES

$$N\!=\!N\!=\!CH\!-\!\overset{\overset{\displaystyle O}{\|}}{C}\!-\!O\!-\!CH_2\!\overset{\overset{\displaystyle NH_2}{|}}{\underset{\underset{\displaystyle H}{|}}{C}}\!-\!COOH$$

azaserine

$$N\!=\!N\!=\!CH\!-\!\overset{\overset{\displaystyle O}{\|}}{C}\!-\!CH_2\!-\!CH_2\!-\!\overset{\overset{\displaystyle NH_2}{|}}{\underset{\underset{\displaystyle H}{|}}{C}}\!-\!COOH$$

6 – diazo – 5 – oxo–norleucine
(DON)

$$H_2N\!-\!\overset{\overset{\displaystyle H}{|}}{\underset{\underset{\displaystyle CH_3}{|}}{C}}\!-\!\overset{\overset{\displaystyle O}{\|}}{C}\!-\!NH\!-\!\overset{\overset{\displaystyle H}{|}}{\underset{\underset{\displaystyle CH_2}{|}}{C}}\!-\!\overset{\overset{\displaystyle O}{\|}}{C}\!-\!NH\!-\!\overset{\overset{\displaystyle H}{|}}{\underset{\underset{\displaystyle CH_2}{|}}{C}}\!-\!\overset{\overset{\displaystyle O}{\|}}{C}\!-\!OH$$

CH₂ CH₂

CH₂ CH₂

C=O C=O

CH CH
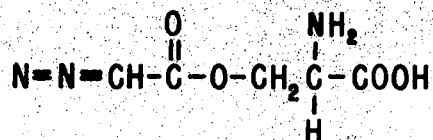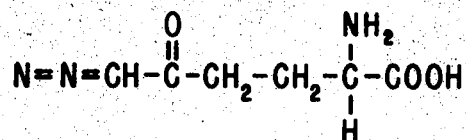
N=N N=N
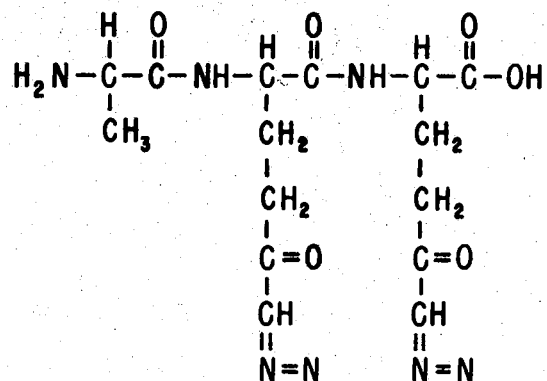
L–alanyl–(6–diazo–5–oxo)–L–norleucyl–(6–diazo–5–oxo)–L–norleucine

(alazopeptin)

$$CH_3\!-\!\overset{}{\underset{\underset{\displaystyle CH_3}{|}}{N}}\!-\!CH_2\!-\!\overset{\overset{\displaystyle NH_2}{|}}{C}\!-\!COOH$$

azaleucine

$$H_2N\!-\!\overset{\overset{\displaystyle O}{\|}}{C}\!-\!CH_2\!-\!CH_2\!-\!\overset{\overset{\displaystyle NH_2}{|}}{CH}\!-\!COOH$$
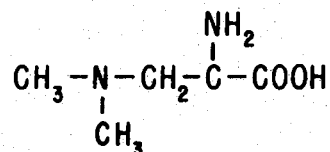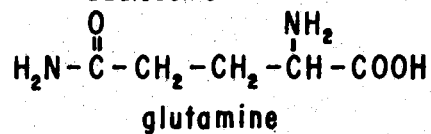
glutamine

Figure 4. Structures of Selected Inhibitors and Glutamine

azaserine (42,43). It has not been previously tested as an inhibitor of the pyridine nucleotide cycle.

Figure 4 shows the structures of these inhibitors compared with glutamine. The similarity of all these structures lends support to the postulation that each acts as a glutamine antagonist (32,42,45).

6-Azauracil, an analogue of uracil was found to inhibit orotic acid biosynthesis and the conversion of uracil to uridine diphosphoglucose (46).

Ricininic acid, or 0-demethyl ricinine, was shown to inhibit the conversion of nicotinic acid to ricinine (48).

CHAPTER III

EXPERIMENTAL METHODS

A. Materials and Chemicals Used

1. Plants

Series A and Series B experiments were conducted using castor bean

plants of the Cimarron variety were grown in port clay loam soil at the

Agronomy farm of Oklahoma State University in Stillwater, during the

summer of 1971, while Series C experiments were conducted using plants

grown in vermiculite-soil mixtures in the horticulture greenhouse. The

plants varied in weight from 75 to 200 grams. Table I shows the planting

TABLE I

PHYSIOLOGICAL STAGE OF THE CASTOR BEAN PLANTS
USED IN RICININE BIOSYNTHESIS EXPERIMENTS

Experiments	Planting Dates	Plant Age	Physiological State
Series A	May 1, 1971	8 weeks	non-flowering
Series A	May 1, 1971	11 weeks	flowers, no seeds
Series B	May 15, 1971	13 weeks	flowers, immature seeds
Series B	May 15, 1971	16 weeks	immature, few mature seeds
Series C	July 15, 1971	9 weeks	non-flowering

dates, plant age at the beginning of the experiment and physiological state of development.

2. Inhibitors

DL-4-azaleucine, azaserine and azauracil were purchased from Cal-biochem, Los Angeles, California, while ricininic acid was obtained from General Biochemicals, Chagrin Falls, Ohio and alazopeptin was obtained as a gift from Lederle Laboratories, Pearl River, New York*. Ricinine and ethionine were obtained from General Biochemicals, Chagrin Falls, Ohio.

3. Radioactive Compounds

Quinolinic acid-6-[14]C (specific activity of 43.7 mCi/mmole) was purchased from Nuclear-Chicago Corporation, Arlington Heights, Illinois. It was subjected to paper chromatography using 1M ammonium acetate : 95% ethanol (3 : 7, v/v) as a solvent system, and the radioactivity located using a Nuclear Chicago Actigraph III Model 1002 4π Chromatogram Scanner. The results indicated a radiochemical purity in excess of 99%.

Nicotinamide adenine dinucleotide phosphate-carbonyl-[14]C (specific activity of 26.2 mCi/mmole) was purchased from Nuclear Chicago Corporation, subjected to the same paper chromatography system and found to be greater than 99% radiochemically pure.

4. Chemical Reagents

Solvents and chemical reagents were of analytical reagent grade unless otherwise noted. Non-radioactive pyridine nucleotide cycle reference compounds were purchased from Sigma Chemical Company, St. Louis,

*Courtesy of Dr. E. L. Patterson

Missouri, Biochemical Research Company, Los Angeles, California, Nutri-
tional Biochemicals Corporation, Cleveland, Ohio, or Merck and Company,
Rahway, New Jersey.

Dowex 1 x 8 Cl⁻ form, 200-400 mesh was purchased from J. T. Baker
Chemical Company, Phillipsburg, New Jersey. BioRad AG 1 x 4 Cl⁻ form,
200-400 mesh was purchased from Calbiochem, Los Angeles, California.
Both were converted to the formate form by washing successively with
several volumes of deionized H_2O, 2N HCl, H_2O, 2N NaOH, H_2O, 6N HCOOH
and finally deionized water until the pH was approximately neutral.

B. Methods

1. Administration of Inhibitors and Labeled Compounds

Inhibitors were injected into the hollow internodular stem section
of the castor bean plant using a micro syringe. The labeled compounds
(1 μCi) were administered into the stem by the same technique, 1.0 ± 0.5
hours after the injection of the inhibitors. The plants were allowed to
metabolize for varying time periods up to 20 hours.

2. Isolation of Metabolites

Each castor bean plant was cut into small pieces with scissors,
placed in a Waring blender with 300 ml of 80% methanol at 50-60°C and
homogenized to a coarse slurry. The extract was filtered through a
sintered glass funnel (coarse porosity) under vacuum and the residue
extracted several more times until it was nearly colorless. The residue
was dried, ground, weighed and stored in vials and analyzed for radio-
activity by wet combustion and gas counting using a Cary Model 31 Vi-
brating Reed Electrometer. The combined 80% methanol extracts were
evaporated to dryness using a rotary evaporator and taken up in 150 ml

of deionized water. This water phase was extracted with diethyl ether

three times; the diethyl ether phase was dried on a steam plate, 90-100°

C, weighed, stored in vials and checked for radioactivity. The aqueous

phase was evaporated to near dryness on a rotary evaporator, and then

taken up in 10 ml of deionized water and stored in a 10 ml volumetric

flask at 2-5°C. Aliquots, usually 2 ml, were then subjected to thin-

layer chromatography on silica gel HF in chloroform : methanol (5 : 1,

v/v) along with authentic ricinine for identification purposes. The

ricinine was removed by elution with methanol, while the remainder of

the silica gel from the plate was extracted five times with 50% meth-

anol. Absorbance readings at 255 and 307 nm were taken of the ricinine

solution and the specific activity determined by liquid scintillation

spectrometry. This ricinine solution was dried, weighed and stored in

vials at 2-5°C. The 50% methanol extract of the remainder of the

silica gel was evaporated to near dryness using a rotary evaporator,

taken up in a minimal amount of deionized water and analyzed on either

a Dowex 1 x 8 or BioRad 1 x 4 formate column. This procedure is out-

lined in the flow diagram shown in Figure 5.

3. Chromatography

Anion Exchange Column Chromatography (33,34,47): Analysis of the

ricinine-free aqueous phase extract was achieved by placing an aliquot

on a Dowex 1 x 8 formate or BioRad AG 1 x 4 formate column, 1.4 x 42 cm.

The compounds were eluted using a formic acid concentration gradient,

which began with 200 ml of deionized water in the mixing chamber, and

into which 150 ml of deionized water, 150 ml of .05 M HCOOH, 300 ml of

0.5 M HCOOH and 400 ml of 3N HCOOH, were successively introduced. Two

fraction collectors, one a National Instrument Laboratories, Inc.

photoelectric drop counter and the other an Instrumentation Specialties

Company, Inc. volumetric fraction collector, were used to collect six

ml fractions at the rate of 80 ml per hour. These fractions were used

for the measurement of radioactivity and ultraviolet absorption at 260 nm.

Reference compounds were also subjected to column chromatography on

Dowex 1 x 8 formate and BioRad AG 1 x 4 formate columns to determine

their elution positions.

RICINUS COMMUNIS PLANTS

    80% methanol extraction
     filtration

evaporated under vacuum
to near dryness
dissolved in 150 ml H_2O

RESIDUE
(dried and
weighed)

H_2O SOLUTION

ETHER PHASE (dried and weighed) H_2O PHASE

evaporated under
vacuum to 10 ml

CONCENTRATED H_2O PHASE

TLC

POLAR COMPOUNDS   RICININE

Dowex 1 x 8 formate   (dried and weigh-
or BioRad AG 1 x 4   ed)
formate column chro-
matography

PYRIDINE NUCLEOTIDE
CYCLE INTERMEDIATES

Figure 5.   Isolation Procedure for Ricinine and the Pyridine Nucleotide
        Cycle Intermediates.

Paper Chromatography: The fraction from the Dowex 1 x 8 formate
and BioRad AG 1 x 4 formate columns containing radioactive peaks were
combined and dried by lyophilization. The residue was dissolved in
either methanol or deionized water, then spotted on Whatman No. 3 paper
strips along with standard compounds and chromatographed in 1 M ammonium
acetate : 95% ethanol (3 : 7, v/v), or isobutyric acid : ammonia : water,
(66 : 1.7 : 33, v/v/v).

4. Ultraviolet Spectrophotometry

All ultraviolet spectra or absorbance readings made on individual
samples were obtained on either a Beckman DB recording spectrophotometer
or a Hitachi-Perkin Elmer 124 Double Beam Spectrophotometer.

5. Measurement of Radioactivity

Each of the six ml fractions from the Dowex 1 x 8 formate or BioRad
AG 1 x 4 formate columns were analyzed for radioactivity by placing 2 ml
from each fraction with 10 ml of Bray's scintillation solution (49), and
counting on a Model 3320 Packard Tri-Carb Scintillation Spectrophoto-
meter. The gain was set at 16.5% and the windows at 25 to 1000. Bray's
solution was prepared with 4 grams of 2,5-diphenyloxazole (PPO), 0.2
grams of p-bis-2-(5-phenyloxazolyl)benzene (POPOP), 60 grams of naptha-
lene, 20 ml of ethylene glycol, 100 ml of methanol and the proper volume
of p-dioxane for 1 liter of solution.

The counting efficiency of 10 ml of Bray's solution with 2 ml of
formic acid from 1.0 to 2.0 M added was approximately 70%, while the
counting efficiency between 0.0 and 1.0 M formic acid was approximately
72%. The effect of formic acid concentration on counting efficiency is
shown in Figure 6. Corrections for formic acid quenching were made us-
ing Figure 6.
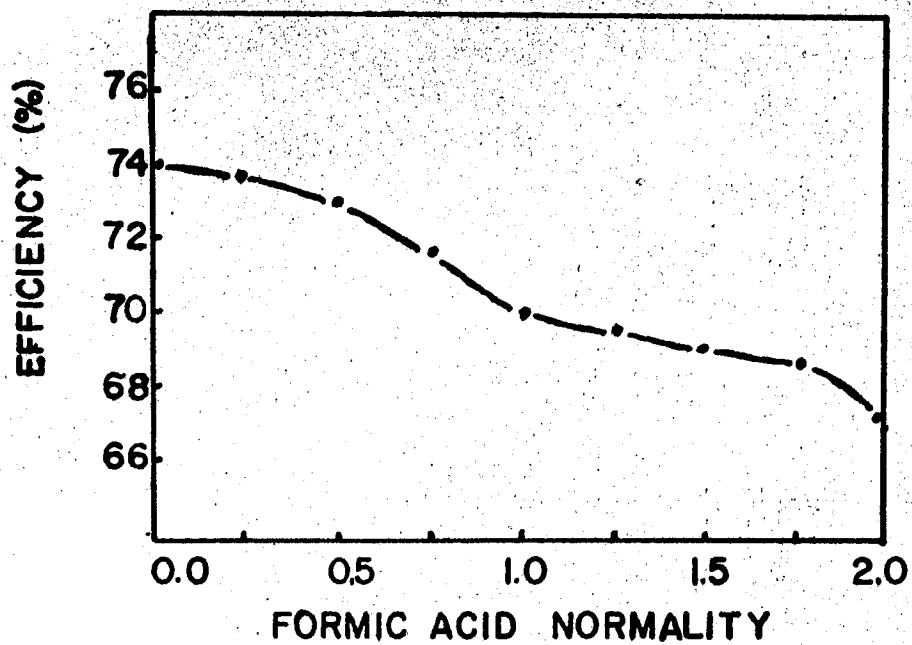
Figure 6. Efficiency of Radioactivity Counting at
Various Concentrations of Formic Acid
Using Liquid Scintillation Spectrometry.
Two ml of water per 10 ml of scintilla-
tion cocktail.
Counting efficiency (%) = (cpm/dpm) X 100

CHAPTER IV

RESULTS AND DISCUSSION

A. Administration of Inhibitors and Labeled Compounds

Administration of the inhibitors, azauracil and ricininic acid, was
difficult since both were sparingly soluble in water and/or methanol.
The solubility of these compounds never exceeded 5 mg/ml in either
methanol, water, or mixtures of these solvents. Quantities in excess of
1 ml were injected into the plants to obtain the appropriate amounts of
inhibitor. The amounts of inhibitor injected and the times allowed for
metabolism for each of the experiments are shown in Table IV. Azaserine
and azaleucine were very soluble in water and quantities less than 100
μl were injected into the plants. Only a small amount of alazopeptin
was obtained so only one experiment was conducted with this inhibitor.
All of the inhibitors were injected approximately one hour before the
labeled precursor were administered.

Ten μl of a solution containing one μCi/μl of quinolinic acid-6-^{14}C
(specific activity of 43.7 μCi/μmole), were injected into each plant.
This quinolinic acid-6-^{14}C was analyzed on Dowex 1 x 8 column chromatog-
raphy before administration to the plants. A single symmetrical radio-
active peak was observed.

No noticeable physical effects due to the inhibitors were noted
with the exception of azaleucine. Injection of large quantities of
azaleucine caused a slight weakening of the stem structure indicated by

a partial collapse at the stem at the point of injection. No wilting or discoloration was observed.

Several experiments were conducted with NADP-carbonyl-^{14}C as the precursor and azaserine and azaleucine as the inhibitors. One μCi of NADP-carbonyl-^{14}C (specific activity of 20 μCi/μmole) was injected into the plants one hour after injection of the inhibitors.

B. Isolation and Identification of Metabolites

The isolation procedure shown in Figure 6 had as one of its last steps a thin-layer chromatographic analysis in which ricinine was separated from the polar pyridine nucleotide cycle intermediates by development in chloroform : methanol (5 : 1, v/v). Figure 7 shows a radio chromatographic scan of one of these developed thin-layer plates. Peak A, at the origin, contains the various pyridine nucleotide cycle intermediates while peak B was shown to be ricinine. Since the compounds present in peak A could not be readily separated by paper or thin-layer chromatography, they were subjected to anion exchange chromatography on a Dowex 1 x 8 formate column as previously described.

Figure 8 shows a plot of absorbance at 260 nm (A_{260}) and radio-activity versus tube number for Dowex 1 x 8 column chromatography of quinolinic acid-6-^{14}C injected control plant, after removal of the ricinine by the previously described thin-layer chromatography. Eight major radioactive peaks were observed. This general elution pattern was observed for all control plants.

Tubes representing each peak were pooled, lyophilized to dryness and identified by paper chromatography and thin-layer chromatography with authentic samples, as well as comparison of elution volumes on
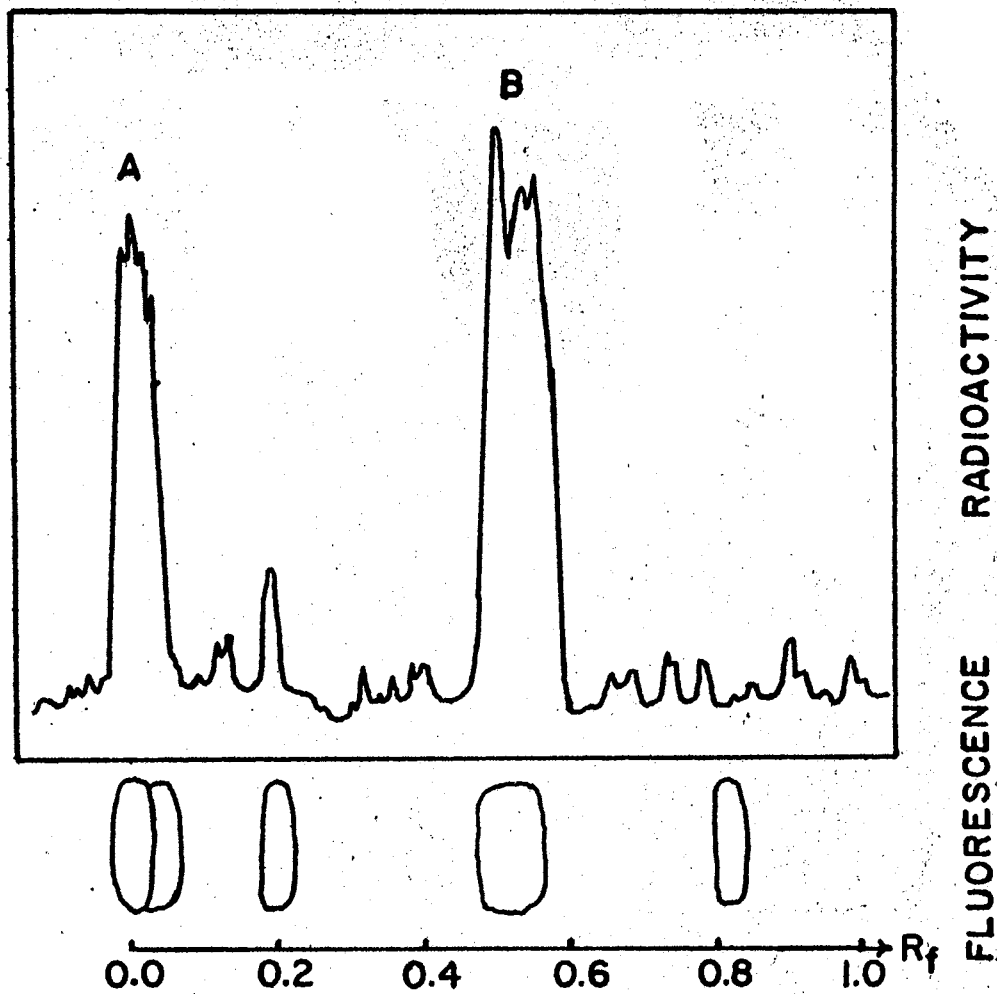
Figure 7. Thin-Layer Radiochronatogram Tracing of an 80%
Methanol Extract from a Castor Bean Plant Fed
Quinolinic Acid-6-^{14}C. (Solvent; Chloroform:
Methanol, 5 : 1, v/v)

A - Polar Compounds
B - Ricinine
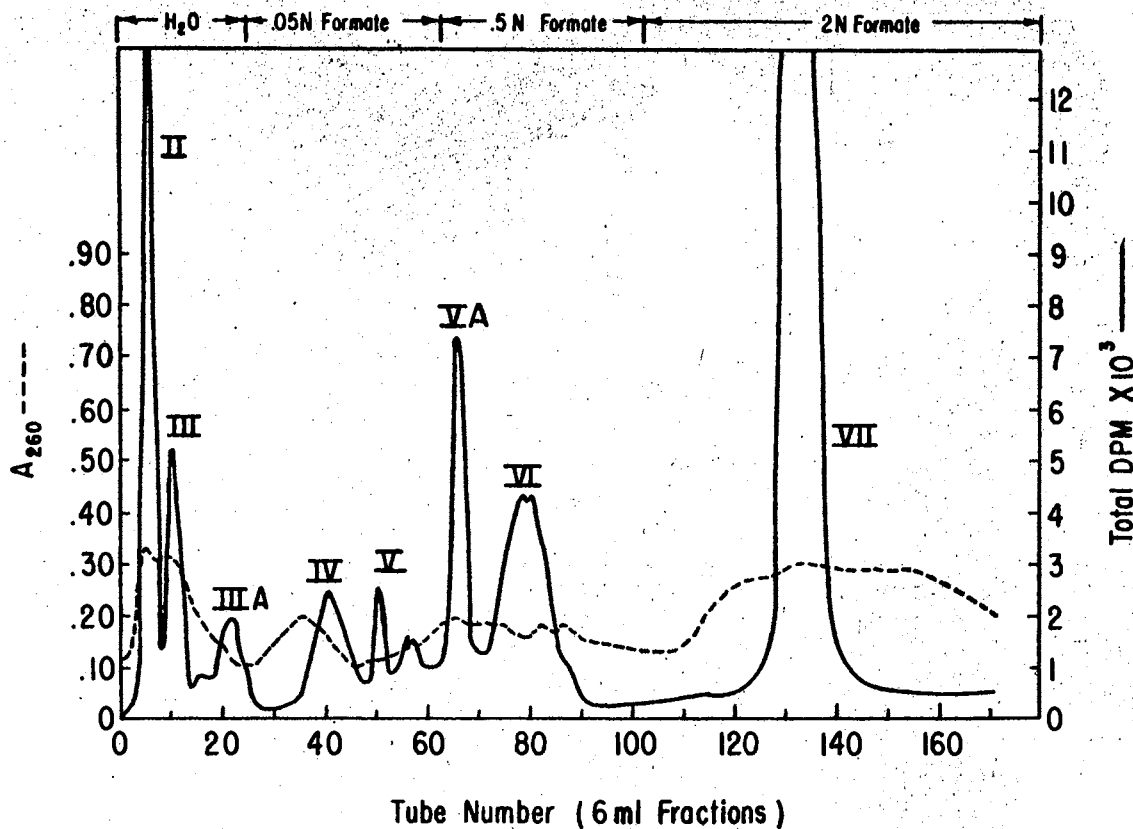
Figure 8. Dowex 1 x 8 Formate Column Chromatography of the Aqueous
Phase of an 80% Methanol Extract of a Control Castor
Bean Plant Injected with one Microcurie of Quinolinic
Acid-6-^{14}C. Peak identities shown in Fig. 10 and
Table II.

Dowex 1 x 8 formate columns of authentic and unknown samples and finally by comparison of ultraviolet spectra of authentic and unknown samples. Based on the criteria previously mentioned, the following radioactive peaks, II, III, IV, V, VA, VI and VII were tentatively identified as a mixture of N-methyl nicotinic acid and N-methyl nicotinamide, nicotin- amide, ricinine, NAD, nicotinic acid, desamido NAD and quinolinic acid, respectively. The possibility of minor contributions from compounds other than the one assigned to the radioactive peaks cannot be excluded, and minor radioactive peaks were not identified because of low concen- trations and insufficient radioactivity. Table II shows the R_f values of the various metabolites from both paper- and thin-layer chromato- graphic systems. Figure 9 shows the elution pattern of several reference compounds from a Dowex 1 x 8 formate column.

C. Quinolinic Acid-6-^{14}C As a Precursor

1. Inhibitor Effects on Ricinine Biosynthesis

The biosynthesis of ricinine as well as the pyridine nucleotide cycle intermediates in higher plants have been studied by measuring the incorporation of labeled precursors into these compounds. It has been postulated that ricinine was biosynthesized both from pyridine nucleo- tide cycle intermediates (2) or by a pathway operating independently of the cycle from quinolinic acid (5).

To help clarify this situation, experiments were undertaken in which labeled quinolinic acid was fed to castor plants previously fed with compounds known or suspected to be pyridine nucleotide cycle in- hibitors. These compounds, described previously, were ricininic acid, azauracil, alazopeptin, azaserine and azaleucine. Also large amounts of
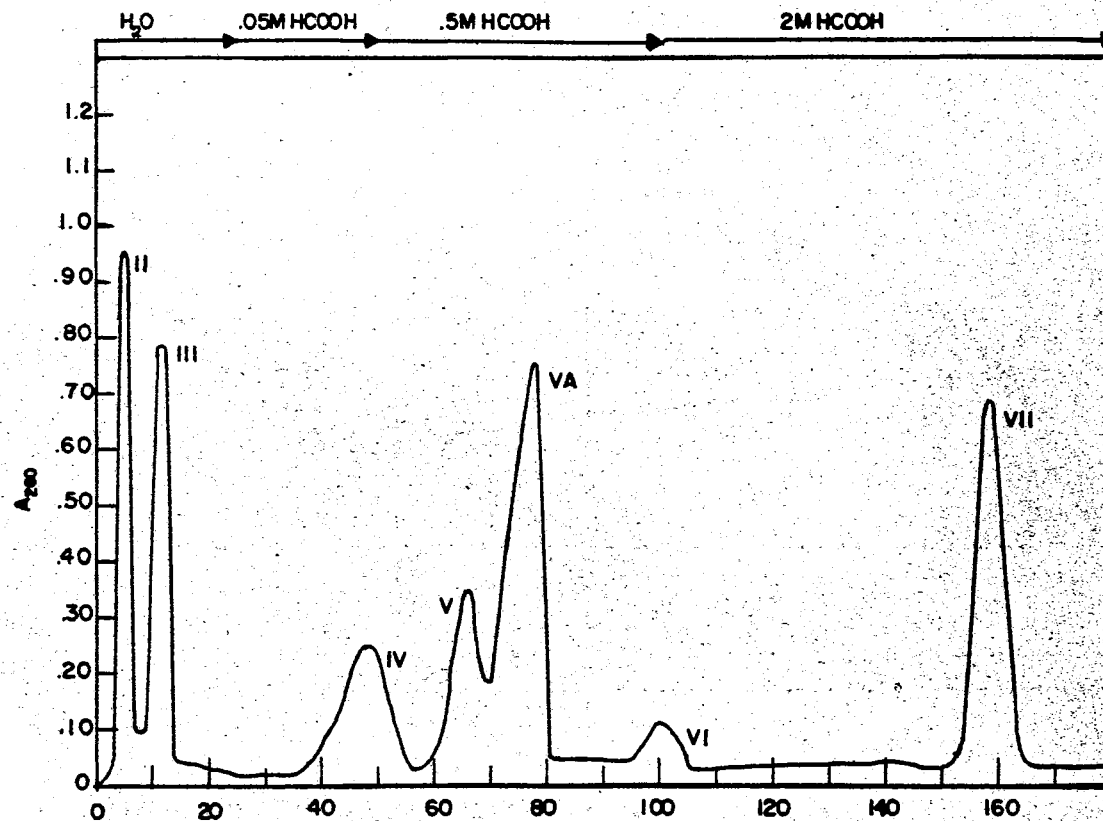
Figure 9. Dowex 1 x 8 Formate Column Chromatography of Standard
Pyridine Nucleotides Cycle Intermediates. II, III,
IV, V, VA, VI and VII were N-methyl nicotinic acid,
nicotinamide, ricinine, NAD, nicotinic acid, desamido
NAD and quinolinic acid.

ricinine and ethionine were injected into castor bean plants in an attempt to block the synthesis of ricinine at the latter stages of biosynthesis and to observe any effects on the pyridine nucleotide cycle.

TABLE II

R_F VALUES FROM PAPER CHROMATOGRAPHY OF THE METABOLITES
OF QUINOLINIC ACID-6-^{14}C IN RICINUS COMMUNIS L.

Compound	Solvent 1	Solvent 2
II (N-methyl nicotinic acid) (N-methyl nicotinamide)	.71	.80
III (nicotinamide)	.77	.85
IV (ricinine)	.88	–
V (NAD)	.22	.35
VA (nicotinic acid)	.57	.71
VI (desamido-NAD)	.18	.39
VII (quinolinic acid)	.42	.32

solvent 1: 1M ammonium acetate : 95% ethanol (3 : 7, v/v)

solvent 2: isobutyric acid : ammonia : water (66 : 1.7 : 33, v/v/v).

Two preliminary experiments (Series A) were undertaken in which these inhibitors were tested as to their effect on the biosynthesis of ricinine and of the pyridine nucleotide cycle intermediates. Quinolinic acid-6-^{14}C (1 μCi) was used as a precursor in these experiments. Four plants were injected with only quinolinic acid-6-^{14}C, two plants with

ricininic acid (10 mg/100 gm) followed by one μCi of quinolinic acid-6-^{14}C, two plants with alazopeptin (15 mg/100 gm) followed by one μCi of quinolinic acid-6-^{14}C, three plants with azauracil (20 mg/100 gm) followed by 1 μCi of quinolinic acid-6-^{14}C, three plants with azaleucine (20 mg/100 gm) followed by 1 μCi of quinolinic acid-6-^{14}C, and three plants with azaserine (20 mg/100 gm) followed by 1 μCi of quinolinic acid-6-^{14}C.

Three more groups of experiments were undertaken after observation of the results of the preliminary experiments. In the first of these experiments (Series B) the concentration of the inhibitors was increased to 45 mg/100 gm and the time the plants were allowed to metabolize in the presence of the quinolinic acid-6-^{14}C and inhibitors was varied. Duplicate control plants, azaleucine-treated plants and azaserine-treated plants were allowed to metabolize for four-, eleven- and twenty-hour periods before analysis. The results from the 4-hour experiments were extremely variable and inconclusive and so were not used. The eleven- and twenty-hour experiments produced more significant results. In the second of the Series B experiments two plants were treated only with quinolinic acid-6-^{14}C, two plants with quinolinic acid-6-^{14}C plus azaserine (75 mg/100 gm) and quinolinic acid-6-^{14}C plus azaleucine (75 mg/gm).

In the third group of experiments duplicate young non-flowering plants were injected with 1 μCi of quinolinic acid-6-^{14}C, with 1 μCi of quinolinic acid-6-^{14}C plus 1 mg/gm of unlabeled ricinine or with 1 μCi of quinolinic acid-6-^{14}C plus 40 mg/100 gm of ethionine.

In all experiments ricinine was isolated from each plant by thin-layer chromatography and was quantitatively analyzed and its

incorporation of radioactivity determined directly, while the pyridine nucleotide cycle intermediates were isolated by Dowex 1 x 8 formate column chromatography and also quantitatively analyzed for incorporation of radioactivity. Table III shows the effects of inhibitors on the amount of ricinine in the plant and the incorporation of label into ricinine from quinolinic acid-6-^{14}C.

In the preliminary experiments, (Series A), the amount of ricinine in the plants remained approximately the same. This was to be expected since there is a very high concentration of ricinine in the plants (about 1 mg/gm fresh weight) and even a reduced biosynthetic rate would not affect the net amount of ricinine in the plant since the turnover of ricinine is relatively slow. The % incorporation of label from quinolinic acid-6-^{14}C into ricinine varied somewhat, however, the only really significant change occurred in the alazopeptin-treated plants where the incorporation into ricinine was about one-half that of the control plants. These results are shown in the Series A section of Table III. Unfortunately, not enough alazopeptin was available to continue these experiments so no further experimentation using alazopeptin was not done. The insolubilities of ricininic acid and azauracil in both methanol and water prevented further experimentation using higher dosages, so only azaserine and azaleucine were used in the Series B experiments.

In the Series B experiments, the amount of ricinine present in the plants was again essentially unchanged, however, the effects of the inhibitors on the incorporation of label into ricinine was marked, especially in the case of azaleucine. The results shown in Table III indicated that in the eleven-hour experiments, azaserine caused a

TABLE III

EFFECTS OF INHIBITORS ON THE
BIOSYNTHESIS OF RICININE

One μCi of quinolinic acid-6-^{14}C (specific activity of 43.7 μCi/ μmole) was administered as a precursor.

Inhibitors		Duration	Ricinine			Isotope Dilution
Exp.	Conc.		Conc.	Incorp.	Sp. Act.	
	$\frac{mg}{100gm}$	hours	$\frac{mg}{100gm}$	%	$\frac{m\mu Ci}{\mu mole}$	
Series A						
Control	−	11	3.6	35.4	1.14	32,988
Ricininic Acid	10	11	3.4	42.5	1.32	26,638
Azauracil	20	11	3.6	36.6	1.22	35,812
Alazopeptin	15	11	3.9	19.9	1.53	28,483
Azaleucine	20	11	3.7	38.1	1.64	25,179
Azaserine	20	11	3.7	35.6	1.57	29,832
Series B						
Control-11	−	11	2.6	25.6	1.27	34,409
Azaserine-11	45	11	2.6	20.6	0.79	55,564
Azaleucine-11	45	11	1.9	6.5	0.18	99,993
Control-20	−	20	2.5	20.8	0.82	52,914
Azaserine-20	75	20	2.7	16.0	0.74	59,011
Azaleucine-20	75	20	2.4	4.6	0.19	223,369
Control	−	20	3.4	35.5	4.26	10,288
Ricinine	100	20	5.4	5.7	0.56	78,035
Ethionine	40	20	4.1	8.6	0.96	45,521

reduction in the incorporation of label into ricinine of about 20%. In the 20-hour experiments the reduction of label incorporation into ricinine by azaserine was about 23%

In the 11-hour experiments, azaleucine caused a massive 75% reduction of incorporation of label from quinolinic acid-6-^{14}C into ricinine, and in the 20-hour experiments, the reduction was about 80%. This indicated a sharp decrease in the biosynthesis of ricinine from quinolinic acid.

In all cases of decreased incorporation into ricinine a reduction in specific activity and an increase in the isotope dilution verified the results.

In the ricinine overloading and ethionine inhibition experiments large decreases in incorporation of label into ricinine from quinolinic acid-6-^{14}C were noted. These amounted to an 84% decrease and a 76% decrease, respectively. The specific activity of ricinine was reduced considerably and the isotope dilution values verify these results.

2. Inhibitor Effects on the Pyridine Nucleotide Cycle

Dowex 1 x 8 formate column chromatography was used to separate the pyridine nucleotide cycle intermediates. Plots of absorbance at 260 nm and total radioactivity versus fraction number yielded elution patterns similar to that shown in Figure 10, however, there were some noticeable differences in the incorporation of radioactivity into some of the pyridine nucleotide cycle intermediates in the presence of these inhibitors. Table IV shows the distribution of radioactivity in the pyridine nucleotide cycle intermediates from quinolinic acid-6-^{14}C in the presence and absence of inhibitors.

Figure 10. Dowex 1 x 8 Formate Column Chromatography of the Quino-
linic Acid-6-^{14}C Metabolites of Castor Bean Plants
Injected with Azaserine (45mg/100 gm). Legend is the
same as described under Figure 9. VIA and VIB could
not be identified.

TABLE IV

EFFECTS OF INHIBITORS ON THE DISTRIBUTION
OF RADIOACTIVITY IN PYRIDINE NUCLEOTIDE
CYCLE INTERMEDIATES

One μCi of quinolinic acid-6-^{14}C (specific activity of 43.7 $\mu Ci/\mu mole$) was administered as a precursor.

II = mixture of N-methyl nicotinic acid and N-methyl nicotinamide
des NAD = nicotinic acid adenine dinucleotide
NAD = nicotinamide adenine dinucleotide
QA = quinolinic acid
N-Amide = nicotinamide
N-Acid = nicotinic acid

Inhibitor	Conc.	Distribution of Radioactivity					
		QA	des-NAD	NAD	N-Amide	N-Acid	II
	$\frac{mg}{100gm}$	%	%	%	%	%	%
Series A							
Control	–	11.3	1.0	1.7	0.6	1.1	12.2
Ricininic Acid	10	8.6	0.7	0.5	0.5	0.5	12.1
Azauracil	20	7.7	1.4	1.9	1.1	0.9	16.4
Alazopeptin	15	15.9	1.5	1.4	1.1	1.1	20.8
Azaleucine	20	10.1	0.8	1.2	2.0	0.7	17.7
Azaserine	20	11.2	1.1	2.0	1.6	1.5	15.6
Series B							
Control-11	–	19.5	2.0	1.0	2.2	1.0	2.8
Azaserine-11	45	38.3	6.2	2.0	4.0	1.3	9.1
Azaleucine-11	45	38.2	1.4	0.8	4.2	0.7	4.4
Control-20	–	14.1	2.7	0.8	1.6	0.6	4.7
Azaserine-20	75	22.9	3.3	1.1	5.3	1.3	7.1
Azaleucine-20	75	37.0	2.6	0.4	1.2	0.7	5.1
Control	–	7.7	0.7	0.8	2.6	1.0	4.3
Ricinine	100	14.3	0.4	0.3	10.6	3.3	8.0
Ethionine	40	20.1	0.7	0.7	13.8	2.2	7.4

In the Series A experiments most of the data were not significant, however, in the case of alazopeptin-treated plants a 41% increase in the amount of label remaining in unreacted quinolinic acid was noted. This was an indication of a partial blockage of the cycle with respect to the control plants. Some increase in the amount of label present in desamido-NAD was observed, indicating that the cycle inhibition was occurring at the amidation of desamido-NAD to NAD, catalyzed by NAD synthetase. These data were quite variable and this increase in label in desamido-NAD may or may not be significant. The other inhibitors produced no significant changes in the pattern of label incorporation into the cycle intermediates in this set of experiments.

In the Series B experiments, the inhibition of the cycle as well as of ricinine biosynthesis, was marked. Figure 10 shows a plot of A_{260} and radioactivity versus tube number for Dowex 1 x 8 chromatography of an 80% MeOH extract of an azaserine-treated plant. In the 11 hour experiments, azaserine-treated plants showed a marked 3-fold increase in incorporation of label into desamido-NAD indicating a definite inhibition of the NAD synthetase catalyzed amidation of desamido-NAD to NAD. Further proof of the inhibition of the cycle was shown in the data on the amount of label remaining in unreacted quinolinic acid. A 2-fold increase in the label remaining in quinolinic acid in the 11-hour azaserine-treated plants was observed. This indicated a definite inhibition of the cycle perhaps at the quinolinic acid decarboxylase-catalyzed conversion of quinolinic acid to nicotinic acid mononucleotide. In the 20-hour experiments with azaserine-treated plants this inhibition was again present but not quite as marked. A 23% increase in the label incorporation into desamido-NAD compared to the controls was noted

and a 63% increase in the amount of label remaining in quinolinic acid was observed. Again this indicated a definite inhibition of the cycle. The effects of azaserine on the other cycle intermediates was somewhat variable, however, a definite increase in the amount of label in peak II, (3-fold and 2-fold, respectively) which contains N-methyl nicotinic acid and N-methyl nicotinamide, was observed. This could be due to an inhibition of the demethylation reactions which convert these storage compounds to nicotinamide and nicotinic acid, respectively, or it could be that the peak incorporation of label from quinolinic acid into these compounds was more closely approached by the azaserine inhibited plants at the times of analysis than by the control plants, perhaps because the highest incorporation levels were reached by the control plants before analysis and at the time of analysis a great portion of the label had been further metabolized. In the case of nicotinamide a 2- to 3-fold increase in label incorporation was observed in both the eleven-hour and twenty-hour azaserine-treated plants compared with the value for the control plants. This increase could be due to an inhibition of the deamidation of nicotinamide to nicotinic acid, catalyzed by nicotinamide deamidase. Since azaserine has been shown to be an inhibitor of the amidation of desamido-NAD to NAD, it may also inhibit the deamidation of nicotinamide to nicotinic acid.

Figure 11 shows a plot of A_{260} and radioactivity versus tube number for Dowex 1 x 8 formate column chromatography of an 80% methanol extract of a plant treated with azaleucine. In the Series B experiments, azaleucine caused decreases in incorporation of label from quinolinic acid-6-^{14}C into the cycle intermediates and large amounts of label remained in unreacted quinolinic acid. Nicotinamide and peak II were the
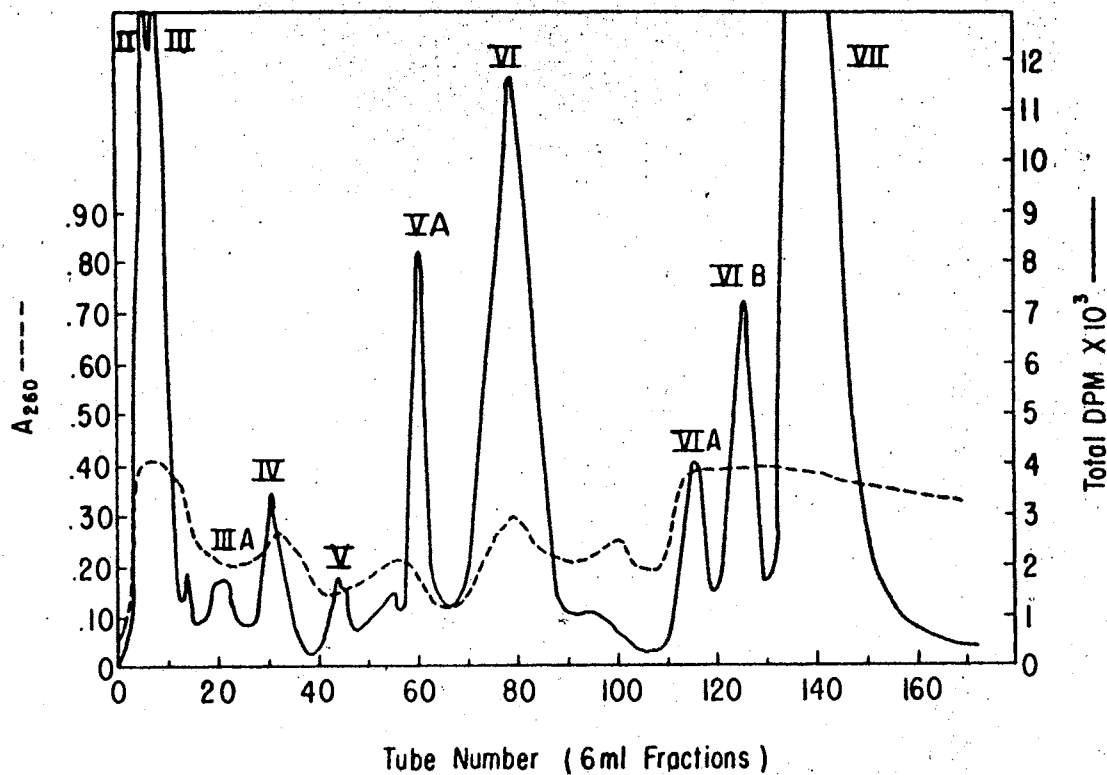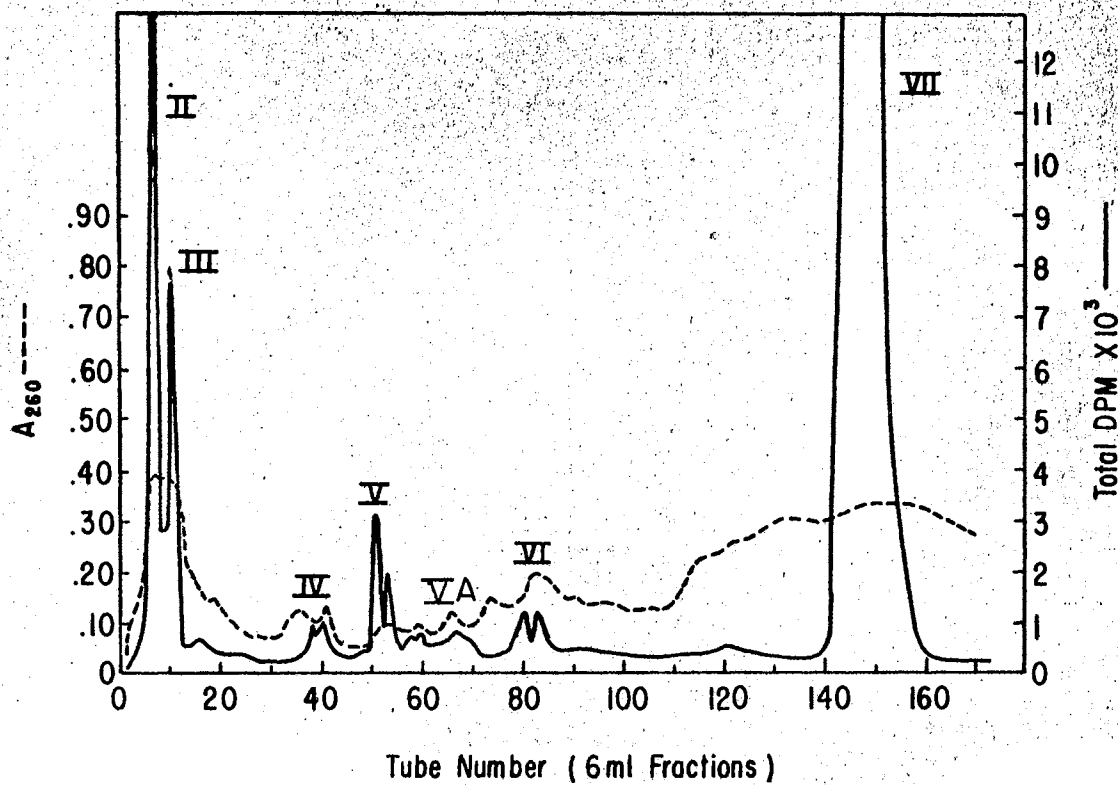
Figure 11.   Dowex 1 x 8 Formate Column Chromatography of the Quino-
            linic Acid-6-[14]C Metabolites of Castor Bean Plants
            Injected with Azaleucine (45 mg/100 gm). Legend is
            the same as described in Figure 9.

only cycle intermediates which incorporated more radioactivity than the controls. In the eleven-hour experiments a 2-fold increase in the amount of unreacted labeled quinolinic acid was observed. This was probably due to an inhibition of quinolinic acid decarboxylase, which slowed down the entrance of labeled quinolinic acid into the cycle. A general reduction in the amount of label found in most of the cycle intermediates was also noted, probably due to the reduction in amount of labeled quinolinic acid entering the cycle. In the 20-hour experiments the same type of results were observed. A 2.5-fold increase in the amount of label remaining in quinolinic acid was seen, again probably due to an inhibition of quinolinic acid decarboxylase. Again there was a reduction in the amount of label incorporated into the cycle intermediates with the exception of peak II and nicotinamide which increased.

In both the 11- and 20-hour experiments azaserine to some extent and azaleucine to a greater extent inhibited both ricinine biosynthesis and the pyridine nucleotide cycle. This indicates a connection or relationship between ricinine biosynthesis and the pyridine nucleotide cycle.

Figures 12, 13 and 14 show plots of radioactivity and A_{260} versus tube number for Dowex 1 x 8 column chromatography of 80% methanol extracts of control plants, ricinine-treated plants and ethionine-treated plants respectively. In the ricinine overloading and ethionine inhibition experiments the amount of label remaining in quinolinic acid increased 2- to 3-fold indicating an inhibition of the operation of the cycle. A 2- to 4-fold increase in the radioactivity found in nicotinamide in the presence of both excess ricinine and ethionine as well as a 2-fold increase in incorporation of radioactivity into peak II was
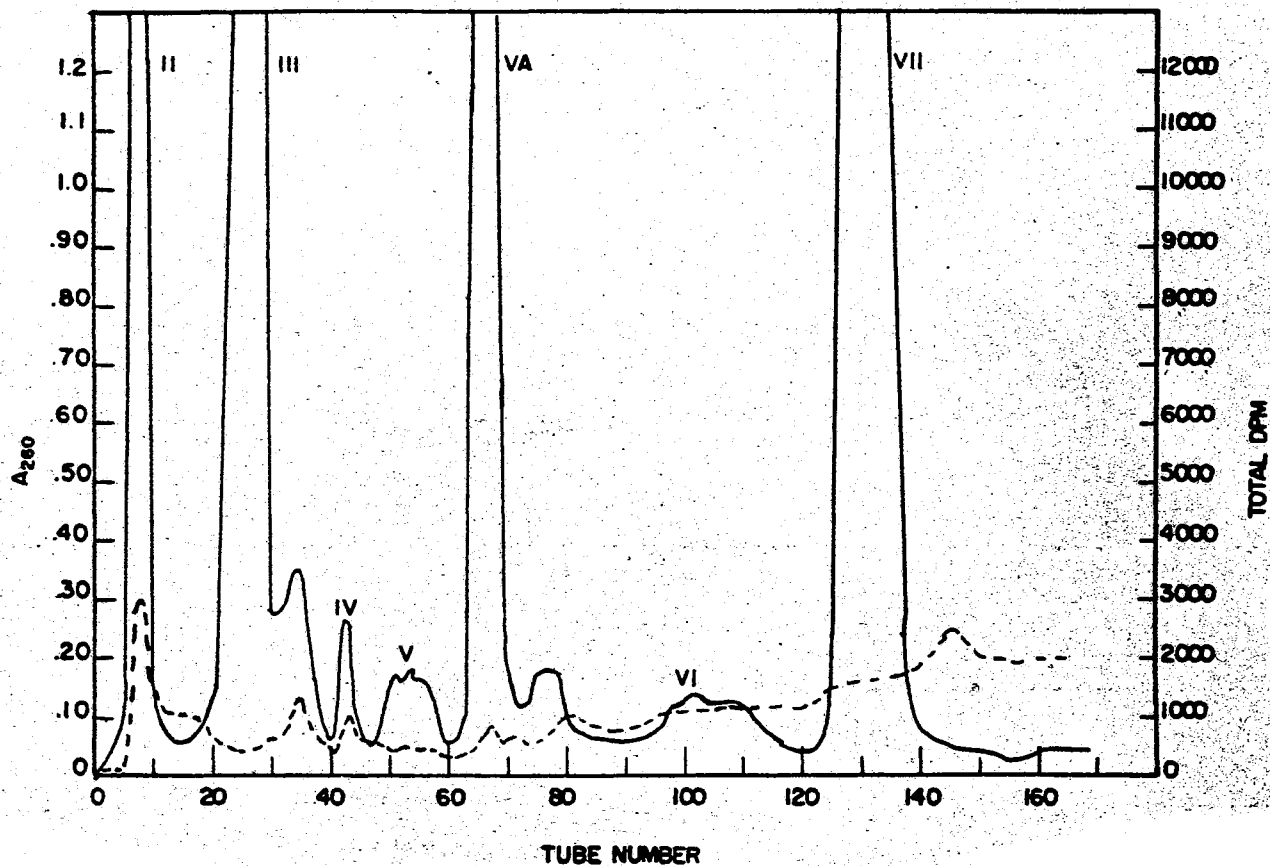
Figure 12. Dowex 1 x 8 Formate Column Chromatography of the Aqueous
Phase of an 80% Methanol Extract of a Control Castor
Bean Plant Treated With one Microcurie of Quinolinic
Acid-6-^{14}C. Peak Identities are Shown in Figure 10
and Table II.
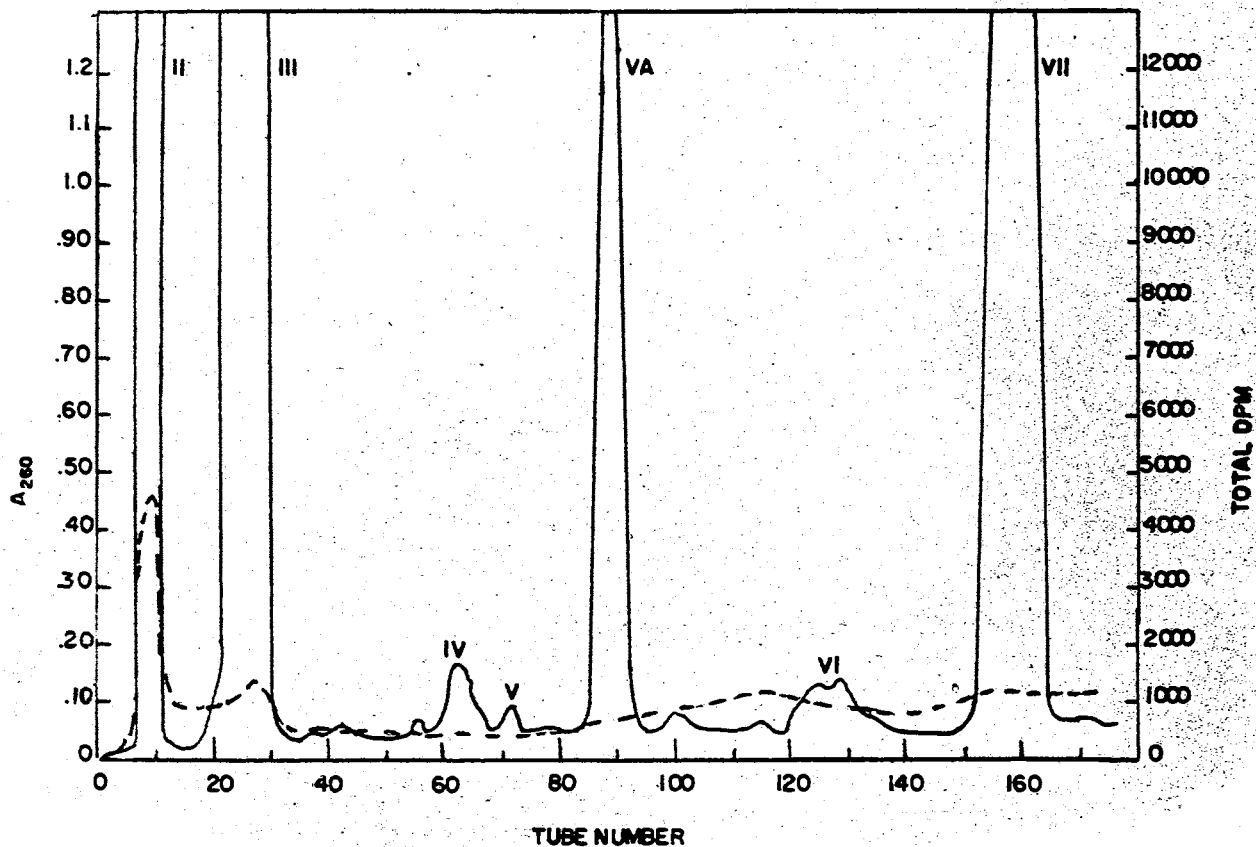
Figure 13. Dowex 1 x 8 Formate Column Chromatography of the Aqueous
Phase of an 80% Methanol Extract of a Castor Plant
Treated with a Two-Fold Excess of Ricinine plus Quino-
linic Acid-6-^{14}C (1μCi). Peak identities are shown in
Figure 10 and Table II.
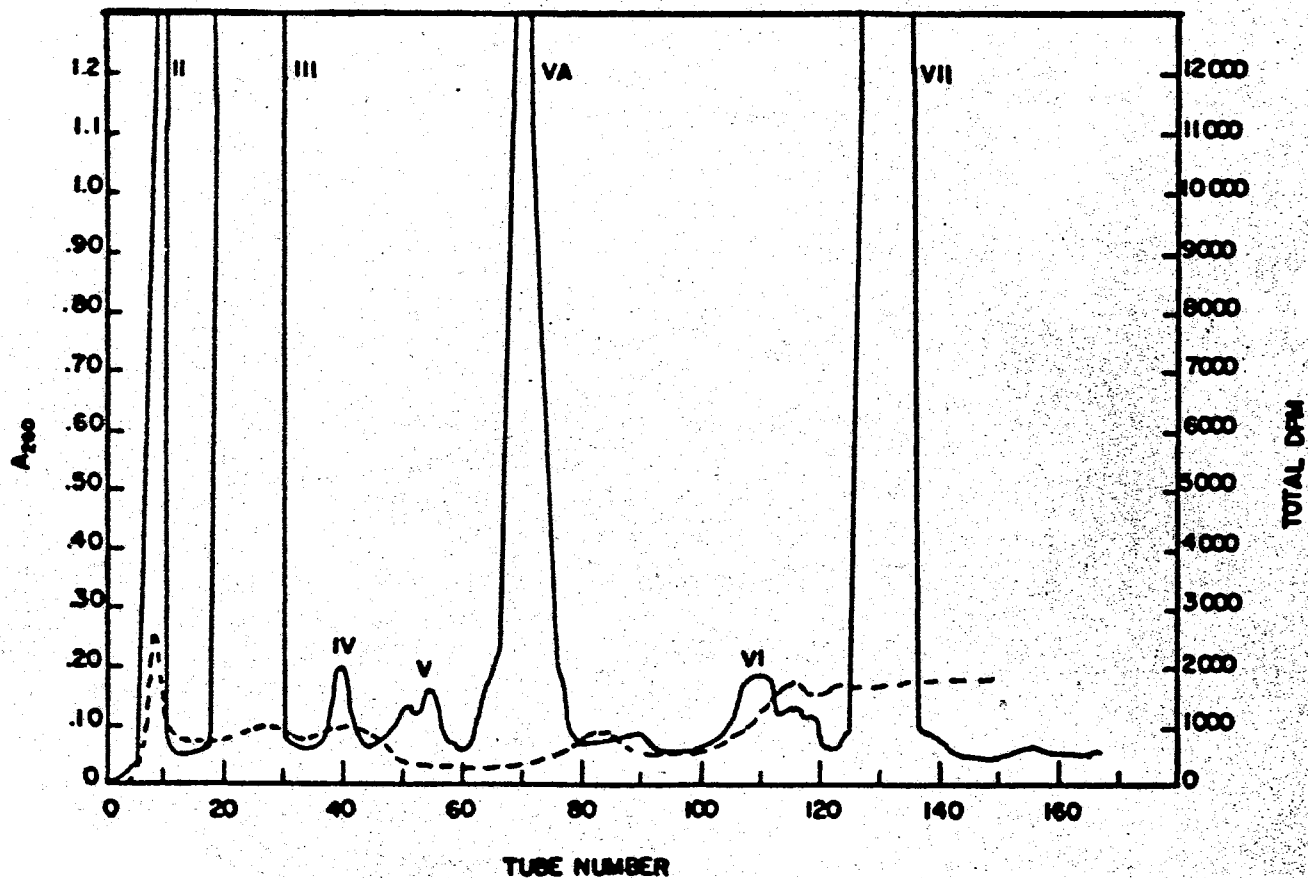
Figure 14. Dowex 1 x 8 Formate Column Chromatography of the Aqueous
Phase of an 80% Methanol Extract of a Castor Plant Treat-
ed with Ethionine (40 mg/100 gm) plus Quinolinic Acid-
6-^{14}C (1μCi). Peak identities are shown in Figure 10
and Table II.

observed. A 2- to 3-fold increase in the radioactivity found in nico-
tinic acid was also found, however the other cycle intermediates
incorporated about as much radioactivity as was found in the controls.
These data indicated that either a 2-fold excess of ricinine or a 40
mg/100 gm concentration of ethionine caused a definite inhibition in the
incorporation of label from quinolinic acid-6-^{14}C into ricinine, 6-fold
and 4-fold, respectively. The increase in the amount of label remain-
ing in quinolinic acid, 2-fold and 3-fold respectively, also indicated
an inhibition of the pyridine nucleotide cycle and again linked the
cycle to ricinine biosynthesis.

Wet combustion and gas counting was used to determine the amount of
label left in the residue of the plant extract. With these data a
total radioactivity determination was achieved. Table V shows the amount
of label in the residue of the plants from the various experiments and
the total radioactivity values.

The total radioactivity varied as shown in Table V; however, in all
cases greater than 50% of the administered label was recovered. In only
one case, the 11-hour azaserine experiments, did the total label closely
approach 100% recovery (96.1%). This was due mostly to a large amount
of the label found in the extract (83.5%), however, the amount of label
in the residue was also rather high (18.5%). No definite pattern in
the amounts of label present in the residue seem evident, except for a
2- to 3-fold increase in the label present in the residue from the 11-
hour azaserine- and azaleucine-treated plants. This was not found in
the 20-hour azaserine-treated plants but in the azaleucine-treated
plants at this same time period about a 2-fold increase was noted. In
the ricinine overloading and ethionine inhibition experiments a 4-fold

TABLE V

TOTAL RADIOACTIVITY ANALYSIS

Inhibitor		Radioactivity			
Experiment	Conc.	Extract	Residue	Ether Extract	Total
	mg/100 gm	%	%	%	%
Series A					
Control	–	53.3	6.5	–	59.8
Ricininic Acid	10	65.4	8.8	0.7	64.9
Azauracil	20	66.0	8.4	0.2	74.6
Alazopeptin	15	61.7	9.6	0.5	71.8
Azaleucine	20	70.6	6.7	0.3	77.6
Azaserine	20	68.6	10.6	0.3	79.5
Series B					
Control-11	–	54.1	7.2	0.6	61.9
Azaserine-11	45	77.5	18.5	0.1	96.1
Azaleucine-11	45	56.2	16.1	0.3	72.6
Control-20	–	45.3	7.6	0.5	53.4
Azaserine-20	75	57.0	7.9	0.6	65.5
Azaleucine-20	75	51.6	12.0	0.6	64.2
Series C					
Control	–	52.6	2.8	0.9	56.3
Ricinine	100	42.6	11.8	0.6	55.0
Ethionine	40	53.5	7.3	0.6	61.4

and 3-fold increase in residue label compared to control values was
found, respectively. The reasons for this increase are not clear,
however, a reasonable explanation could be that inhibition of ricinine
and the pyridine nucleotide cycle caused an increase in label incorpor-
ation into either metabolites or precursors, or both, of ricinine and
the pyridine nucleotide cycle intermediates, which are insoluble or
bound.

The ether extracts of the various plants extracted contained less
than 1% of the administered label and indicated that no metabolism of
pyridinium compounds resulting in the formation of ether soluble prod-
ucts occurred.

Although the results of these experiments have indicated an inter-
dependency of operation between ricinine biosynthesis and the pyridine
nucleotide cycle, the details concerning the order of intermediates in
ricinine biosynthesis have not been elucidated. The conflicting evi-
dence concerning which pyridine nucleotide cycle intermediate is the
most immediate precursor of ricinine may best be explained by a more
complicated relationship between the cycle intermediates and ricinine
biosynthesis. Such a relationship is expressed by a metabolic grid,
which is defined as a series of parallel reactions in which analagous
transformations occur, but at different rates; thus a compound may be
transformed to a product by several different parallel pathways (49).
A similar type of metabolic grid was proposed by Waller and Nowacki con-
cerning the conversion pathways of quinolizidine alkaloids (50). The
metabolic grid shown in Figure 15 shows a series of possible inter-
relationships which help explain the known results. Quinolinic acid
(A1) has been shown to be converted directly to nicotinic acid
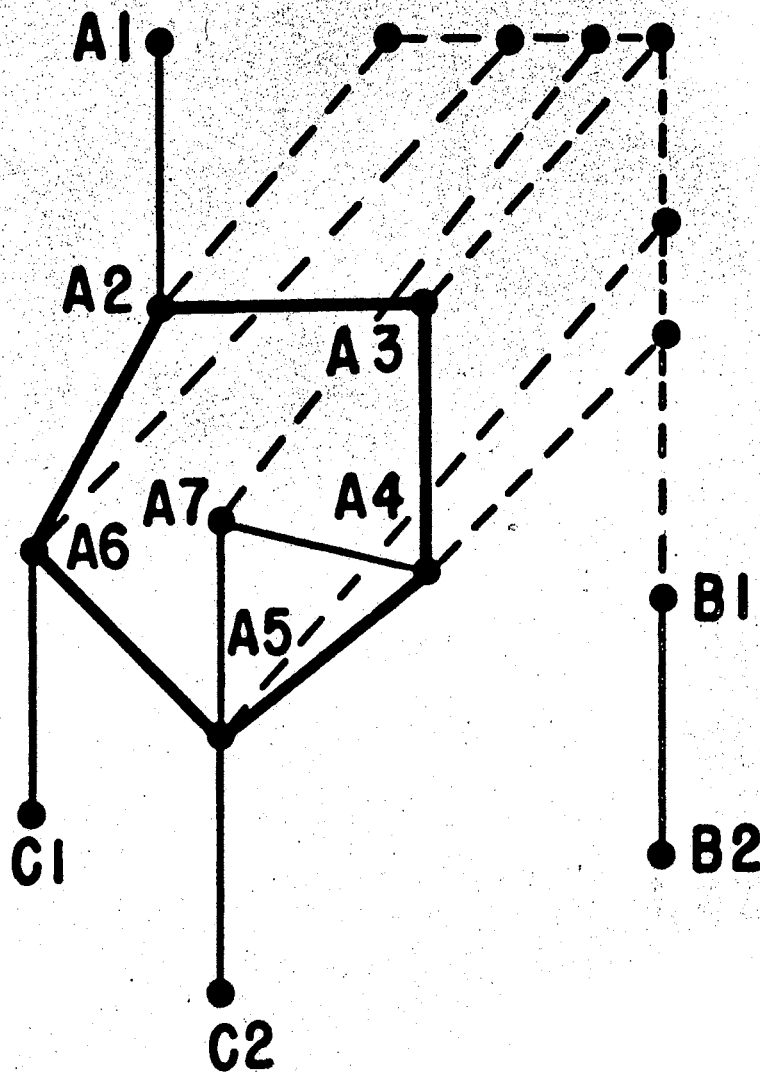
Figure 15. Proposed Metabolic Grid for
Ricinine Biosynthesis.
A1 = Quinolinic acid
A2 = Nicotinic acid mono-
nucleotide
A3 = Nicotinic acid
adenine dinucleotide
A4 = Nicotinamide adenine
dinucleotide
A5 = Nicotinamide
A6 = Nicotinic acid
A7 = Nicotinamide mono-
nucleotide
B1 = N-demethyl ricinine
B2 = Ricinine
C1 = N-methyl nicotinic
acid
C2 = N-methyl nicotinamide
_____ Pyridine Nucleotide Cycle
---- Postulated Reactions

mononucleotide (A2) and also converted indirectly to ricinine (B2),

through the cycle (2). It has been postulated that quinolinic acid can

also be converted to ricinine independent of the cycle (5). However,

the results previously presented have shown that inhibition of the

cycle was accompanied by inhibition of the biosynthesis of ricinine,

thus the main pathway for ricinine formation was probably through the

cycle. All of the cycle intermediates were proven to be precursors of

ricinine but the incorporation of radioactivity from these intermediates

into ricinine and isotope dilution values for these conversions were

similar and did not indicate which of these intermediates was the most

immediate precursor (2). The proposed metabolic grid, shown in Figure

15, explains these results by postulating that all of these intermedi-

ates may be incorporated into the biosynthetic pathway of ricinine dir-

ectly. This would explain the similarity of radioisotope incorporation

and isotope dilution data of all of these intermediates. The results

of Hiles and Byerrum (5) which indicated that a large excess (10-fold)

of NAD added to castor bean plants caused an increase in the incorpora-

tion of label into ricinine from quinolinic acid-^{14}C rather than the

expected decrease, do not have to be interpreted as proof of a separate

route of ricinine biosynthesis independent of the cycle, but can be

explained by the metabolic grid concept. If NaMN (A2) and desNAD (A3)

can enter the biosynthetic pathway of ricinine without conversion to

NAD (A4) then blockage of the cycle by excess NAD would not necessarily

block synthesis of ricinine from QA (A1) but could cause an increase

due to an increase in the amount of QA (A1) diverted to ricinine (B2).

In terms of the metabolic grid, if the pathway QA (A1) to NaMN (A2) to

desNAD (A3) to NAD (A4) were blocked at the desNAD to NAD (A3 to A4)

step, then label from QA (A1) would be diverted into the alternate
pathways QA (A1) to NaMN (A2) to NDR (B1) to ricinine (B2) and QA (A1)
to NaMN (A2) to desNAD (A3) to NDR (B1) to ricinine (B2). Despite evi-
dence to the contrary the possibility remains that QA (A1) could be
incorporated into ricinine (B2) without going through the cycle, but
this pathway is certainly not necessary to explain the data of Hiles and
Byerrum. The NMN (A7) shuttle in which NAD (A4) can either be conver-
ted directly to Nam (A5) or shuttled through NMN (A7) and then to Nam
(A5) was postulated to be present in barley (30) and may be present in
Ricinus communis. Previous work has indicated that the carbon-14 to
nitrogen-15 ratio in the nitrile group of ricinine remained the same as
the ratio in the carboxamide group of the administered nicotinamide
(19). This indicated that nicotinamide was converted to ricinine with-
out any deamidation occurring. This metabolic grid also accounts for
these data. The metabolic grid concept permits more than one, in fact
probably all, cycle intermediates to enter the ricinine biosynthetic
pathway, and inhibition of the cycle at one point may slow but will not
stop the conversion of QA to ricinine. The exception to this may be
the QA to NaMN conversion, which, if blocked, could cause a drastic
decrease in QA conversion to ricinine, provided that there is no path-
way from QA to ricinine independent of the cycle. The results with
the inhibitor azaleucine indicated that there was probably little
liklihood of the existence of an independent pathway, thus it may be
concluded that total inhibition of QA decarboxylase should cause total
inhibition of incorporation of labeled quinolinic acid into ricinine.

D. NADP-Carbonyl-^{14}C as a Precursor

The procedure for the NADP-carbonyl-^{14}C experiments was the same as described previously. Duplicate control plants were injected with 1 µCi of NADP-carbonyl-^{14}C; duplicate plants were injected first with 45 mg/ 100 gm of azaserine or azaleucine then, one hour later, one µCi of NADP-carbonyl-^{14}C. The plants were allowed to metabolize for 20 hours and were then analyzed by methods described previously. These results from this experiment indicated that there was little effect of the inhibitors on either ricinine biosynthesis or the pyridine nucleotide cycle. Table VI shows the effect of inhibitors on the biosynthesis of ricinine from NADP-carbonyl-^{14}C. The effect was negligible since the incorporation into ricinine varied only from 7.6% in the controls to 9.3% in the aza-serine-treated plants to 6.5% in the azaleucine-treated plants. The amount of ricinine in the plants remained constant. There seemed to be no noticeable effect of the inhibitors upon the incorporation of label from NADP-carbonyl-^{14}C into ricinine. Specific activities and isotope dilution values for ricinine were also very similar and verified the incorporation data. Table VII shows the effect of inhibitors on the distribution of radioactivity in the pyridine nucleotide cycle inter-mediates. The radioactivity present in nicotinic acid (VA), des-NAD (VI) and unreacted NADP was expressed as one value because of a lack of separation of these components on Dowex 1 x 8 formate column chromatog-raphy. There were no large differences in label incorporation into the cycle intermediates with respect to control and inhibitor-treated plants. However, in the azaleucine-treated plants there was a small reduction in the amount of label incorporated into peak II. This amounted to a 32% decrease, however, the data in these experiments were

TABLE VI

INHIBITOR EFFECTS ON THE BIOSYNTHESIS
OF RICININE FROM NADP–CARBONYL–^{14}C

One µCi of NADP–carbonyl–^{14}C (specific activity of 26.2 µCi/µmole) was administered as a precursor.

Inhibitors		Duration	Ricinine			Isotope Dilution
Experiment	Conc.		Conc.	Incorp.	Sp. Act.	
	$\dfrac{mg}{100gm}$	hours	µmoles/gm	%	$\dfrac{mµCi}{µmole}$	
I						
Control	–	20	4.0	7.8	0.36	55,556
Azaserine	75	20	3.6	9.3	0.44	45,455
Azaleucine	75	20	3.8	6.5	0.35	57,143

TABLE VII

INHIBITOR EFFECTS ON THE DISTRIBUTION OF
RADIOACTIVITY IN THE PYRIDINE NUCLEOTIDE
CYCLE FROM NADP-CARBONYL-^{14}C

One μCi of NADP-carbonyl-^{14}C (specific activity of 26.2 μCi/μmole)
was administered as a precursor.

II = a mixture of N-methyl nicotinic acid and N-methyl nicotina-
     mide
VA = nicotinic acid
VI = des-NAD
N-Amide = nicotinamide

Inhibitors	Conc.	Distribution of Radioactivity			
		II	N-Amide	NAD	VA + VI + NADP
	mg/100 gm	%	%	%	%
Control	-	32.7	3.8	6.0	13.2
Azaserine	75	36.1	3.8	2.2	7.5
Azaleucine	75	22.3	6.2	5.8	4.9

more variable than the data for the quinolinic acid-6-^{14}C because of the smaller number of plants subjected to the same conditions. A 2- to 3-fold decrease in the peak containing nicotinic acid, desamido-NAD and NADP was found in the azaleucine-treated plants, but no data on the amounts of label in each of these three components was obtained. In the azaserine-treated plants, a 3-fold reduction in the label incorporated into NAD was found. Since azaserine blocks the desNAD to NAD step in the cycle and since labeled NADP is converted directly to labeled NAD by the action of phosphatases present in the plant, one might expect an increase in the label present in NAD, instead of the decrease found. However, in a long term experiment (20 hours) such as this, label was probably shunted out of the cycle into the storage forms, N-methyl nicotinic acid, and N-methyl nicotinamide and ricinine; consequently label would not be cycled back into NAD through the cycle due to blockage by azaserine. Other than these changes, the inhibitors seemed to have little effect on the cycle or on ricinine biosynthesis.

A SELECTED BIBLIOGRAPHY

(1) Leete, E. and Leitz, F. H. B., Chem. and Ind. (London), 1572 (1957).

(2) Waller, G. R., Yang, K. S., Gholson, R. K., Hadwiger, A. L. and Chaykin, S., J. Biol. Chem., 241, 441 (1966).

(3) Waller, G. R. and Yang, K. S., Phytochem., 4, 881 (1965).

(4) Frost, G. M., Yang, K. S. and Waller, G. R., J. Biol. Chem., 242, 887 (1967).

(5) Hiles, R. A. and Byerrum, R. U., Phytochem., 8, 1927 (1969).

(6) Tuson, R. V., J. Chem. Soc., 17, 195 (1964).

(7) Maqueune, L. and Phillippe, L., Compt. Rend., 139, 840 (1904).

(8) Manske, R. H. F. and Holmes, H. L., The Alkaloids, Vol. I, Academic Press, Inc., New York, 1950, p. 206.

(9) Skursky, L., Burleson, D. and Waller, G. R., J. Biol. Chem., 244, 3228 (1969).

(10) Dubeck, M. and Kirkwood, S., J. Biol. Chem., 199, 307 (1952).

(11) Waller, G. R. and Henderson, L. M., Biochem. Biophys. Res. Commun., 5, 5 (1961).

(12) Juby, P. F. and Marion, L., Biochem. Biophys. Res. Commun., 5, 461 (1961).

(13) Essery, J., Juby, P. F., Marion, L. and Trumbull, E., J. Amer. Chem. Soc., 84, 4597 (1962).

(14) Essery, J., Juby, P. F., Marion, L. and Trumbull, E., Can. J. Chem., 41, 1142 (1963).

(15) Chandler, J. L. and Gholson, R. K., Biochim. Biophys. Acta (in press).

(16) Suzuki, N. and Gholson, R. K., (unpublished results).

(17) Hadwiger, L. A. and Waller, G. R., Plant Physiol., 39, 244 (1964).

(18) Waller, G. R. and Nakazawa, K., Plant Physiol., 28, 318 (1963).

(19) Waller, G. R. and Henderson, L. M., J. Biol. Chem., 236, 1186
        (1961).

(20) Hadwiger, L. A., Badiei, S. E., Waller, G. R. and Gholson, R. K.,
        Biochem. Biophys. Res. Commun., 13, 466 (1963).

(21) Andreoli, A. J., Ikeda, M., Nishizuka, Y. and Hayaishi, O., Biochem.
        Biophys. Res. Commun., 12, 92 (1963).

(22) Packman, P. M. and Jacoby, W. B., Biochem. Biophys. Res. Commun.,
        18, 710 (1965).

(23) Nishizuka, Y. and Hayaishi, O., J. Biol. Chem., 238, PC483 (1963).

(24) Gholson, R. K., Ueda, I., Ogasawara, N. and Henderson, L. M., J.
        Biol. Chem., 239, 1208 (1964).

(25) Joshi, J. G. and Handler, P., J. Biol. Chem., 237, 929 (1962).

(26) Preiss, J. and Handler, P., J. Biol. Chem., 233, 488, 493 (1958).

(27) Sarma, D. S. R., Rajalakshmi, S. and Sarma, P. S., Biochem. Bio-
        phys. Res. Commun., 6, 389 (1961).

(28) Gholson, R. K., Nature, 212, 934 (1966).

(29) Keller, J., Liersch, M. and Grunicke, H., Eur. J. Biochem., 22,
        263 (1971).

(30) Ryrie, I. J. and Scott, K. J., Biochem. J., 115, 679 (1969).

(31) Levenberg, B., Melnick, I. and Buchanan, J. M., J. Biol. Chem.,
        225, 163 (1957).

(32) Langan, T. A., Jr., Kaplan, N. O. and Shuster, L., J. Biol. Chem.,
        234, 2161 (1959).

(33) Priess, J. and Handler, P., J. Amer. Chem. Soc., 79, 4246 (1957).

(34) Priess, J. and Handler, P., J. Biol. Chem., 233, 488 (1958)

(35) Narrod, S. A., Bonavita, V., Ehrenfeld, E. R. and Kaplan, N. D.,
        J. Biol. Chem., 236, 931 (1961).

(36) Slater, T. F. and Sawer, B. C., Biochem. Pharmacol., 15, 1267
        (1966).

(37) Bonasera, N., Magione, G. and Bonavita, V., Biochem. Pharmacol.,
        12, 633 (1963).

(38) Greenlees, J. and LePage, G. A., Cancer Res., 16, 808 (1956).

(39) Barclay, R. K. and Phillips, M. A., Cancer Res., 26, 282 (1966).

(40) Jacquez, J. A. and Sherman, J. H., *Cancer Res.*, 22, 56 (1962).

(41) Reilly, H. C., *Ciba Foundation Symposium on Amino Acids and Peptides with Antimetabolic Activity*, J. and A. Churchill, Ltd., 1958, p. 62.

(42) Smith, S. S., Bayliss, N. L. and McCord, T. J., *Arch. Biochem. Biophys.*, 102(2), 313 (1963).

(43) Argoudelis, H. D., Herr, R. R., Mason, D. J., Pyke, T. R. and Zieserl, J. F., *Biochemistry*, 6(1), 165 (1967).

(44) Hartman, S. C., *J. Biol. Chem.*, 238, 3036 (1963).

(45) Peterson, E. L., Johnson, B. L., DeVoe, S. E. and Bohonos, N., *Antimicrobial. Agents Chemotherapy*, 115 (1965).

(46) Ross, C. W., *Biochim. Biophys. Acta*, 87(4), 564 (1964).

(47) Purko, J. and Stewart, H. B., *Can. J. Biochem.*, 45, 179 (1967).

(48) Nowacki, E. and Waller, G. R., *Abh. Deutch, Acad. Wiss. Berlin*, 00,000 (1971).

(49) Bray, G. A., *Anal. Biochem.*, 1, 127 (1960).

(50) Bu'Lock, J. D., *The Biosynthesis of Natural Products*, McGraw-Hill Publishing Co., New York, 1965, p. 81-82.

(51) Nowacki, E. and Waller, G. R., personal communication.

PART TWO

BIOCHEMISTRY OF METHYLCYCLOPENTANE MONOTERPENOIDS

CHAPTER V

INTRODUCTION

The biosynthesis of the methylcyclopentane ring system in higher plants has been the subject of a number of studies using various carbon-14 labeled precursors including acetate, mevalonate, geranylpyrophosphate and carbon dioxide. However, the part of the biosynthetic route leading to cyclization of either the five- or six-membered ring is unknown.

Of particular interest in this study were the methylcyclopentane monoterpenoid feline attractants, which are nepetalactone, produced by Nepeta cataria, actinidine, iridomyrmecin and isoiridomyrmecin, produced by Actinidia polygama and actinidine and two actinidine-like alkaloids produced by Valeriana officinalis. The biosynthesis of nepetalactone, iridomyrmecin, isoiridomyrmecin and actinidine have been postulated to involve iridodiol (nepetadiol), iridodial or perhaps a pyrophosphorylated intermediate (65,73).

The main objectives of this research were: (a) to develop a rapid and efficient synthesis of carbon-14 labeled iridodiol (nepetadiol) and carbon-14 labeled dihydronepetalactone and (b) to test these compounds as possible precursors of nepetalactone and epinepetalactone in Nepeta cataria, in order to gain some insight into the metabolism of these compounds.

The synthesis of ^{14}C-labeled nepetadiol and ^{14}C-labeled dihydro-nepetalactone was undertaken and upon completion the metabolism of these compounds in Nepeta cataria was investigated.

CHAPTER VI

LITERATURE REVIEW

A. Structure and Occurrence

1. Simple Iridoids

According to their structure some 80 natural products have been

classified as methylcyclopentane monoterpenoids (simple iridoids), true

iridoids or seco-iridoids (1). Of particular interest were the simple

iridoids or methylcyclopentane monoterpenoids. All have two methyl

groups, one in position 4, the other in position 8. Figure 1 shows the

structures of a number of these iridoids (1).

Iridodiol (II), a group of isomeric dialcohols, were isolated from

the galls of Actinidia polygama and synthesized by Sakan, et al. (2).

They were also synthesized and separated by gas chromatography by

Regnier, et al. (15).

Iridodial (III), a dialdehyde isolated from insects such as the

Australian ants species, Iridomyrmex detectus and Iridomyrmex conifer

(3), was also isolated from several Dolichoderus and other Iridomyrmex

species (4) and Tapinomia nigerrimum (5). Cavill, et al. determined

the structure of iridodial (3) while Clark, et al. synthesized iridodial

from citronellal (6).

The dialdehyde, dolichodial (IV), was isolated from Dolichoderus

acanthoclinea clarki and related species by Cavill, et al. (4), who

also determined its structure. Anisomorphal, an epimer of dolichodial,
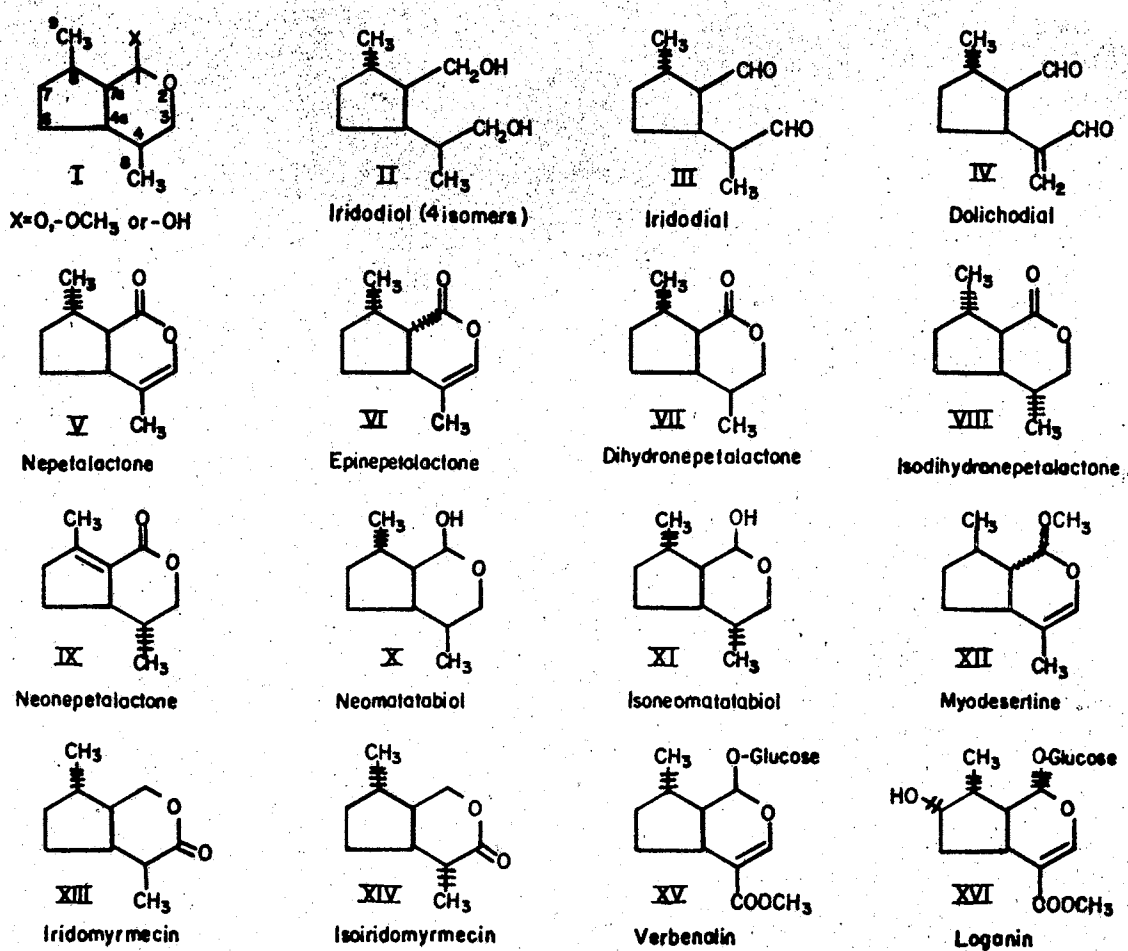
Figure 1. Methylcyclopentane Monoterpenoids.

was isolated from Anisomorpha buprestoides (7) and synthesized by Cavill

and Whitfield in 1964 (8).

Nepetalactone (V) was first isolated from the steam-volatile oil of

Nepeta cataria L. by McElvain, et al. (9). It was shown to be the cis-

trans isomer, and in much greater abundance in Nepeta cataria L. than

the trans-cis isomer, which was designated as epinepetalactone (VI) or

isonepetalactone (10,11,12,13). Nepetalactone was also isolated from

Nepeta hindostana, Nepeta citriodora and Nepeta mussini (14,15) while

epinepetalactone (trans-cis) was found in Nepeta cataria, Nepeta

citriodora and Nepeta mussini (15,19). McGurk later found that cis-cis

nepetalactone was the major isomer present in N. mussini rather than

the trans-cis isomer (13), however, he found no cis-cis nepetalactone

in N. cataria. The configuration of nepetalactone was determined by

Bates, et al. (11), while Sakan, et al. were able to synthesize DL-

nepetalactone (17) and Trave et al. and McGurk synthesized the nepetal-

actone stereoisomers (13,18).

Dihydronepetalactone (VII), isodihydronepetalactone (VIII) and neo-

nepetalactone (IX) were isolated from the leaves and galls of Actinidia

polygama (12). VII and VIII were also found in Nepeta cataria (12).

Isodihydronepetalactone (VIII) was found in the secretions from the anal

glands of Iridomyrmex nitidus (20). The structures of these compounds

were determined by Sakan, et al. (13) and were later synthesized by

Wolinsky and Nelson (21).

Neomatatabiol (X) and isoneomatatabiol (XI) were isolated from

Actinidia polygama by Hyeon, et al. (22). Neomatatabiol was shown to

be derived from dihydronepetalactone by reduction; isoneomatatabiol was

shown to be derived from isodihydronepetalactone by reduction.

Myodesertine (XII) was isolated from <u>Myoporum</u> <u>deserti</u>, by Sutherland and Park (23).

Iridomyrmecin (XIII) and isoiridomyrmecin (XIV) were isolated from the leaves and galls of <u>Actinidia</u> <u>polygama</u> by Sakan, <u>et</u> <u>al</u>. (24) and designated matatabilactone. These isomers were separated and identified by Murai (25). Iridomyrmecin was isolated from the ant, <u>Iridomyrmex</u> <u>humilis</u> (3,26). Isoiridomyrmecin was found in various colonies of <u>Dolichoderus</u> and <u>Iridomyrmex</u> species, where it accompanied iridodial and dolichodial (4). It was also found in the secretion of the anal glands of <u>Iridomyrmex</u> <u>nitidus</u> (20). Minato (26) determined the absolute configuration. Clark, <u>et</u> <u>al</u>. (6) synthesized isoiridomyrmecin from citronellal via iridodial.

2. Monoterpenoid Alkaloids

The following compounds may be considered as nitrogen derivatives of 1,2-dimethyl-3-isopropyl-cyclopentane (1). The similarity of the structures of iridoids and the methylcyclopentane monoterpene alkaloids suggest a common biogenetic relationship, especially since they have been found in the same botanical families (1). Figure 2 shows the structures of the methylcyclopentane monoterpenoid alkaloids.

Alkaloid RW47 (XVII) was isolated by Arthur, <u>et</u> <u>al</u>. from <u>Rauwolfia</u> <u>verticillata</u> Bail., where it coexists with several indole alkaloids (28). It was shown to be monoterpenoid in origin and related to the actinidine group (28). It was shown to be a C_9 alkaloid and thus classified as a degenerate monoterpenoid.

Actinidine (XVIII) was isolated by Sakan, <u>et</u> <u>al</u>. from <u>Actinidia</u> <u>polygama</u> (24). It was synthesized by Sakan, <u>et</u> <u>al</u>. (29) and its absolute structure elucidated by Sakan, <u>et</u> <u>al</u>. (30). Actinidine has also been

XVIII : R=CH₃ **Actinidine**
XIX : R=CH₂OH **Tecostidine**
XX : R=CH₂OCH₃ **8-Methoxyactinidine**

XXI : R=H **4-Noractinidine**
XXII : R=CHO **Indicain**
XXIII : R=COOH **Plantagonin**

XVII
RW 47

XXV : R=H **Venoterpin**
XXVI : R=COOCH₃ **Jasminum-Alkaloid**

XXIV
Boschniakin

XXVII **Tecostanine**
XXVIII **Tecomanine**
XXIX **Skytanthine** (3 isomers)

XXX **Hydroxyskytanthine I**
XXXI **Hydroxyskytanthine II**
XXXII **Dehydroskytanthine**

XXXIII : R=CH₃
XXXIV : R=CH₂OH

Valeriana Alkaloids

Figure 2. Methylcyclopentane Monoterpenoid Alkaloids.

isolated from Valeriana officinalis by Gross, et al. (31) and also by Johnson, et al. (32). 8-Methoxyactinidine (XX) was isolated from Valeriana officinalis by Franck (33) while boschniakin (XXIV) was isolated from Bosschniakia rossica by Sakat, et al. (34). Plantagonin (XXIII) and indicain (XXII) were isolated from Plantago indica L., Pedicularis olgae Rgl. and P. dolichorrhiza S. (35-41), while 4-noractinidine (XXI) was isolated from Tecoma stans by Dickinson and Jones (42). Venoterpin (XX) has been isolated from Rawolfia verticillata Bail. by Arthur, et al. (42,43), and from Alstonia venenata by Roy, et al. (45) and by Hart, et al. (46), while the Jasminum-alkaloid (XXVI) was isolated from a new Jasminum species by Hart, et al. (46).

Tecostidine, (XIX) tecostanine (XXVII) and tecomanine (XXVIII) have been isolated from Tecoma stans Juss. and their structures elucidated by Hammouda, et al. (47-50).

Skytanthine (XXIX) has been isolated from Skytanthus actus Meyen by three independent groups (51-53) and its structure established by Djerassi, et al., using catalytic dehydrogenation yielding actinidine (51). Skytanthine exists in three isomeric forms (54). Hydroxyskytan-thines I (XXX), hydroxyskytanthine II (XXI) and dehydroskytanthine (XXXII) were also isolated from this plant (54,55).

Two quarternary substituted alkaloids (XXXIII, XXXIV) were isolated from Valeriana officinalis L. by Torsell and Wahlberg (56,57). The quarternary substituent was shown by these authors to be a p-hydroxy-phenethyl group.

B. Biological Activity

Unlike most monoterpenoids, the methylcyclopentane monoterpenoids are physiologically active in a number of organisms. Their varied and

somewhat exotic biological activities have caused a surge of interest in these compounds.

Nepetalactone has been known for years to be a powerful feline attractant. Todd has postulated that nepetalactone imitates a feline pheromone which cuases courtship displays (58). Evidence to support this hypothesis was as follows:

1. The catnip responses and courtship were very similar.

2. Field observations indicated that catnip-like displays occur at sites known to have been marked by the urine of tomcats.

3. Catnip-like activity was found in ether extracts of tomcat urine.

4. Cross fatigue of the catnip response and the courtship display appeared to occur.

5. The "central neural substrate" of the catnip response and courtship behavior appeared to be intimately related.

6. Mounting activity of two male snow leopards was provided by catnip responses of two females.

7. There was no correlation between the distribution of plants having catnip-like activity and that of cats which were sensitive to them.

8. There was a striking difference in response to catnip between lions and tigers which may be due to the unknown mechanism which reproductively isolated these two species in nature (but not in captivity).

Nepetalactone has also been shown to be an insect repellant (59). The lactones iridomyrmecin, dihydronepetalactone, isodihydronepetalactone and neonepetalactone also have feline attracting capabilities (12).

Neomatobiol from <u>Actinidia</u> <u>polygama</u> was shown to attract the adult male lacewing (<u>Chrysopa septempunctata</u>) (22), while iridodiols isolated from this plant also had a similar biological activity (2). The antibiotic activity of iridomyrmecin was determined (26), and D-(+)-isoiridomyrmecin was shown to inhibit the growth of <u>Rhizopus</u>, <u>Pennicillum</u> and <u>Aspergillus</u>, but not <u>Staphylococcus</u> or <u>Pseudomonas</u> (60). Other results have indicated that the iridomyrmecins have canine attracting capabilities and are involved in arthropod defense (61,62). Iridodial was found to be involved in arthropod defense also (61).

The skytanthine alkaloids were found to possess feline attracting capabilities, the ability to stimulate the learning capacity of rats (63,64) and to act as an antidiabetic (62).

Actinidine was demonstrated to be a potent feline attractnat (2, 24,30), while tecomanine and tecostanine were found to have antidiabetic effects (65).

C. Biosynthesis

The biosynthesis of the iridoids has been studied more frequently in recent years since they have provided a structural link between terpenes and alkaloids, two previously divergent classes of natural products (66).

One of the earlies reports on the biosynthesis of a methylcyclopentane monoterpenoid was on skytanthine (XXVII) (66,67,68), and a later report indicated that the N-methyl group of skytanthine originated from L-methionine (69). Mevalonate-2-^{14}C was also used as a precursor and label appeared in carbons 3,4,7 and 9 indicating a definite isoprenoid origin (69). It was found that randomization of label between

carbons 3 and 8 did not occur in 3 year old S. actus plants but did

occur in 1 year old plants (69). It was postulated that this phenomenon

was controlled by different levels of inhibitors and/or enzymes in the

young and old plants (69).

Using mevalonic acid-2-^{14}C as a precursor, it was determined that

a limited randomization of the carbon-14 found in carbons 3 and 8 and

also 6 and 9 of nepetalactone occurred (V) (70).

Actinidine (XVIII), isolated from Actinidia polygama, was shown to

be isoprenoid in origin (71). This finding was also of interest in the

field of alkaloid chemistry, since it represented the third pathway for

the biosynthesis of pyridine alkaloids in plants (66). Mevalonic acid-

2-^{14}C, acetate-2-^{14}C and geranyl pyrophosphate-1-^{14}C were all incorpor-

ated into actinidine with mevalonic acid-2-^{14}C showing the highest in-

corporation (71).

DL-Mevalonolactone-2-^{14}C was shown to be incorporated into

dolichodial (IV) in Anisomorpha buprestoides and into nepetalactone (V)

in Nepeta cataria (72).

Iridodial (III) was postulated to be the precursor of iridomyrmecin

(XIII) in Dolichoderus and Iridomyrmex (4). It has been suggested (73)

that citronellol, its aldehyde and iridodial could be biosynthetic in-

termediates between geraniol and loganin (XVI).

Verbenalin (XV), a methylcyclopentane monoterpenoid glucoside, was

shown to incorporate label from mevalonic acid-2-^{14}C in young Verbena

officinalis plants with randomization of label occurring between carbons

3 and 8 (75). Horodysky, et al. (76) showed that little randomization

of label occurred in XV produced by mature, flowering V. officinalis

plants. Further studies indicated that randomization of label between

carbons 3 and 8 occurs in young V. officinalis plants, decreased in intermediate aged plants and ceased in mature plants (76).

Some recent results have indicated that the main alkaloid (XXXIII) found in Valeriana officinalis, which is composed of an actinidine segment and a p-hydroxy phenethyl side chain, is derived from mevalonic acid and from tyrosine, respectively. Actinidine (XVIII) was also isolated from this plant and its origin is isoprenoid (31).

Several biogenetic schemes have been postulated concerning the methylcyclopentane monoterpenoids, however, only the most recent proposal, which incorporates the most recent biosynthetic data, will be discussed (66,74). This proposal is shown in Figure 3. Geranyl pyrophosphate (XXXV), because of its biological reactivity and its widespread occurrence was considered to be a likely intermediate for the stepwise cyclization to the proposed methylcyclopentane aldehydropyrophosphate (XXXIX), which was postulated to be the key biological intermediate in this scheme (66,74). From XXXIX, transamination to XXXX could occur, followed by cyclization to XLI. By dehydration of XLI, the dihydro-actinidines (XLIIa, XLIIb, XLIIc) could be formed and direct oxidation could form actinidine (XVIII) or by oxidation and hydroxylation tecostidine (XIX) could be formed. From the dihydroactinidines, skytanthine (XXIX) (3 isomers), hydroxy skytanthine (XXXI), tecomanine (XXVIII), dehydroskytanthine (XXXII) and tecostamine (XXVII) could be formed by various hydroxylations, reductions and methylations (66,74).

From XXXIX, reduction to XLV could occur and removal of pyrophosphate could result in XLVI which could be oxidized to iridodial (III) or reduced to iridodiol (II) through the semialdehyde XLVI. From XLVI, III and XLVII, cyclization and oxidation could form iridomyrmecin (XIII),
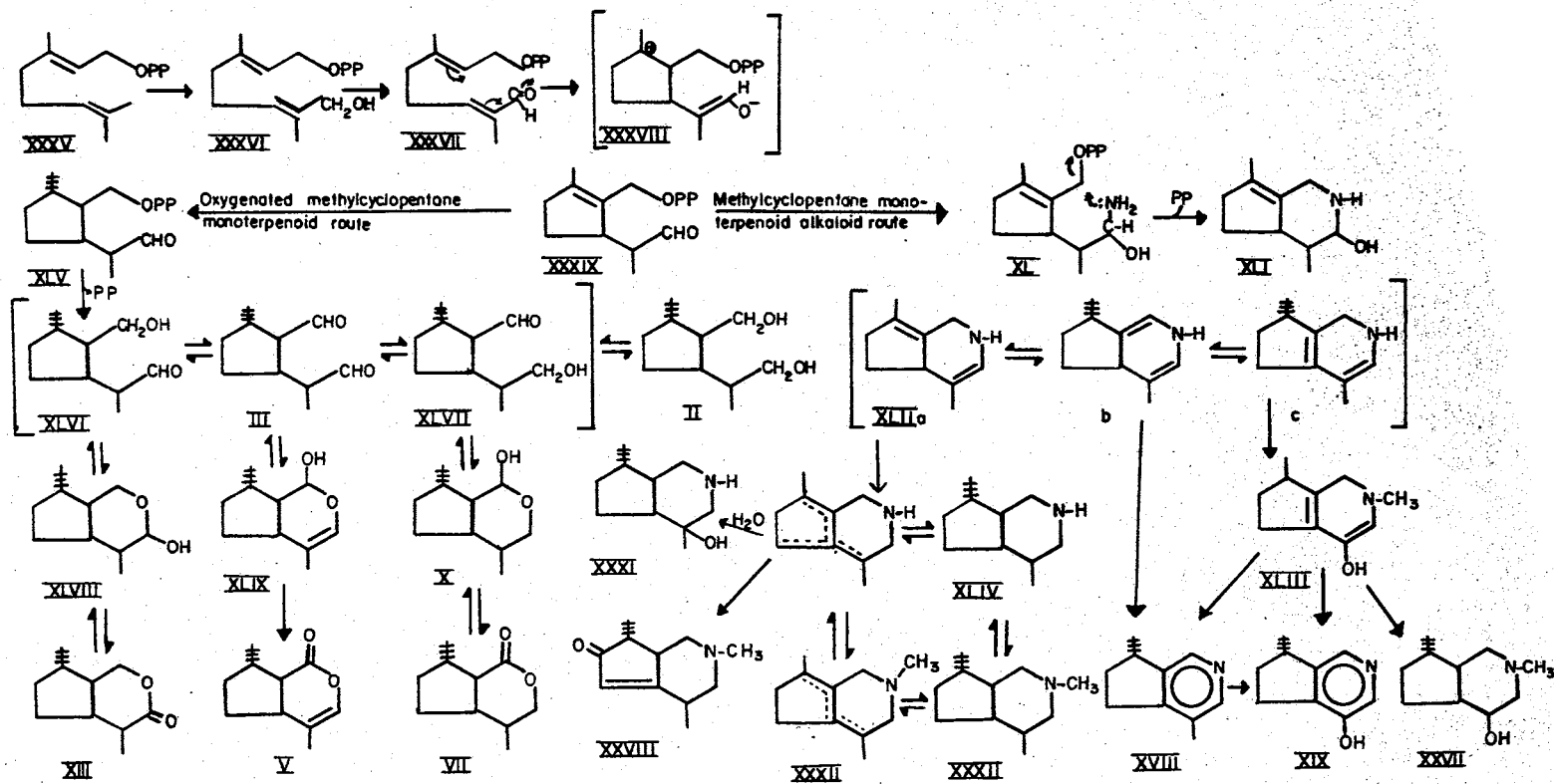
Figure 3. Biogenesis of the Methylcyclopentane Monoterpenoids.

nepetalactone (V) and dihydronepetalactone (VII), respectively (66, 74).

This hypothesis provides for the formation of almost all methyl cyclopentane monoterpenoids which vary at carbons 4a and 7a (66,74).

Other biogenetic schemes and similar pertinent information can be found in references 1, 77 and 78.

CHAPTER VII

EXPERIMENTAL METHODS

A. Materials and Chemicals Used

1. Plants

Nepeta cataria L. plants were grown in vermiculite-soil mixtures
in the horticulture greenhouse at Oklahoma State University in the fall
of 1971. The plants were propagated from cuttings and were approximately
eight to twelve weeks old when the experiments were initiated.

Valeriana officinalis and Actinidia polygama Miq. plants were
grown in vermiculite-soil mixtures in the horticulture greenhouse. V.
officinalis roots were obtained as a gift from Dr. C. F. Van Sumere,
Laboratorium voor Plantenbiochemie, Gent, Belgium. A. polygama plants
were originally obtained from Japan and propagated by cuttings.

2. Radioactive Compounds

Barium carbonate-^{14}C (specific activity of 50.2 mCi/mmole) was
purchased from Amersham/Searle Corporation, Arlington Heights, Illinois.
It was used without further purification.

3. Chemical Reagents

Solvents and chemical reagents were of analytical reagent grade
unless otherwise specified.

Silica gel G and silica gel HF were purchased from Brinkmann In-
struments, Westbury, New York. Commercially prepared analytical and

preparative silica gel HF plates were purchased from Brinkmann Instruments, Westbury, New York and Analtech, Inc., Newark, Delaware.

Palladium on charcoal, a hydrogenation catalyst, was purchased from Matheson, Coleman and Bell, Norwood, Ohio. Lithium aluminum hydride was purchased from K and K Laboratories, Hollywood, California.

Gas chromatography column packing material was purchased from Analabs, Inc., Hamden, Connecticut.

B. Methods

1. Preparation of Nepetalactone-G-^{14}C

$^{14}CO_2$ Incorporation Into Nepetalactone: Nepetalactone-G-^{14}C was prepared by allowing young Nepeta cataria plants to photosynthesize in the presence of 1 mCi of $^{14}CO_2$ for 36 hours. Figure 4 shows a diagram of the photosynthetic chamber used in this preparation. Two Nepeta cataria plants were placed in the chamber, and the top replaced and sealed with high vacuum grease. One millicurie (2.3 mg) of Ba$^{14}CO_3$ was then placed in the sidearm tube and the tube placed in the 29/42 joint and sealed with vacuum grease. The vacuum pump was turned on and a considerable portion of the atmosphere was removed. Stopcock A was then closed and 2 ml of 6 X H_2SO_4 was injected with a syringe through the serum cap and onto the Ba$^{14}CO_3$. A bunsen burner was then used to complete the liberation of $^{14}CO_2$ from the Ba$^{14}CO_3$, leaving BaSO$_4$ in the sidearm. Air was allowed to flow back into the partially evacuated chamber until the pressure on the inside was just slightly less than atmospheric pressure. A bank of Gro-Lux fluorescent lights were used to provide a light source and the plants were allowed to photosynthesize. At the end of 36 hours, the vacuum pump was turned on, stopcock

A - Count Rate Meter

B - Recorder

Geiger-Müller Tube

Serum Cap

$\mathbf{S}$ 29/42

Ba^{14}CO$_3$

Stopcock A

Vacuum →
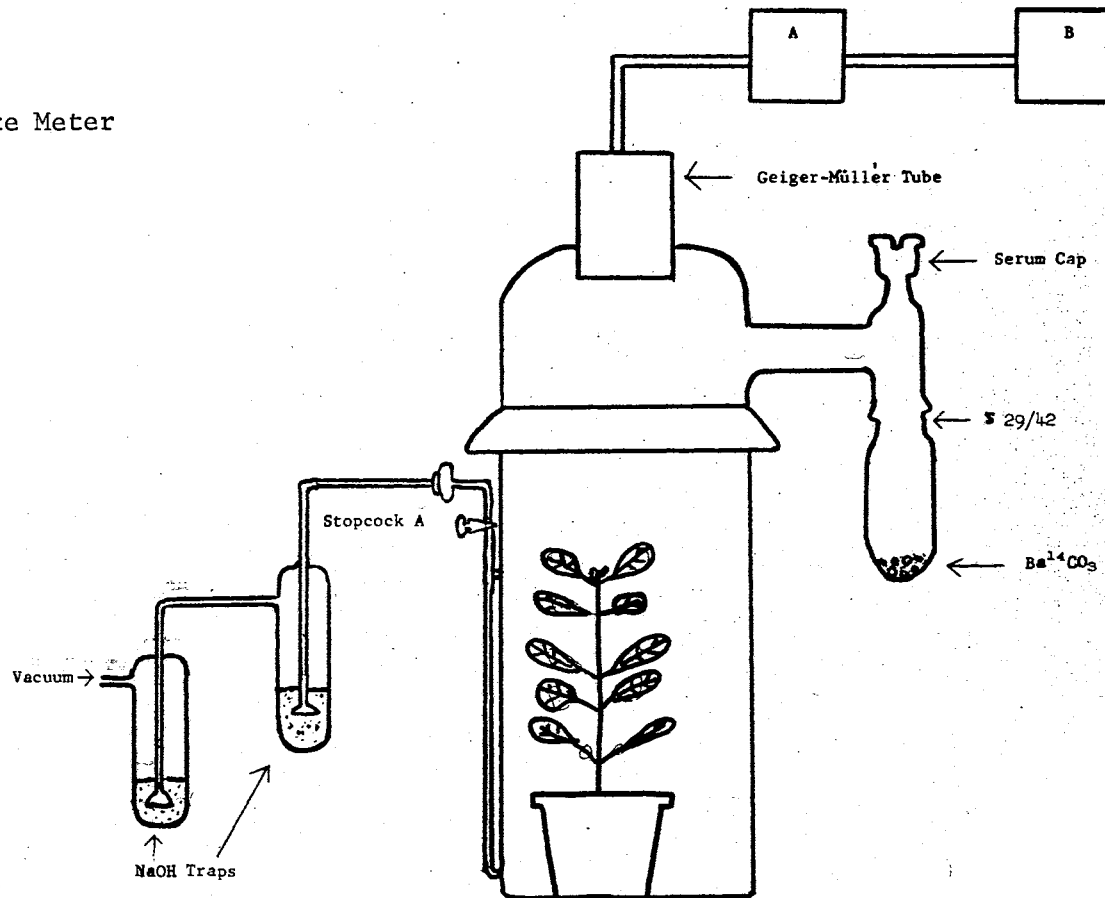
NaOH Traps

Figure 4. Photosynthesis Chamber

A opened, and the system was evacuated through the NaOH traps to trap any remaining $^{14}CO_2$ as $NaCO_3$.

Isolation and Purification of Nepetalactone-G-^{14}C: The plants were removed and cut into small pieces with scissors and homogenized in a Waring blender with 500 ml of deionized water. This homogenate was steam distilled and 500 ml of steam distillate collected. The steam distillate was saturated with NaCl and extracted 4 times with 200 ml of diethyl ether each time. The combined ether extract was dried over anhydrous Na_2SO_4 and reduced under N_2 to near dryness. The concentrated ether extract was then streaked on two preparative thin layer plates and developed in hexane : acetone : ethanol (40 : 10 : 4, v/v/v). The nepetalactone bands were scraped from the plates, eluted from the silica gel HF with diethyl ether, filtered, dried, weighed and stored in a vial in 2 ml of ether.

2. Hydrogenation of Nepetalactone-G-^{14}C

Amounts of nepetalactone-G-^{14}C from 50 mg to 420 mg were subjected to catalytic hydrogenation to produce dihydronepetalactone-G-^{14}C. The labeled nepetalactone was placed in a thick-walled (3 mm) glass hydrogenation vessel with 25 to 175 mg of palladium on charcoal (10%) and 30 ml of dry ethanol. The vessel was then wrapped in a heating tape and placed on a Parr Pressure Reaction Apparatus. The system was flushed with hydrogen gas repeatedly and then pressurized at 4.5 atmospheres. The heating tape rheostat was adjusted so that the temperature remained between 45°C and 60°C. The shaker was turned on and the reaction allowed to proceed for 36 hours. The resulting reaction mixture was analyzed by thin-layer and gas chromatography, mass spectrometry and liquid scintillation counting.

3. Lithium Aluminum Hydride Reduction of Dihydronepetalactone-G-^{14}C

Amounts of purified dihydronepetalactone-G-^{14}C from 25 to 350 mg were dissolved in 2 to 3 ml of diethyl ether. From 50 to 250 mg of powdered LiAlH$_4$ was placed in a 50 ml two-necked micro distillation flask along with 15 to 25 ml of dry diethyl ether or dry tetrahydrofuran and a micro magnetic stirring bar. A reflux apparatus was set up using a micro condenser and a micro heating mantle. A magnetic stirrer was placed under the heating mantle to stir the reaction mixture. The ether solution containing the dihydronepetalactone-G-^{14}C was added dropwise to the stirred LiAlH$_4$ mixture either by a pasteur pipette or by a small separatory funnel. Upon completion of the slow dropwise addition of the reactant, the flask was sealed, and refluxed with stirring for three to five hours. Upon completion the mixture was removed from the flask and the excess LiAlH$_4$ converted to LiAl(OH)$_4$ with 0.01N HCl. The resulting reaction mixture was filtered through a fritted glass funnel (coarse porosity) and the filtrate dried over anhydrous Na$_2$SO$_4$ and then the solution filtered through a fritted glass funnel (fine porosity) and washed with ethanol. The filtrate was then evaporated, using a rotary evaporator, to dryness. The reduction product, nepetadiol-G-^{14}C was only slightly soluble in ether, and so was taken up in 1 to 2 ml of ethanol. This concentrated solution was subjected to analytical, and preparative gas chromatography, mass spectrometry and liquid scintillation counting.

4. Metabolic Studies

Administration of Labeled Compounds: Nepetadiol-G-^{14}C and dihydronepetalactone-G-^{14}C were administered into the plant stems by injection using a microsyringe.

Isolation of Metabolites From Plants Administered Labeled Compounds:

$\underline{N}$. $\underline{cataria}$ plants which had been injected with either nepetadiol-G-^{14}C

or dihydronepetalactone-G-^{14}C were steam distilled and the crude oil

isolated and analyzed by gas chromatography and mass spectrometry. A

number of major components were purified by preparative gas chromatog-

raphy. The purified metabolites were analyzed by liquid scintillation

spectrometry and their amounts estimated by analytical gas chromatography

using previously determined relative response factors for nepetalactone

and dihydronepetalactone. The residues from the steam distillations

of these plants were treated with 2N HCl at 100°C for 2 hours, then

steam distilled again and the analysis procedures repeated. The remain-

ing residue was analyzed by wet combustion and gas counting. In

nepetadiol-G-^{14}C biosynthesis experiment I, a methanol extraction was

conducted on the initial steam distillation residue. This extract was

analyzed by thin-layer chromatography as well as gas chromatography and

mass spectrometry.

5. Isolation of Actinidine from Actinidia Polygama Miq.

Actinidine was isolated from Actinidia polygama plants by homogen-

izing the plant material in a Waring blender in 200 ml of .01 N NaOH,

then thoroughly steam distilling this homogenate until 400 to 700 ml of

distillate was collected. This distillate was saturated with NaCl,

adjusted to pH = 10 with NaOH and extracted with diethyl ether 4 times.

The ether extract was dried over anhydrous sodium sulfate, filtered

through a coarse fritted glass filter, evaporated to dryness, weighed

and stored at -10°C. This crude oil sample was then subjected to thin-

layer chromatography in hexane : acetone : diethylamine (4 : 1 : 1,

v/v/v). The alkaloid was detected using Dragendorff's reagent. It was

scraped, eluted in ether, dried, weighed, taken back up in ether and analyzed on a 15% Carbowax 20 M column as previously described. Gas chromatography-mass spectrometry was used to positively identify this alkaloid.

6. Isolation of Actinidine from Valeriana Officinalis

The alkaloid was isolated from dried roots of Valeriana officinalis by a series of extractions. The roots were first extracted with diethyl ether, the residue then extracted 3 times with chloroform : methanol (5 : 2, v/v). This extract was then filtered, concentrated on a rotary evaporator, taken up in diethyl ether and extracted 5 times with 1/3 volume of 10% HCl. This extract was neutralized, extracted with chloroform : methanol (3 : 2, v/v) and concentrated. Column chromatography first on silicic acid, then on neutral alumina according to the method of Torssell and Wahlberg (57), yielded a purified alkaloid fraction.

Thin-layer chromatography or the purified alkaloid fraction, or of the chloroform : methanol extract on silica gel HF in chloroform : methanol (5 : 1, v/v), or in ethyl acetate : isopropanol : ammonium hydroxide (45 : 36 : 20, v/v/v) yielded several Dragendorff's positive spots. Preparative thin-layer chromatography of the band with the highest R_f value in hexane : acetone : diethylamine (40 : 10 : 4, v/v/v) yielded a purified alkaloid fraction. Mass spectrometry on the previously described instrument and co-chromatography on the previously described gas chromatography equipment were used to identify this alkaloid. A 10 foot column packed with 15% Carbowax 20 M was used. The column temperature was held at 180°C, the injector temperature at 225°C and the flow rate was 80 ml/min of helium.

7. Chromatography and Instrumental Analysis

Thin-Layer Chromatography: The reaction mixtures of all reduction reactions were purified by thin-layer chromatography on Silica Gel HF plates, both analytical and preparative. The developing solvent used was hexane : acetone : ethanol (40 : 10 : 4, v/v/v). The bands of interest were scrpaed from the plates, eluted with either ether or methanol and concentrated under nitrogen for further study. The radioactivity on the chromatograms was located with a Nuclear Chicago 4π Actigraph III chromatogram scanner.

Gas Liquid Chromatography (GLC): Gas liquid chromatographic analyses were performed on a modified Barber-Colman Model 5000 gas chromatograph equipped with a hydrogen flame ionization detector (79). The column packings used were 20% Apiezon L on Anakrom ABS, 60-80 mesh or 15% Carbowax 20 M on Anakrom ABS. Columns used were all 1/4 inch silanized glass, however, their lengths varied from 8 to 12 feet as indicated.

Mass Spectrometry: Low resolution mass spectra were obtained on a prototype of the LKB-9000 combination gas chromatograph-mass spectrometer, which was constructed in the laboratory of Dr. Ragnar Ryhage, Karolinska Institutet, Stockholm, Sweden, as described by Waller (79). The spectra were obtained on the compounds as they emerged from the gas chromatograph using either Apiezon L or Carbowax 20 M columns, under the following conditions: ionization voltage of 20 or 70 eV, 3.5 kV accelerating voltage, 20 or 60 μamp trap current, 1.7 kV electron multiplier voltage, source temperature of 310°C, separator temperature of 250°C, helium flow rate of 20-30 ml/min and a column temperature of 160°C. A recording of the total ionization current obtained from the

collector plate in the analyzer tube served as the gas chromatographic tracing. The vertical slask marks along the tracings indicate the points at which mass spectra were taken. Spectra were counted and the peak heights measured manually. These data were introduced into the IBM 360/65 computer which was used to drive a Cal Comp Model 565 Plotter, which plotted the spectra.

Measurement of Radioactivity: The measurement of the radioactivity present in the purified samples was achieved by adding quadruplicate aliquots to scintillation vials containing 10 ml of toluene-ethanol scintillation solution and counting in a Model 3320 Packard Tri-Carb Scintillation Spectrometer described previously. Counting efficiency was determined using triplicate radioactive standards containing 1173 dpm of acetate-2-^{14}C.

CHAPTER VIII

RESULTS AND DISCUSSION

A. Preparation of Labeled Precursors

1. Preparation of Nepetalactone-G-^{14}C

The preparation of nepetalactone-G-^{14}C was achieved by allowing

Nepeta cataria L. plants to photosynthesize in the presence of $^{14}CO_2$ then

isolating the nepetalactone as described previously. The results of

several preparations are shown in Table I. The specific activity of the

nepetalactone-G-^{14}C, which was purified by thin-layer chromatography,

varied from 11,653 dpm/mg to 29,634 dpm/mg. These preparations of

nepetalactone-G-^{14}C were not further purified, but were reduced and then

purified by thin-layer chromatography followed by parparative gas chro-

matography. Figure 5 shows the mass spectrum of nepetalactone-G-^{14}C,

from experiment IV. This spectrum was similar to that of standard

nepetalactone, which was published by Regnier, et al. (15). The molec-

ular ion, M$^+$ 166 was very intense as was the ion at m/e 81 (M$^+$-85).

Intense ions were also found at m/e 151 (M$^+$-15), m/e 138 (M$^+$-28), m/e

123 (M$^+$-43), m/e 109, m/e 67, m/e 55 and m/e 41. Metastable ions were

found at m/e 114.7 verifying the m/e 166 to m/e 138 transition, m/e

109.6 verifying the m/e 138 to m/e 123 transition and m/e 37.4 verifying

the m/e 81 to m/e 55 transition.

TABLE I

PREPARATION OF NEPETALACTONE-G-^{14}C

Exp. No.	Plant Weight	Crude Oil		Nepetalactone-G-^{14}C		
		Wt.	Radioactiv-ity	Wt.	Radioactiv-ity	Specific Activity
	gm	mg	dpm	mg	dpm	dpm/mg
I	550	425	5,520,000	366	4,272,000	11,653
II	500	400	4,120,000	202	3,000,000	14,851
III	260	270	3,675,000	150	2,708,823	18,059
IV	330	228	5,820,000	164	4,860,000	29,634
V	305	196	2,388,306	121	1,449,000	11,975
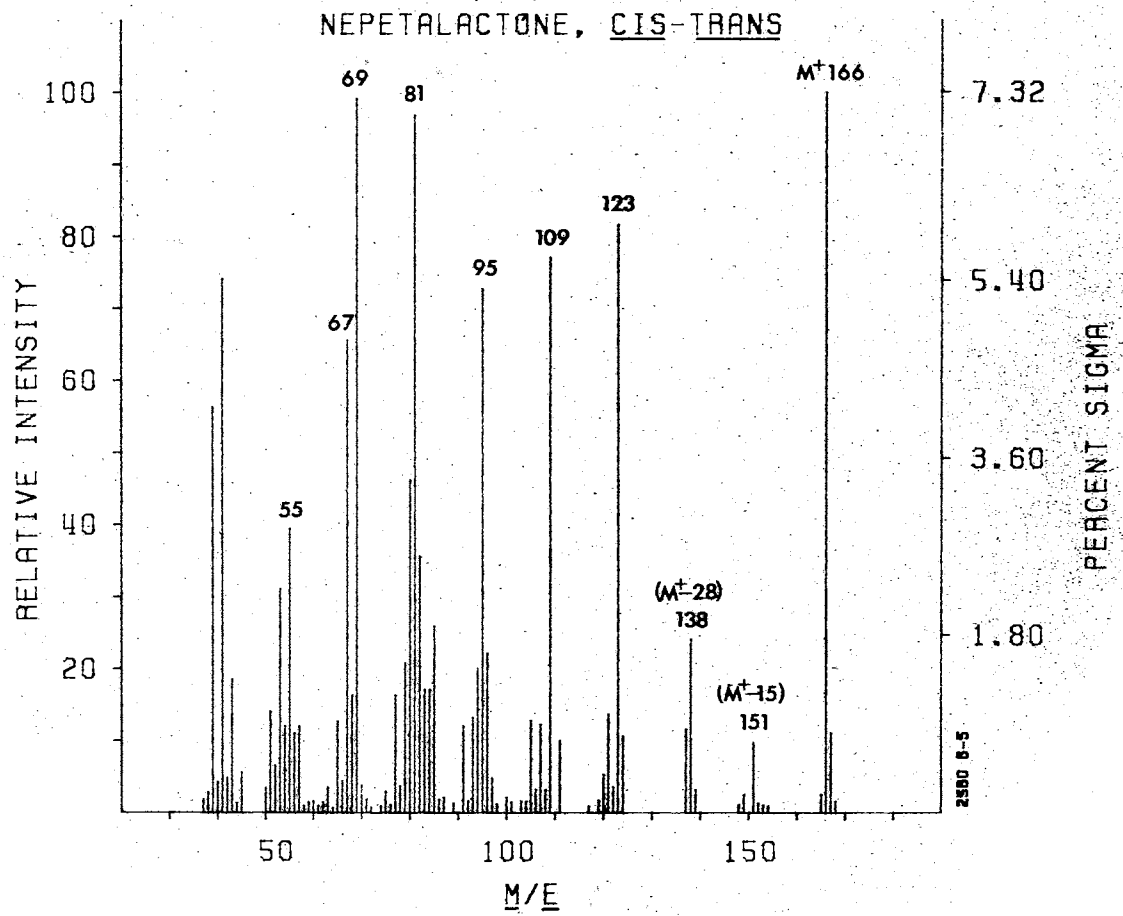
Figure 5. Mass Spectrum of Cis-Trans Nepetalactone.

2. Recuction of Nepetalactone-G-^{14}C to Dihydronepetalactone-G-^{14}C

The reduction of nepetalactone to dihydronepetalactone was achieved in this laboratory by Regnier, et al. (14) previously, using both plat-inum oxide and palladium on strontium carbonate as catalysts; however, an easier and more rapid reduction was achieved by using palladium on charcoal. A series of reductions of unlabeled nepetalactone with vary-ing conditions were undertaken and the conditions shown in Figure 6 were found to yield dihydronepetalactone rapidly and efficiently. Table II shows the yield of dihydronepetalactone from a series of hydrogena-tions of unlabeled nepetalactone. The percent yields varied from 80.2% to 97.4%. The dihydronepetalactone was purified from the reaction mix-ture by thin-layer chromatography.

Since this reaction worked well, preparation of dihydronepetalactone-G-^{14}C was undertaken. The same reaction conditions were used. Table III shows the results of several of these preparations. The yields var-ied from 80.0% to 94.6%, and the specific activities of the TLC purified dihydronepetalactone remained very similar to the specific activities of the respective nepetalactone samples, however, the preparative GLC purified dihydronepetalactone samples contained sufficient quantities of liquid phase (Apiezon L) from the column to cause slight decreases in their specific activities. These samples were analyzed by analytical gas chromatography and shown to consist of one symmetrical peak. Table IV shows the retention times of isolated nepetalactone-G-^{14}C along with the retention times of standard unlabeled samples of these compounds. The retention times tentatively identified these compounds. Mass spec-trometry was used to confirm these identifications. Figure 7 shows the mass spectra of standard and preparative GLC purified
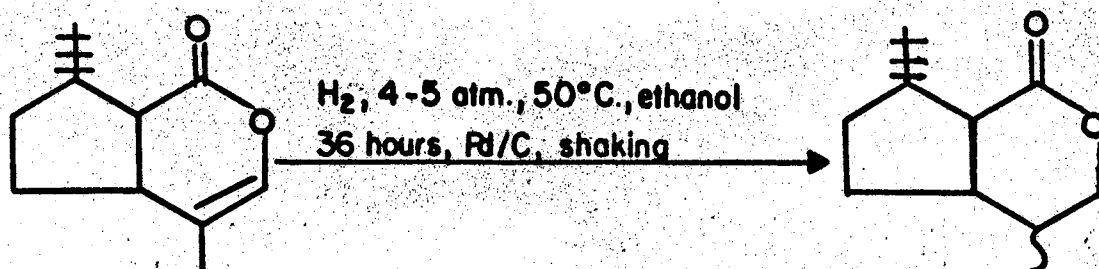
Figure 6. Reduction of Nepetalactone to Dihydronepetalactone.

TABLE II

NEPETALACTONE HYDROGENATION RESULTS

Exp. No.	Nepetalactone	Dihydronepetalactone	Yield
	mg	mg	%
I	250	232	92.8
II	420	409	97.4
III	250	219	87.6
IV	200	170	85.0
V	529	424	80.2

The dihydronepetalactone was purified by thin-layer chromato-graphy as described previously.

TABLE III

PREPARATION AND PURIFICATION OF
DIHYDRONEPETALACTONE-G-^{14}C

Exp. No.	TLC Purified Nepeta-lactone-G-^{14}C		TLC Purified Dihydro-nepetalactone-G-^{14}C			GLC Prepared Dihydro-nepetalactone-G-^{14}C	
	Sp. Act.	Wt.	Sp. Act.	Wt.	Yield	Sp. Act.	Wt.
	dpm/mg	mg	dpm/mg	mg	%	dpm/mg	mg
I	9,300	86	7,900	81	94.6	–	–
II	18,059	150	14,959	118	80.0	–	–
III	29,634	63	27,500	56	88.9	18,400	29
IV	29,634	115	28,077	104	90.4	–	–
V	–	–	11,325	41	–	6,191	35

TABLE IV

GAS CHROMATOGRAPHIC ANALYSIS OF THE
PURIFIED PREPARATIONS

Column: 10 ft., 1/4 silanized glass column packed with 20%
Apiezon L on Anakrom ABS (60-80 mesh).
Conditions: Column temperature: 200°C., Injector temperature:
240°C., He flow rate: 70 mls/minute.

Compound	Retention Time	
	Isolated	Standard
	minutes	minutes
Nepetalactone-G-^{14}C	16.5	16.3
Dihydronepetalactone-G-^{14}C	25.7	25.8
Nepetadiol-G-^{14}C	21.5	–

Figure 7. Mass Spectra of Reference Dihydronepetalactone
and Isolated Dihydronepetalactone.
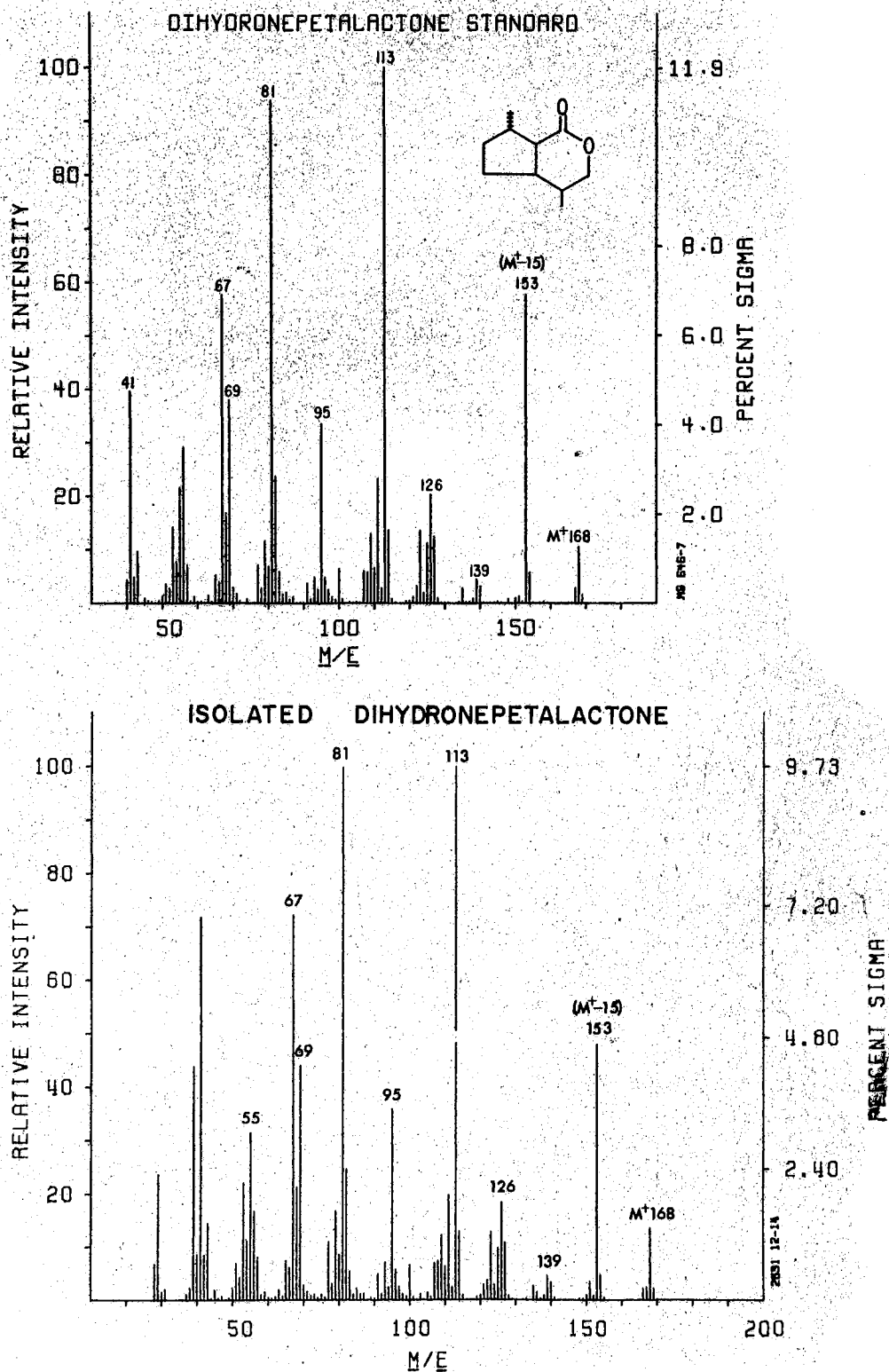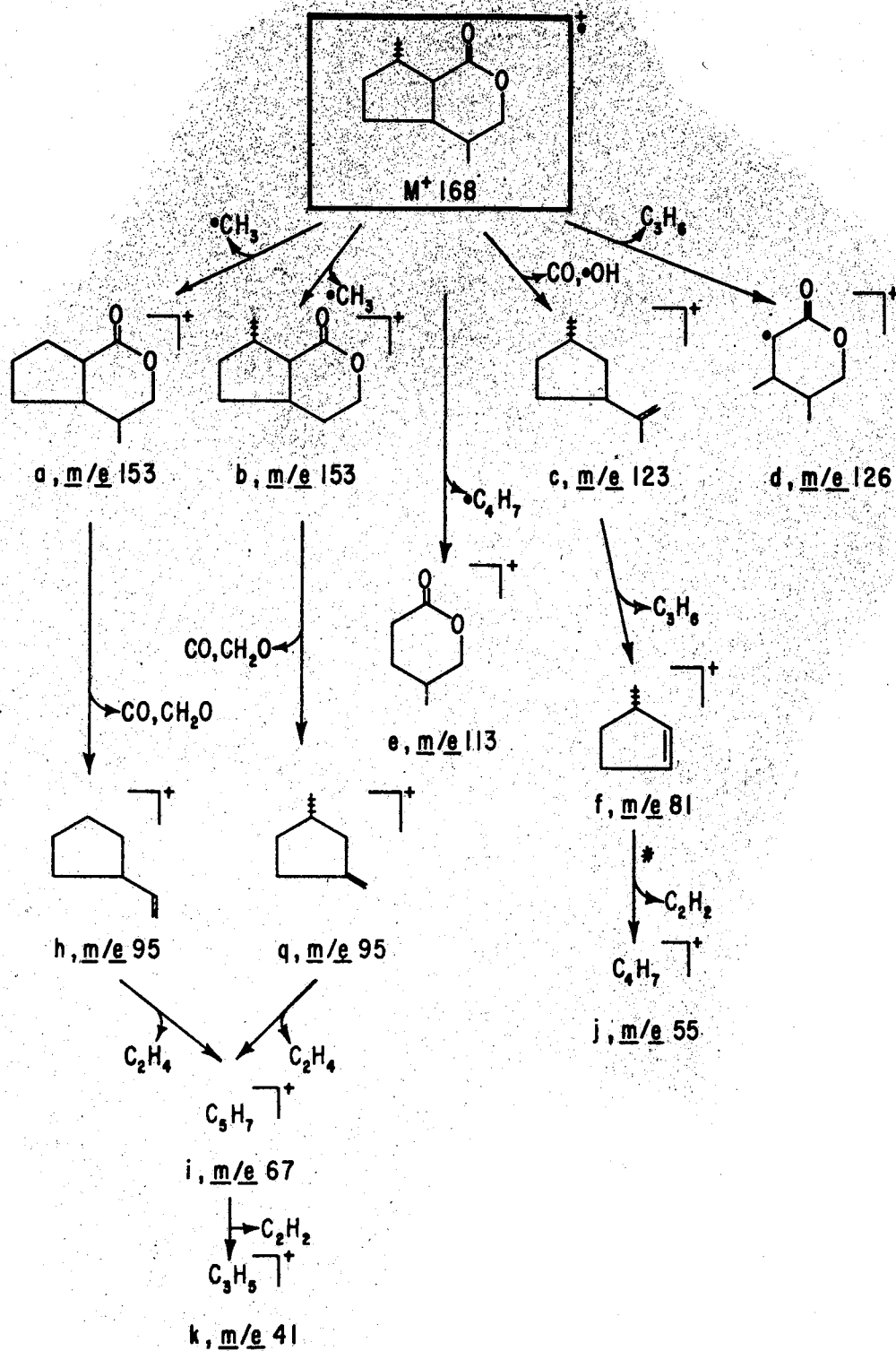
Scheme I. Proposed Partial Fragmentation of Dihydronepeta-lactone.

dihydronepetalactone. The spectra are almost identical. Scheme I shows

the proposed partial fragmentation of dihydronepetalactone. The base

peak in the mass spectrum of isolated dihydronepetalactone is $\underline{m}/\underline{e}$ 67 as

it is in the mass spectrum of standard dihydronepetalactone. The re-

mainder of the two spectra are very similar. In the mass spectrum of

dihydronepetalactone, the molecular ion, M^+ 168, can undergo loss of

either one of two methyl groups to yield ion a, $\underline{m}/\underline{e}$ 153 or ion b, $\underline{m}/\underline{e}$

153. This transition is verified by a metastable ion at $\underline{m}/\underline{e}$ 139.4. The

molecular ion may also undergo successive losses of carbon monoxide and

a hydroxyl group to yield ion c, $\underline{m}/\underline{e}$ 123, it may lose C_3H_6 to yield ion

d, $\underline{m}/\underline{e}$ 126 and it may lose a C_4H_7 fragment to yield ion e, $\underline{m}/\underline{e}$ 113. Ion

a, $\underline{m}/\underline{e}$ 153 and ion b, $\underline{m}/\underline{e}$ 153 may undergo successive loss of carbon

monoxide and CH_2O to yield ion h, $\underline{m}/\underline{e}$ 95 and ion g, $\underline{m}/\underline{e}$ 95 respectively.

Ion c, $\underline{m}/\underline{e}$ 123 may lose C_3H_6 and yield ion f, $\underline{m}/\underline{e}$ 81. Ion h, $\underline{m}/\underline{e}$ 95 and

ion g, $\underline{m}/\underline{e}$ 95 may lose C_2H_4 to yield ion i, $\underline{m}/\underline{e}$ 67. Ion f, $\underline{m}/\underline{e}$ 81 may

lose a C_2H_2 fragment to yield ion j, $\underline{m}/\underline{e}$ 55. This transition is verified

by a metastable ion at $\underline{m}/\underline{e}$ 37.3. Ion j, $\underline{m}/\underline{e}$ 55 may also lose a methylene

fragment to yield ion k, $\underline{m}/\underline{e}$ 41.

3. Reduction of Dihydronepetalactone-G-^{14}C to Nepetadiol-G-^{14}C

The reduction of dihydronepetalactone to nepetadiol was achieved

previously by Regnier, et al. (14), using lithium aluminum hydride. The

reaction was repeated several times on unlabeled dihydronepetalactone

until the most efficient conditions were discovered. In Figure 8, the

reaction and reaction conditions are shown. Table V shows the yields of

nepetadiol obtained from a series of reductions of unlabeled dihydro-

nepetalactone. The yields varied from 68.0% to 92.0%. The nepetadiol

was purified by either thin-layer chromatography in hexane : acetone :
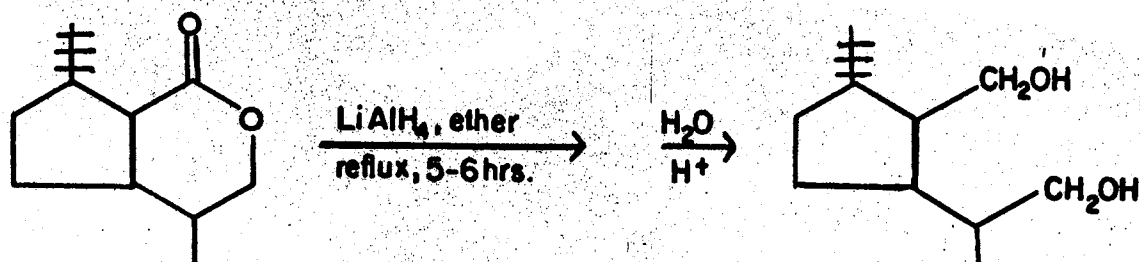
Figure 8. Reduction of Dihydronepetalactone to Nepetadiol.

TABLE V

DIHYDRONEPETALACTONE REDUCTION RESULTS

Exp. No.	Dihydronepetalactone	Nepetalactone	Yield
	mg	mg	%
I	200	184	92.0
II	350	304	86.9
III	175	161	92.0
IV	424	366	86.3
V	325	221	68.0

ethanol (40 : 10 : 4, v/v/v), or by preparative gas chromatography using the column and conditions described previously.

The preparation of nepetadiol-G-^{14}C from dihydronepetalactone-G-^{14}C was undertaken using the same reaction conditions. Table VI shows the results of several of these preparations. Yields were 86.8% and 95.0% for the thin-layer purified nepetadiol-G-^{14}C from the reductions. Preparative gas chromatography allowed the loss of greater than 50% of the sample but resulted in a greater purification than preparative thin-layer chromatography. Analytical gas chromatography on the previously described Apiezon L column showed that the preparative gas chromatographically purified nepetadiol fraction contained one, symmetrical peak. Mass spectrometry in conjunction with gas chromatography was used to identify nepetadiol and verify its purity. Figures 9 and 10 show the spectra of nepetadiol and its trifluoroacetate diester. The molecular weight of nepetadiol is 172 gm/mole, however, no molecular ion at $\underline{m}/\underline{e}$ 172 was seen, so the trifluoroacetate diester was prepared and mass spectra taken to prove the original compound was the dialcohol, nepetadiol. Scheme II shows the proposed partial fragmentation of nepetadiol. No molecular ion at $\underline{m}/\underline{e}$ 172 was found, however, this is not unusual for large molecular weight alcohols and dialcohols. Loss of water can occur to yield either ion a', $\underline{m}/\underline{e}$ 154 or ion b', $\underline{m}/\underline{e}$ 154. Loss of CH_2OH may also occur yielding either ion c', $\underline{m}/\underline{e}$ 141 or ion d', $\underline{m}/\underline{e}$ 141. Ion a', $\underline{m}/\underline{e}$ 154 can either undergo loss of water to yield ion e', $\underline{m}/\underline{e}$ 136 or loss of CH_2OH to yield ion g', $\underline{m}/\underline{e}$ 123. It may also undergo loss of one of two methyl groups to yield ion l', $\underline{m}/\underline{e}$ 139 and ion m', $\underline{m}/\underline{e}$ 139. Ion b', $\underline{m}/\underline{e}$ 154 can either undergo loss of water, to yield ion e', $\underline{m}/\underline{e}$ 136, loss of a CH_2OH fragment to yield ion f', $\underline{m}/\underline{e}$ 123 and loss of a C_3H_7O

TABLE VI

PREPARATION AND PURIFICATION OF
NEPETADIOL-G-^{14}C

Exp. No.	TLC Purified Dihydronepetalactone-G-^{14}C		TLC Purified Nepetadiol-G-^{14}C			GLC Purified Nepetadiol-G-^{14}C	
	Sp. Act.	Wt.	Sp. Act.	Wt.	Yield	Sp. Act.	Wt.
	dpm/mg	mg	dpm/mg	mg	%	dpm/mg	mg
I	14,959	80	11,241	76	95.0	--	--
II	14,959	38	14,242	33	86.8	--	--
III	28,077	51	--	--	--	26,316	11.4
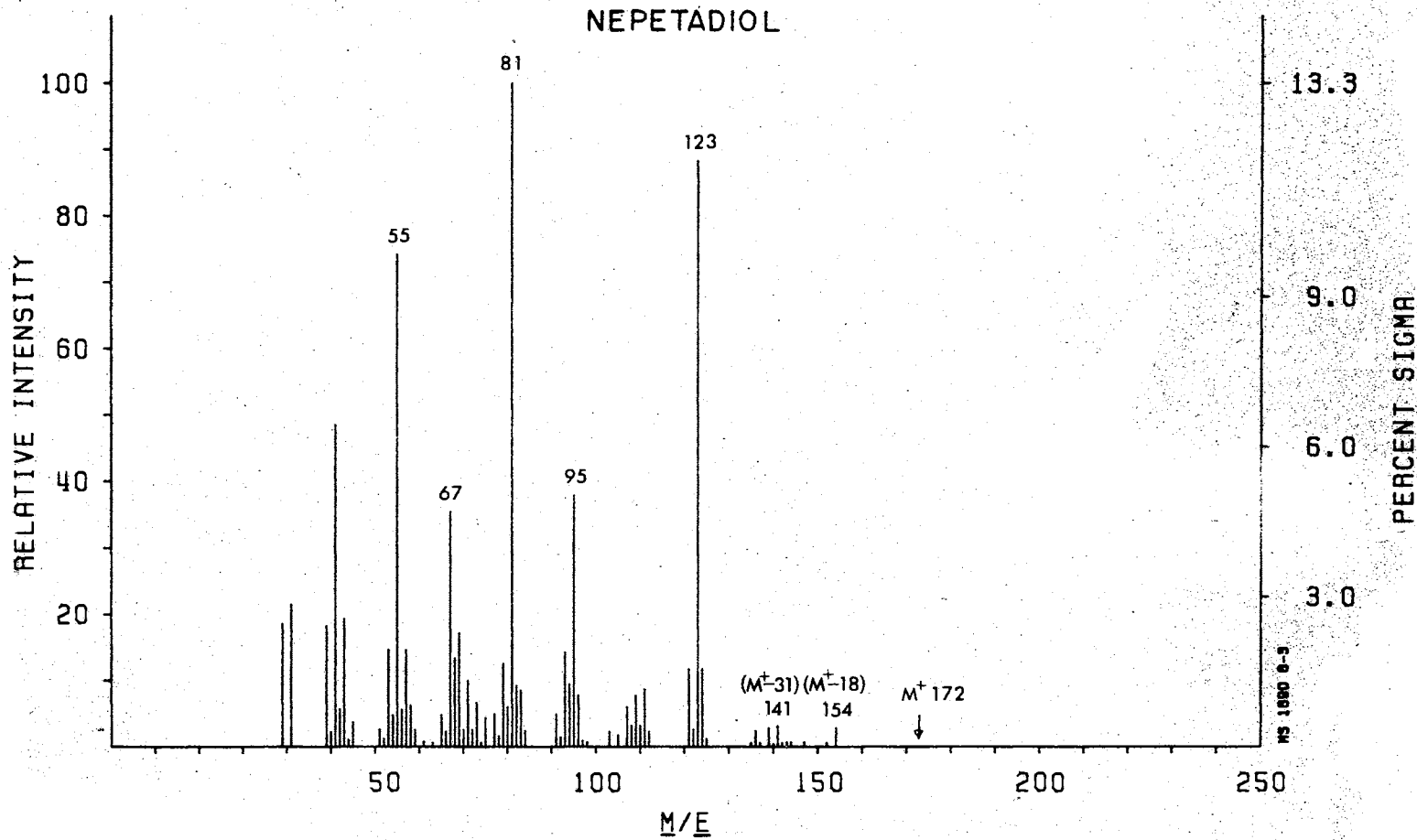
Figure 9. Mass Spectrum of Nepetadiol.
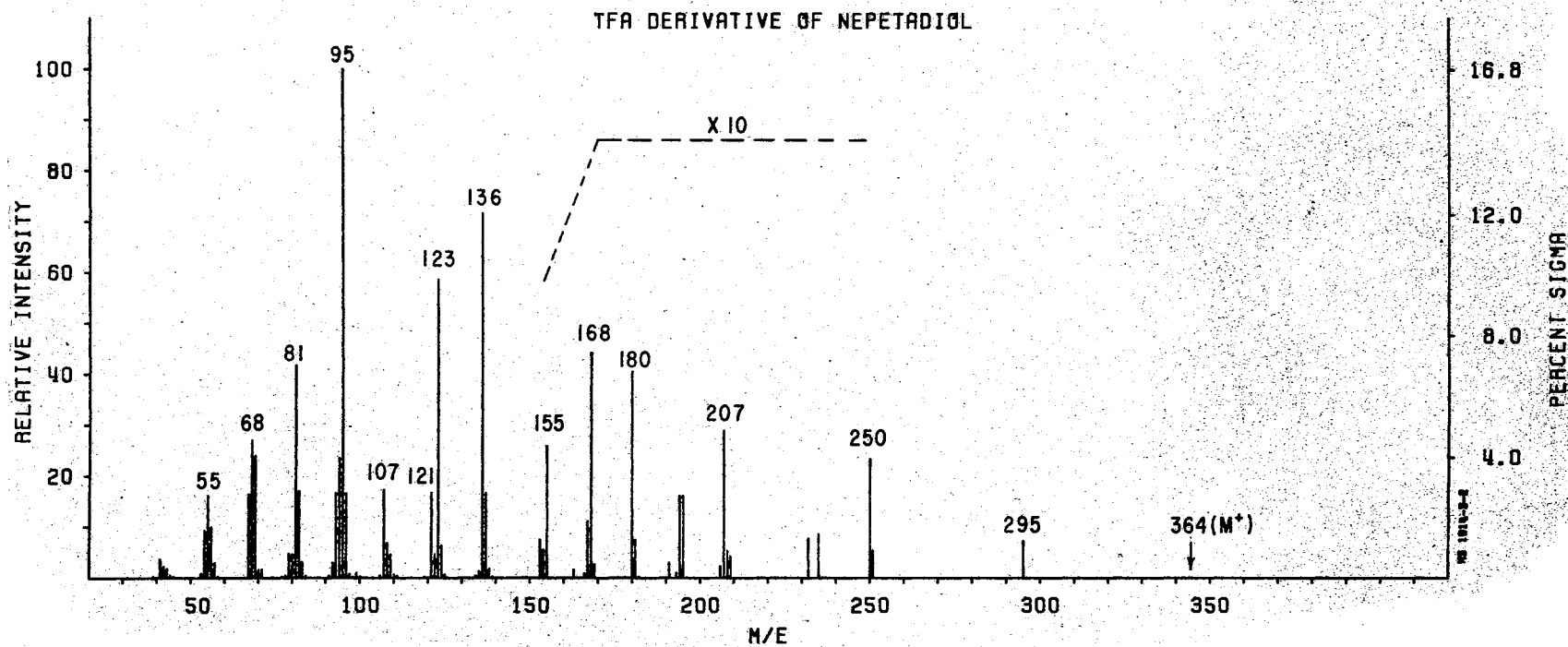
Figure 10. Mass Spectrum of the Trifluoroacetate Diester Derivative of Nepetadiol.

Scheme II. Proposed Partial Fragmentation of Nepetadiol.

fragment to yield ion i', $\underline{m}/\underline{e}$ 95, which is verified by a metastable ion at $\underline{m}/\underline{e}$ 58.6. Ion b', $\underline{m}/\underline{e}$ 154 may also undergo loss of one of two methyl groups yielding ion n', $\underline{m}/\underline{e}$ 139 or ion o', $\underline{m}/\underline{e}$ 139. Ion c', $\underline{m}/\underline{e}$ 141 can lose water to yield ion g', $\underline{m}/\underline{e}$ 123, while ion d', $\underline{m}/\underline{e}$ 141 can also lose water to yield ion f', $\underline{m}/\underline{e}$ 123. These transitions are verified by a metastable ion at $\underline{m}/\underline{e}$ 107.3. Ion d', $\underline{m}/\underline{e}$ 141 can undergo loss of a C_3H_7O fragment and a hydrogen to yield ion h', $\underline{m}/\underline{e}$ 81, which is verified by a metastable ion at $\underline{m}/\underline{e}$ 46.8. Ion e', $\underline{m}/\underline{e}$ 136 can lose either one of two methyl groups to yield ion j', $\underline{m}/\underline{e}$ 121 or ion k', $\underline{m}/\underline{e}$ 121. Ion f', $\underline{m}/\underline{e}$ 123 can undergo loss of C_2H_4 yielding ion i', $\underline{m}/\underline{e}$ 95. This transition is verified by a metastable ion at $\underline{m}/\underline{e}$ 73.3. Ion g', $\underline{m}/\underline{e}$ 123 can lose a C_3H_5 fragment and a hydrogen to yield ion h', $\underline{m}/\underline{e}$ 81 which is verified by a metastable ion at $\underline{m}/\underline{e}$ 53.4. Ion k', $\underline{m}/\underline{e}$ 121 can undergo loss of C_2H_4 to yield ion i', $\underline{m}/\underline{e}$ 95. Ion h', $\underline{m}/\underline{e}$ 81 can lose C_2H_2 to yield ion p', $\underline{m}/\underline{e}$ 55. This transition is verified by a metastable ion at $\underline{m}/\underline{e}$ 37.3.

In order to conclusively prove the identity of the compound isolated from the lithium aluminum hydride reduction of dihydronepetalactone to be nepetadiol, the compound was reacted with trifluoroacetic anhydride and the trifluoroacetate diester was formed. Combination gas chromatography-mass spectrometry of this reaction mixture yielded one major peak which was identified by its mass spectrum. The mass spectrum of the trifluoroacetate diester of nepetadiol is shown in Figure 10 while Scheme III shows the proposed partial fragmentation of the trifluoroacetate diester of nepetadiol. No molecular ion peak at $\underline{m}/\underline{e}$ 364 was observed; however, a peak at $\underline{m}/\underline{e}$ 295 (a") was found. The peak at $\underline{m}/\underline{e}$ 295 (a") provided strong evidence that the isolated compound was
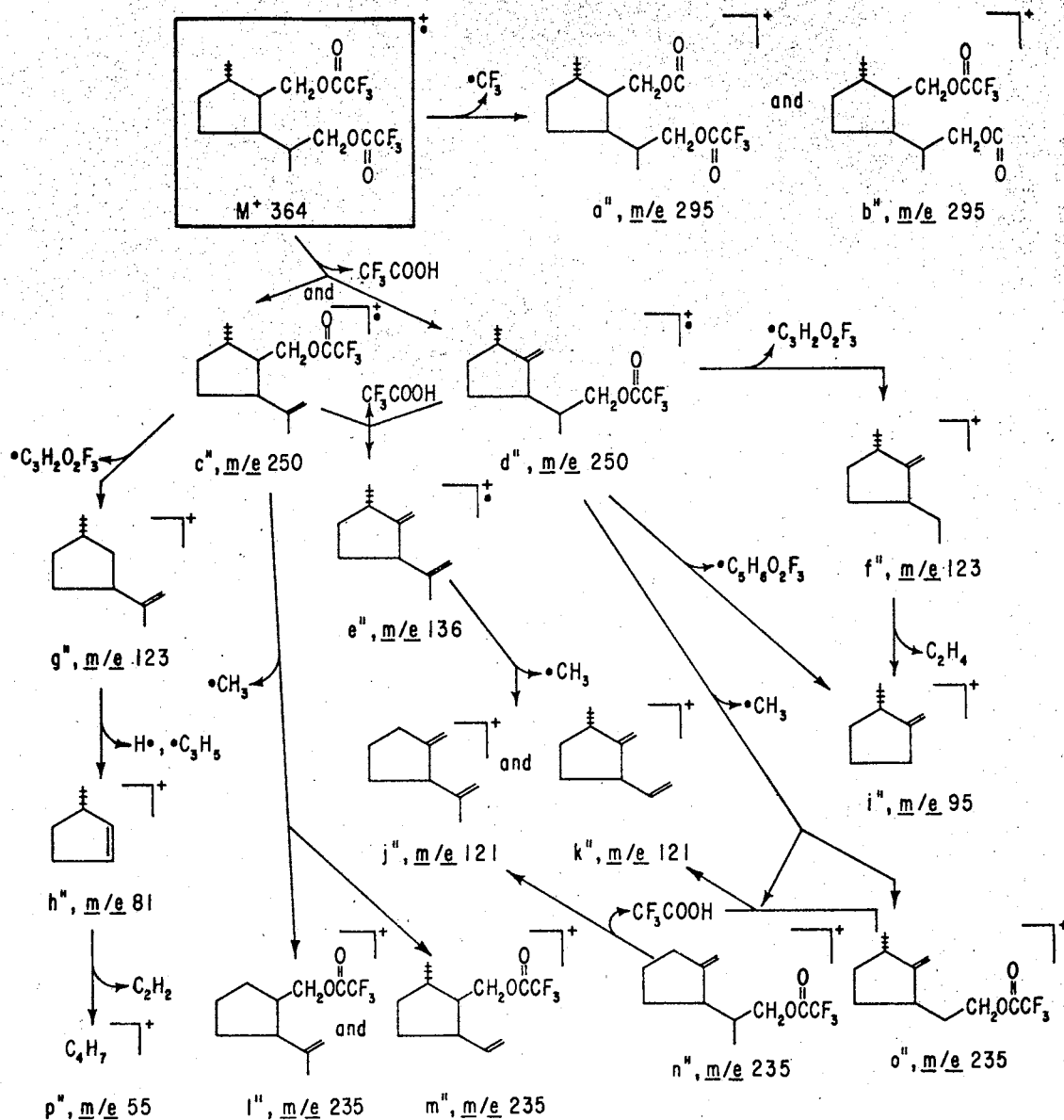
Scheme III. Proposed Partial Fragmentation of the Trifluoroacetate
Diester Derivative of Nepetadiol.

nepetadiol since these fragment ions contain both of the esterified

alcohol groups originating from nepetadiol. Thus the molecular ion,

m/e 364 undergoes loss of a CF_3 fragment to yield ion a", m/e 295 and

ion b", m/e 295. It can also lose trifluoroacetic acid to yield ion c",

m/e 250 and ion d", m/e 250. Ion c", m/e 250 can lose another trifluoro-

acetic acid residue to yield ion c", m/e 136, a methyl fragment to yield

ion l", m/e 235 and ion m", m/e 235, and a $C_2H_2O_2F_3$ fragment to form ion

g", m/e 123. Ion d", m/e 250 can also undergo these same fragmentations

and also can lose a $C_5H_6O_2F_3$ fragment yielding i", m/e 95. Ion c", m/e

136 can undergo loss of one of two methyl groups to form ion j", m/e 121

and ion k", m/e 121. Ion f", m/e 123 can lose C_2H_4 to yield ion i",

m/e 95. Ion g", m/e 123 can undergo loss of a C_3H_5 fragment and a hydro-

gen atom to form ion h", m/e 81. Ion h", m/e 81 can lose C_2H_2 to form

ion p", m/e 55. Ion l", m/e 235 and ion n", m/e 235 can undergo loss of

CF_3COOH to yield ion j", m/e 121 while ion m", m/e 235 and ion o", m/e

235 can lose CF_3COOH to form ion h", m/e 121. Further fragmentation is

similar to that shown in the fragmentation of nepetadiol in Scheme II.

The previously presented data conclusively identified these synthe-

sized compounds as dihydronepetalactone-G-^{14}C and nepetadiol-G-^{14}C so

metabolism experiments in Nepeta cataria were undertaken.

B. Metabolism of Carbon-14 Labeled Methylcyclopentane Monoterpenoids in Nepeta cataria L.

1. Dihydronepetalactone-G-[14]C Metabolism

Two experiments were undertaken in which dihydronepetalactone-G-[14]C

was injected into the plant and allowed to metabolize. In experiment I,

fourteen milligrams (250,000 dpm) of dihydronepetalactone-G-[14]C (specific

activity of 18,400 dpm/mg) were administered to a healthy twelve-week

old N. cataria plant. The plant was allowed to metabolize for 14 hours

then the plant was weighed, homogenized in distilled water, steam dis-

tilled and crude oil isolated and analyzed as described previously. In

experiment II, 11.0 milligrams (200,000 dpm) of dihydronepetalactone-G-

^{14}C (specific activity of 18,400 dpm/mg) were administered to another

N. cataria plant and allowed to metabolize for 24 hours. The plant was

analyzed in the same manner as in experiment I. Table VII shows the

crude radioactivity distribution in these two plants. In these experi-

ments 70% to 80% of the label remained in the residue from the steam

distillation while 20% to 25% was found in the crude oil. Further

steam distillation produced only negligible amounts of labeled crude

oil (approximately 2%). Analysis of the crude oil from both experiments

was achieved using preparative and analytical gas chromatography and

gas chromatography in combination with mass spectrometry. In the gas

chromatography analysis, cis-trans nepetalactone was used as an internal

standard and retention values for the other components were calculated

based on its retention time. The relative retention value of cis-trans

nepetalactone was given the value of 1.00. The following components,

which were identified by gas chromatography-mass spectrometry, had these

relative retention values: trans-cis nepetalactone, 1.15; an unknown

nepetalactone isomer (probably cis-cis) 1.21; recovered dihydronepetal-

actone-G-^{14}C, 1.70 and an unknown compound with a relative retention

value of 1.33, which was not present in the crude oil of the untreated

control plants.

Preparative gas chromatography was conducted using the Apiezon L

column and conditions previously described. Four major fractions were

collected from the crude oil. These fractions were labeled fractions

TABLE VII

CRUDE RADIOACTIVITY DISTRIBUTION IN NEPETA
CATARIA PLANTS FED CARBON-14 LABELED
DIHYDRONEPETALACTONE

Experiment		Dihydronepetalactone-G-^{14}C		Crude Oil		Residue	
	Time	Amount	Radioactivity	Amt.	Radioactivity	Amt.	Radioactivity
	hrs	mg	dpm	mg	dpm	gm	dpm
I	14	14.5	250,000	240	51,000	--	--
II	24	11.0	200,000	493	18,200	12	162,960

TABLE VIII

RADIOACTIVITY DISTRIBUTION AMONG THE PREPARATIVE
GAS CHROMATOGRAPHY FRACTIONS FROM THE
DIHYDRONEPETALACTONE-G-^{14}C METABOLISM
EXPERIMENTS

Total radioactivity and % incorporation values are about 50%
of the actual value, since preparative gas chromatography
allowed the loss of approximately 50% of each component. GLC
column and conditions: column, 3/8 in., 16 ft., 20% Apiezon
L on Anakrom ABS. Column temperature, 210°C. Helium flow
rate, 140 ml/min.

Fraction	Total Radioactivity	Incorporation
	dpm	%
Exp. I		
I	-	-
II	1,050	0.4
III	3,548	1.4
IV	17,451	8.7
Exp. II		
I	1,005	0.5
II	210	0.1
III	5,915	3.0
IV	3,315	1.7

I, II, III and IV. Gas chromatography-mass spectrometry was used to identify the components of these fractions. Fraction II was identified as cis-trans nepetalactone, while fraction IV was identified as dihydro-nepetalactone. The mass spectra of these compounds have been presented and discussed previously. Table VIII shows the distribution of radio-activity among the preparative GLC fractions. Incorporation of radio-activity into cis-trans nepetalactone was shown to be from 0.1 to 0.4%. Analysis of these fractions by combination gas chromatography-mass spectrometry was conducted using the Apiezon L column and conditions described previously. Table IX shows the combination gas chromatography-mass spectrometry analysis of these fractions from experiment II, to-gether with the amount of label in each component. These components were isolated by a second preparative gas chromatography purification on the same Apiezon L column but at a column temperature of 180°C and a helium flow rate of 110 ml/min. The amount of each component isolated was estimated by gas chromatography using relative response factors determined previously for standard nepetalactone and dihydronepetalactone. The specific activity of the recovered dihydronepetalactone was 19,650 dpm/mg compared to 18,400 dpm/mg for the administered dihydronepetalac-tone; these values were essentially the same within experimental error, and this indicated that very little free endogenous dihydronepetalactone was present in the plant.

The identity of the components of the preparative GLC fractions were determined by combination gas chromatography-mass spectrometry. Preparative gas chromatography fraction I was analyzed by combination gas chromatography-mass spectrometry and two components were observed. The larger of the peaks (I-A) was identified by comparison of mass

TABLE IX

COMPONENTS OF THE PREPARATIVE GAS CHROMATOGRAPHY
FRACTIONS FROM DIHYDRONEPETALACTONE-G-^{14}C
METABOLISM EXPERIMENT II

Fraction		Components	Radioactivity	Sp. Act.
			dpm	dpm/mg
I		3-hexen-1-ol	1,005	505
II		cis-trans nepetalactone	210	18
III	B	trans-cis nepetalactone	*396	8,351
	C	unknown nepetalactone isomer		
	D	unknown monoterpenoid	1,320	11,321
IV		dihydronepetalactone	3,315	19,650

*trans-cis nepetalactone and the unknown nepetalactone isomer (probably cis-cis) could not be completely resolved by preparative gas chromatography so the total radioactivity value represents the total label in both compounds.

spectral data with that of authentic 3-hexen-1-ol (81). The minor (10%)

component was not identified. Table X shows a comparison of the ten

most intense ions in the spectra of the major component of fraction I

and of 3-hexen-1-ol. These data are identical in m/e values and almost

identical in order of intensity. The analysis of fraction III indicated

three major components with some contamination with cis-trans nepetal-

actone. Figure 11 shows the recorder tracing of the GC-MS analysis of

fraction III. Peak III-A was identified as cis-trans nepetalactone and

peak III-B as trans-cis nepetalactone. The mass spectrum of peak III-C

was very similar to that of both cis-trans nepetalactone and trans-cis

nepetalactone and is postulated to be cis-cis nepetalactone. Peak III-

D, which contained the majority of the label present in fraction III,

had a molecular weight of 166 as do the nepetalactone isomers, however,

its spectra differed from the spectra of the nepetalactone isomers too

much to be another isomer. Figure 12 shows the mass spectrum of this

compound. There are several key variations from the mass spectra of the

nepetalactone isomers, which yield information concerning its structure.

Scheme IV shows the postulated partial fragmentation pattern of this

compound along with a proposed structure which fits the fragmentation

found in the mass spectrum shown in Figure 12. A postulated structure

for this component is also shown in this figure. The molecular ion,

(M^+), m/e 166 is postulated to have the structure shown. It can undergo

loss of water to yield ion bb, m/e 148, which was verified by a meta-

stable ion at m/e 132.0, or it may undergo loss of CH_2O to form ion bc,

m/e 136. It can also lose CO and a hydroxyl fragment to yield ion bd,

m/e 121, or it may lose one of two methyl fragments to yield ion be,

m/e 151 and ion bf, m/e 151. This transition was confirmed by a

TABLE X

COMPARISON OF THE TEN MOST INTENSE
IONS IN THE MASS SPECTRA OF I—A
AND 3-HEXEN-1-OL

We wish to acknowledge the earlier contribution of uncerti-
fied mass spectra of cis- and trans-3-hexen-1-ol by Western
Utilization Research and Development Division, U. S. Depart-
ment of Agriculture, Albany, California.

Order of	m/e Values		
Intensity	I-A	cis-3-Hexen-1-ol	trans-3-Hexen-1-ol
1	41	41	41
2	67	67	67
3	82	82	69
4	55	55	82
5	69	39	55
6	42	27	39
7	39	31	27
8	31	42	31
9	27	69	29
10	29	29	42
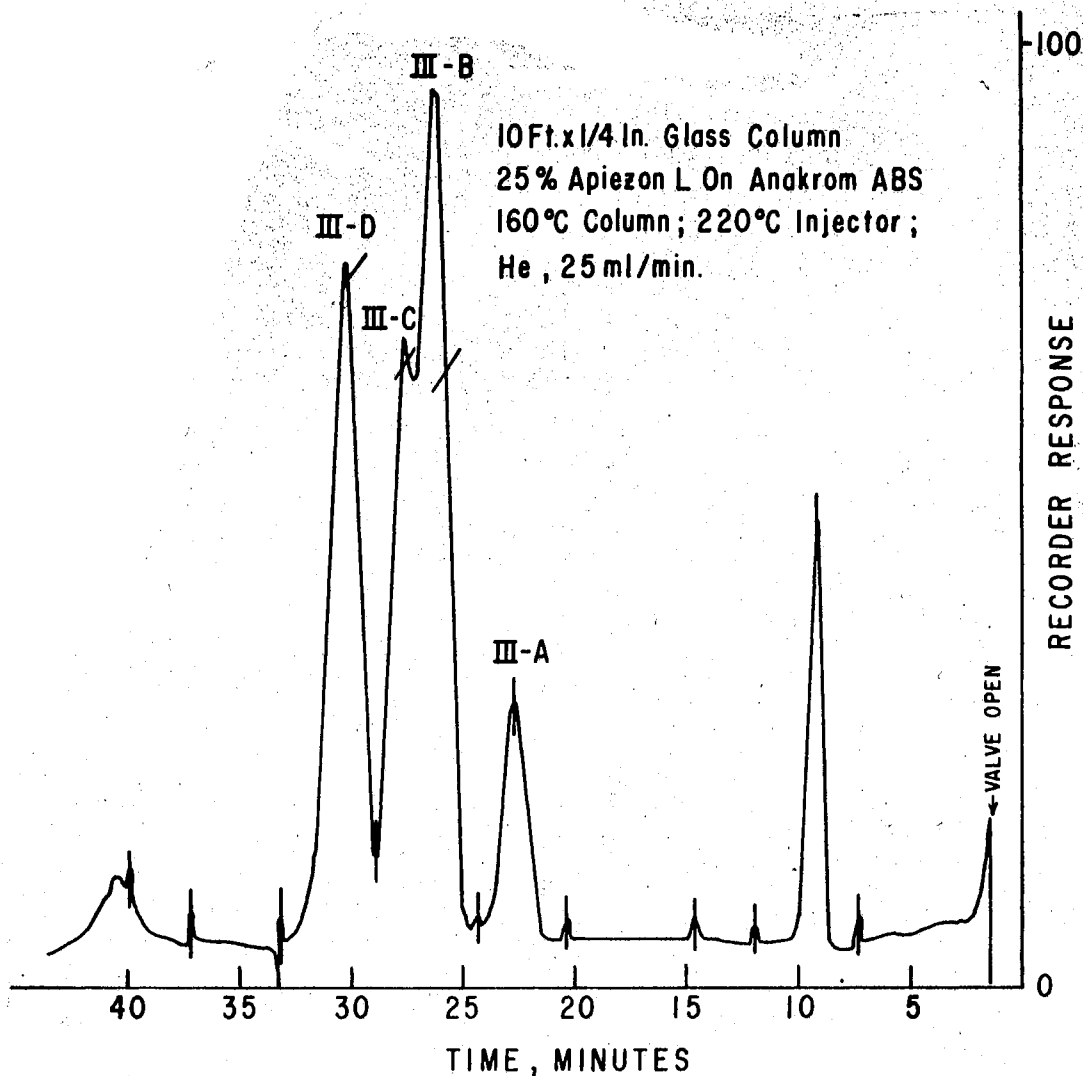
Figure 11. Total Ion Current Tracing of Fraction III of the Pre-
parative GLC Purification of the Crude Oil From
Dihydronepetalactone-G-^{14}C Biosynthesis Experi-
ment I. The slash marks indicate where a mass
spectrum was taken. The column and conditions
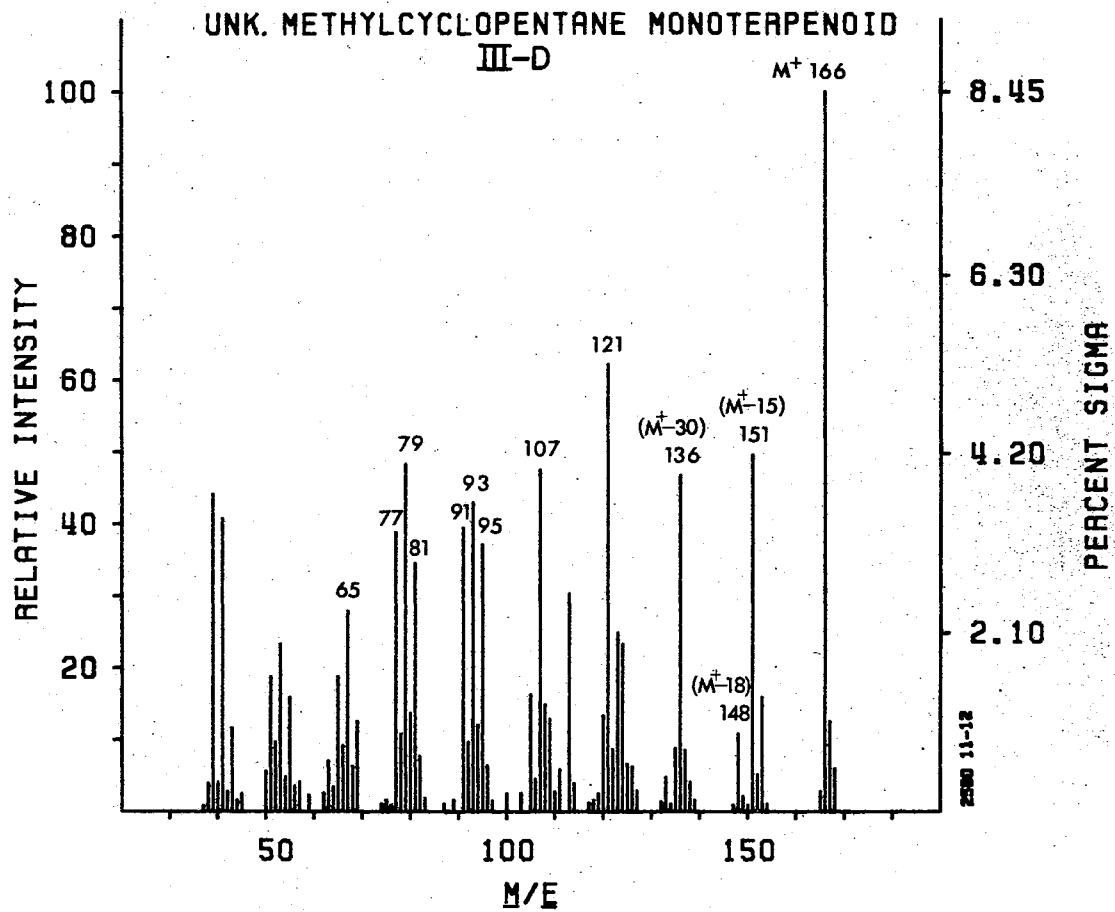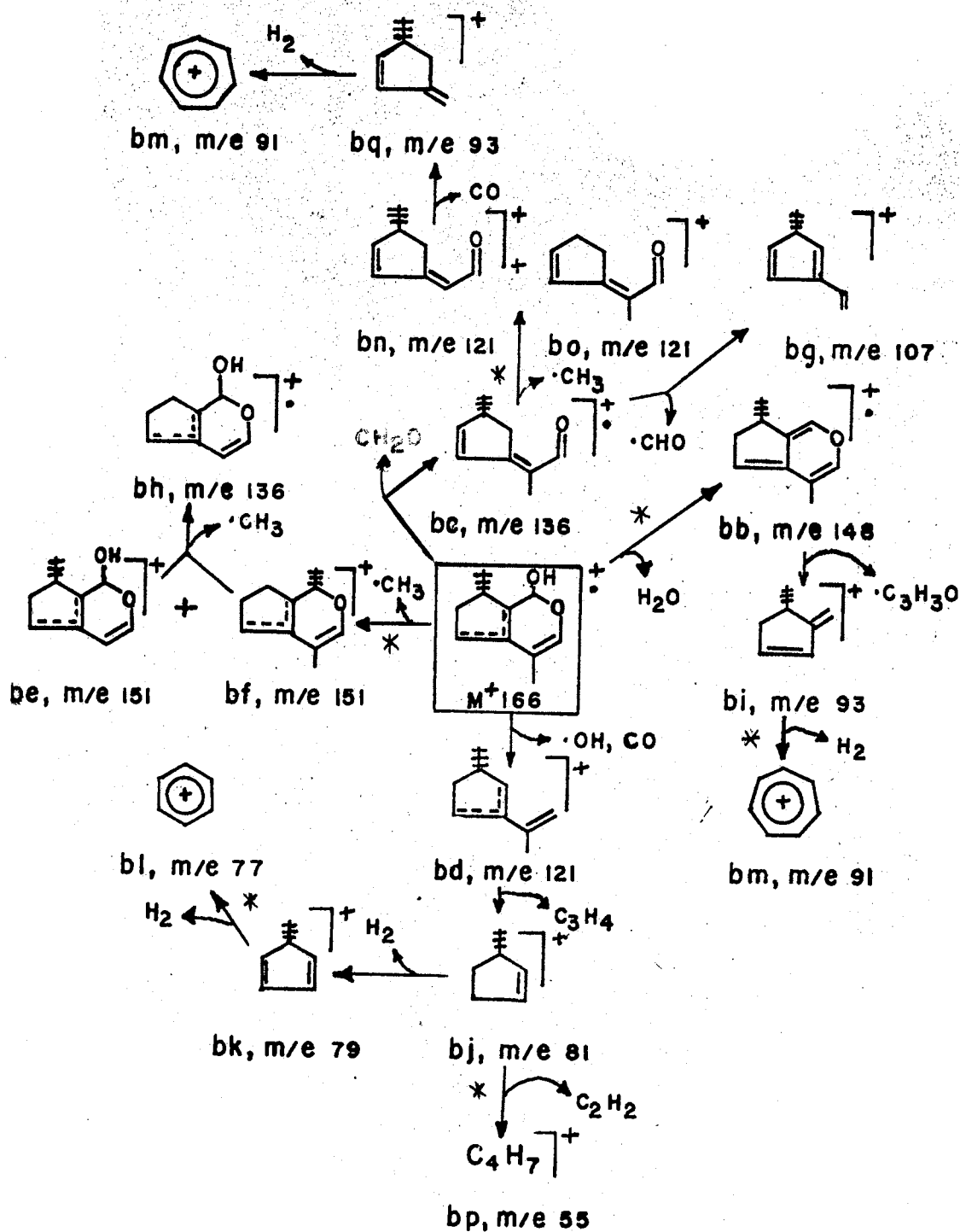were the same as shown in Figure 10.

Figure 12. Mass Spectrum of Compound III-D.

Scheme IV. Proposed Partial Fragmentation of Component III-D

* = means transition confirmed by a metastable ion.

metastable ion at m/e 137.2. Ion bb, m/e 148 can lose a C_3H_3O fragment forming ion bi, m/e 93 which can then undergo loss of molecular hydrogen and rearrange to yield ion bm, m/e 91. This transition was verified by a metastable ion at m/e 89.0. Ion bc, m/e 136 can lose a CHO fragment to yield ion bg, m/e 107 or it can undergo loss of a methyl fragment to yield ion bn, m/e 121 or ion bo, m/e 121. This transition was verified by a metastable ion at m/e 107.6. Ion bd, m/e 121 can lose C_3H_4 to form ion bj, m/e 81 or it can lose C_3H_6 to form ion bk, m/e 79. Ion be, m/e 151 and ion bf, m/e 151 can undergo loss of the remaining methyl group to yield ion bh, m/e 136. Ion bj, m/e 81 can lose molecular hydrogen to yield ion bh, m/e 79 or it can lose C_2H_2 to form ion bp, m/e 55. This transition was verified by a metastable ion at m/e 37.3. Ion bk, m/e 79 can undergo loss of molecular hydrogen and rearrange to form ion bl, m/e 77. This transition was verified by a metastable ion at m/e 75.1. Ion bn, m/e 121 can lose CO to yield ion bg, m/e 93 which can undergo loss of molecular hydrogen and rearrange to yield ion bm, m/e 91. This transition was verified by a metastable ion at m/e 89.0.

The structure of compound (III-D) is tentatively proposed based on the similarity of its mass spectrum to those of the nepetalactone isomers. The specific activity of III-D was quite high, 11,321 dpm/mg compared to a specific activity of 18,400 dpm for the administered dihydronepetalactone-G-^{14}C. It was concluded that III-D is the nearest metabolite of dihydronepetalactone in either its biosynthetic or catabolic pathways. Compound III-D is probably a catabolic metabolite of dihydronepetalactone, however, it is possible that the high concentration of dihydronepetalactone administered to the N. cataria plants could have caused a blockage of the biosynthetic pathway and resulted in a

shift in the equilibrium reaction leading to III-D. This equilibrium shift could allow a reversal of the flow of the biosynthetic pathway and lead to a conversion of dihydronepetalactone-G-^{14}C to its immediate precursor. The tentative structure of III-D indicated that it is more likely a catabolic metabolite of dihydronepetalactone. Figure 13 shows the proposed conversions of dihydronepetalactone to III-D and nepetalactone based on radioisotopic incorporation data.

A suggestion for further study would be to administer large doses of unlabeled dihydronepetalactone (30 to 50 mg); then isolate compound III-D by the procedure previously described, after allowing a 12 to 24 hour period of time to elapse. Compound III-D could then be subjected to infrared spectrophotometry and nuclear magnetic reasonance spectrometry to conclusively determine its structure.

Because of the large amount of radioactivity remaining in the residue of the steam distillation of the dihydronepetalactone-G-^{14}C treated plants (75 to 85%) the residue of one of these plants was steam distilled again, however very little radioactive material (4500 dpm) was found in the steam distillate. This residue was then subjected to hydrolysis in 2N HCl for 2 hours at 100°C and then steam distilled a third time. The crude oil after acid hydrolysis contained 23,250 dpm. Analysis of this fraction by gas chromatography mass spectrometry yielded three large peaks. This analysis is shown in Figure 14. Component A', B' and C comprised more than 95% of the volatile material in this crude oil. Component A' had a molecular ion at $\underline{m/e}$ 154. Its spectrum is shown in Figure 15. It contains many of the same fragment ions as dihydronepetalactone and nepetalactone, except that the fragment ions containing the lactone ring were 14 mass units lower than the

CH$_3$CH$_2$-CH=CH-CH$_2$-CH$_2$OH
3-hexen-1-ol
(Sp.Act. 505 dpm/mg)

0.5% ?

~ 1%

~ 1%

A'
(Sp.Act., 1003 dpm/mg)

Dihydronepetalactone
(Sp.Act., 18,400 dpm/mg)

Nepetalactone isomers

~ 5%

III-D
(Sp.Act., 11,321 dpm/mg)

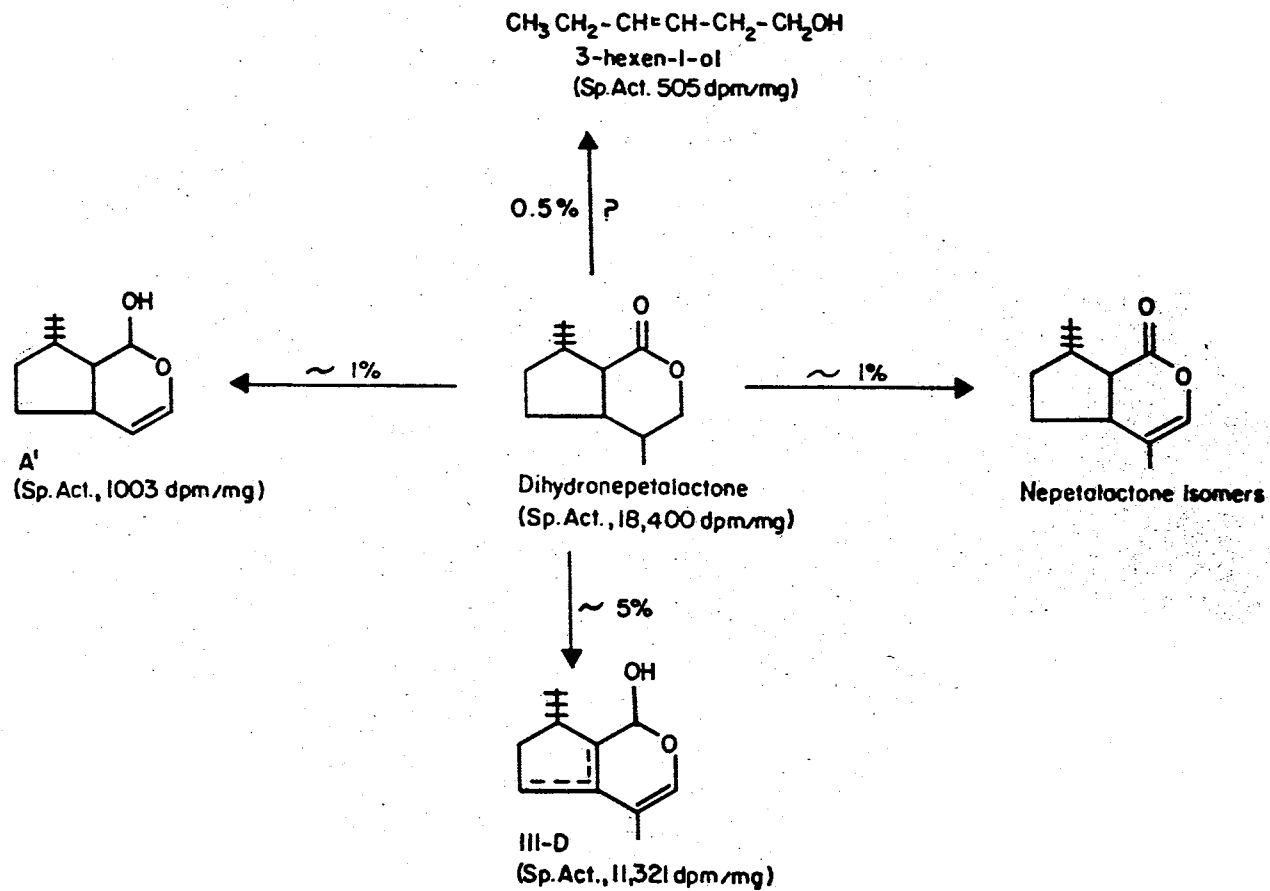Figure 13. Proposed Interconversions of Dihydropetalactone in Nepeta
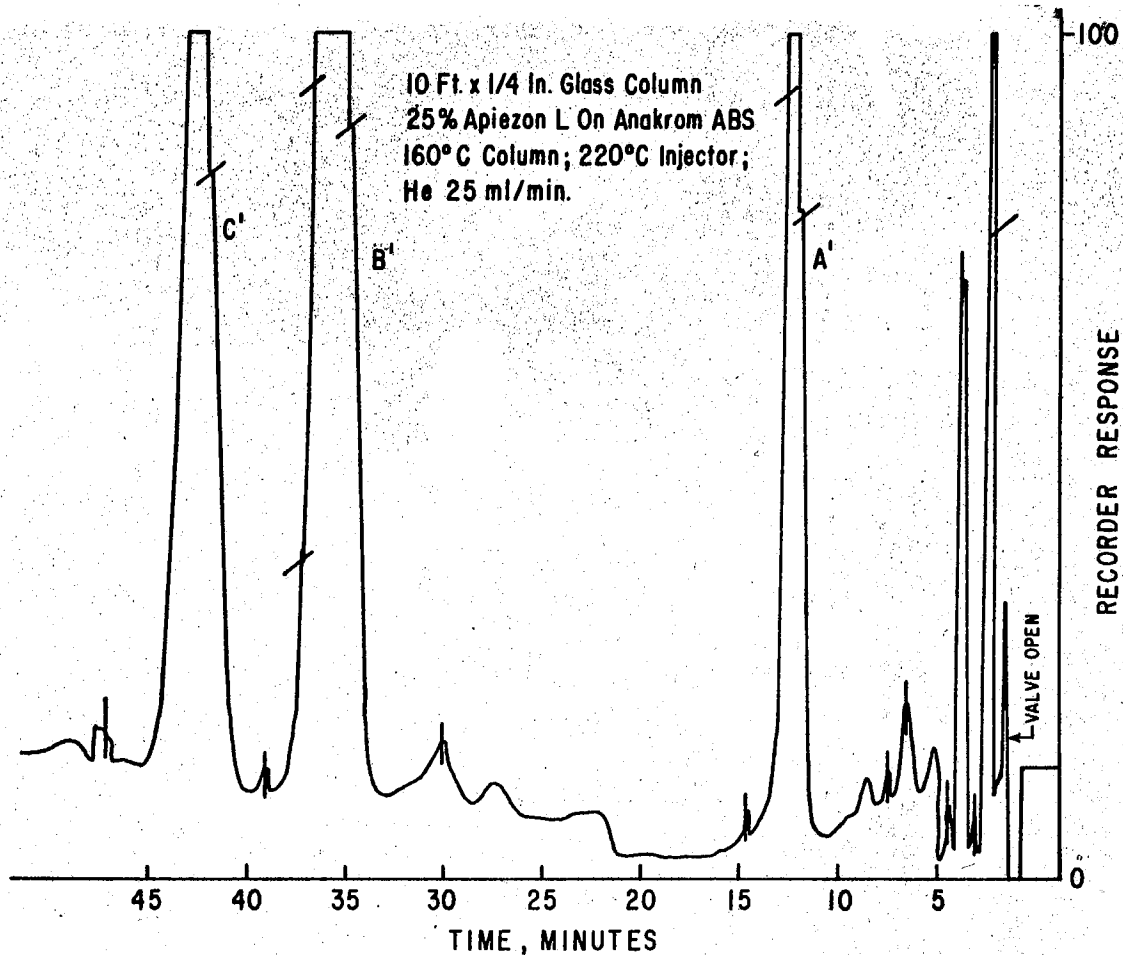cataria L.

Figure 14. Total Ion Current Tracing of Steam Distillate from the
2N HCl Hydrolysis of the Residue from Dihydronepetal-
actone-G-^{14}C Metabolism   Experiment II. The slash
marks indicate where a mass spectrum was taken. The
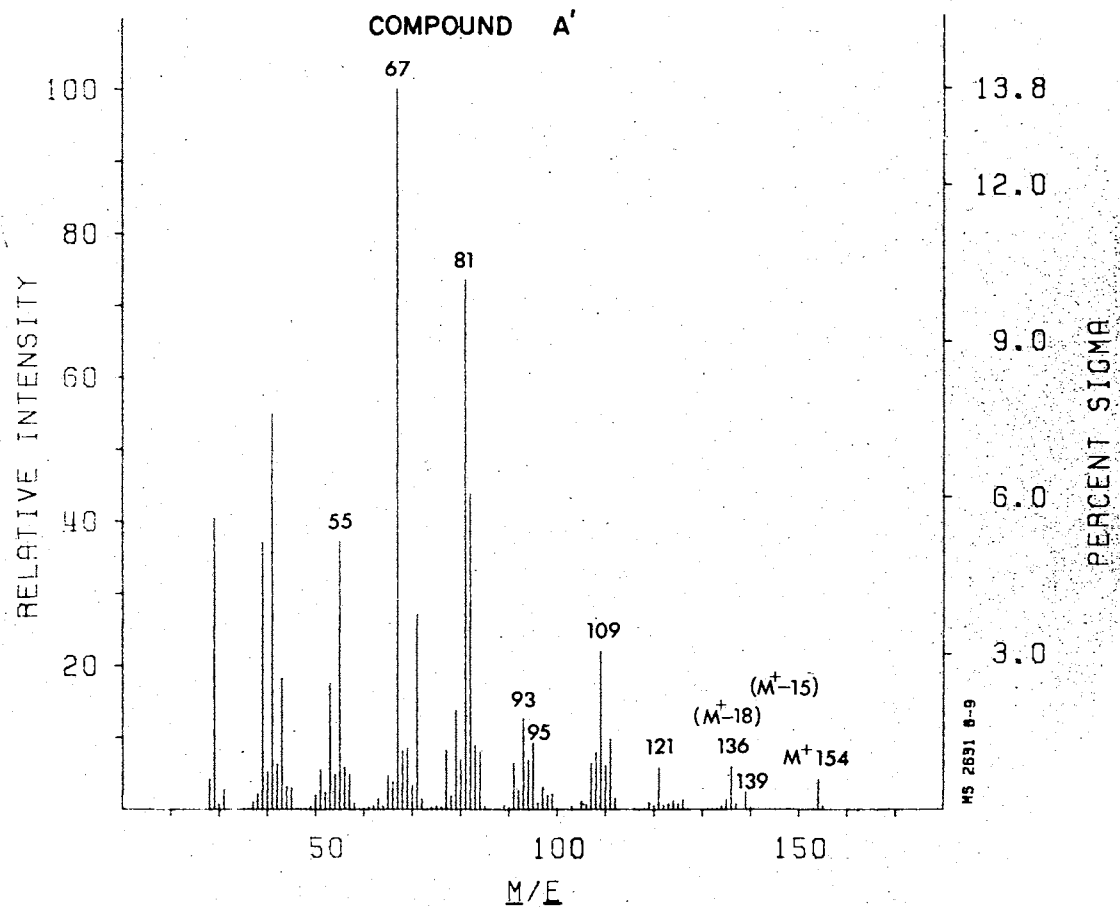column and conditions were the same as shown in Figure
10.

Figure 15. Mass Spectrum of Compound A'.

corresponding ions in the mass spectra of dihydronepetalactone and
nepetalactone. Loss of water was also found in its spectrum and these
data led to the proposed structure and fragmentation pattern shown in
Scheme V. The molecular ion of A' was M^+ 154. It can undergo loss of
a methyl group yielding ion cc, m/e 139 or it can lose water to yield
ion cd, m/e 136 or it may lose a COOH fragment to form ion ce, m/e 109.
The last two transitions were verified by metastable ions at m/e 120.1
and m/e 77.1 respectively. Ion cc, m/e 139 can undergo loss of water
to yield ion cf, m/e 121. Ion cd, m/e 136 may lose a C_2HO fragment to
yield ion cg, m/e 95. Ion ce, m/e 109 can lose C_2H_4 to yield ion ch,
m/e 81. Ion cg, m/e 95 may undergo loss of C_2H_4 to yield ion ci, m/e
67. This transition was verified by a metastable ion at m/e 47.3. Ion
ch, m/e 81 can lose C_2H_2 to yield ion cj, m/e 55. This transition was
verified by a metastable ion at m/e 37.3. Ion ci, m/e 67 can lose C_2H_2
to yield ion ck, m/e 41. This transition was verified by a metastable
ion at m/e 25.1. The similarity of the mass spectrum of component A' to
the mass spectra of dihydronepetalactone and to compound III-D allowed a
tentative structure to be proposed (Scheme V).

Compounds B' and C' were shown by mass spectral analysis to be
dihydronepetalactone diastereoisomers, comprising 90% of the volatile
fraction. Both compounds have mass spectra very similar to that of
authentic dihydronepetalactone, which was obtained by hydrogenation of
nepetalactone, shown in Figure 7. Compound C' was shown by comparison
of gas chromatography retention times and mass spectra to be identical
to dihydronepetalactone synthesized from nepetalactone.

Compounds A', B' and C' were purified by preparative gas chromatog-
raphy and their amounts of radioactivity were determined by liquid

OH

M⁺ 154

·COOH

H₂O

·CH₃

OH

ce, m/e 109

cd, m/e 136

cc, m/e 139

C₂H₄

·C₂HO

·CH₃

H₂O

ch, m/e 81

cg, m/e 95

cf, m/e 121

C_4H_7

C_5H_7

C₂H₂

C₂H₄

cj, m/e 55

ci, m/e 67

C₂H₂

C_3H_5

ck, m/e 41
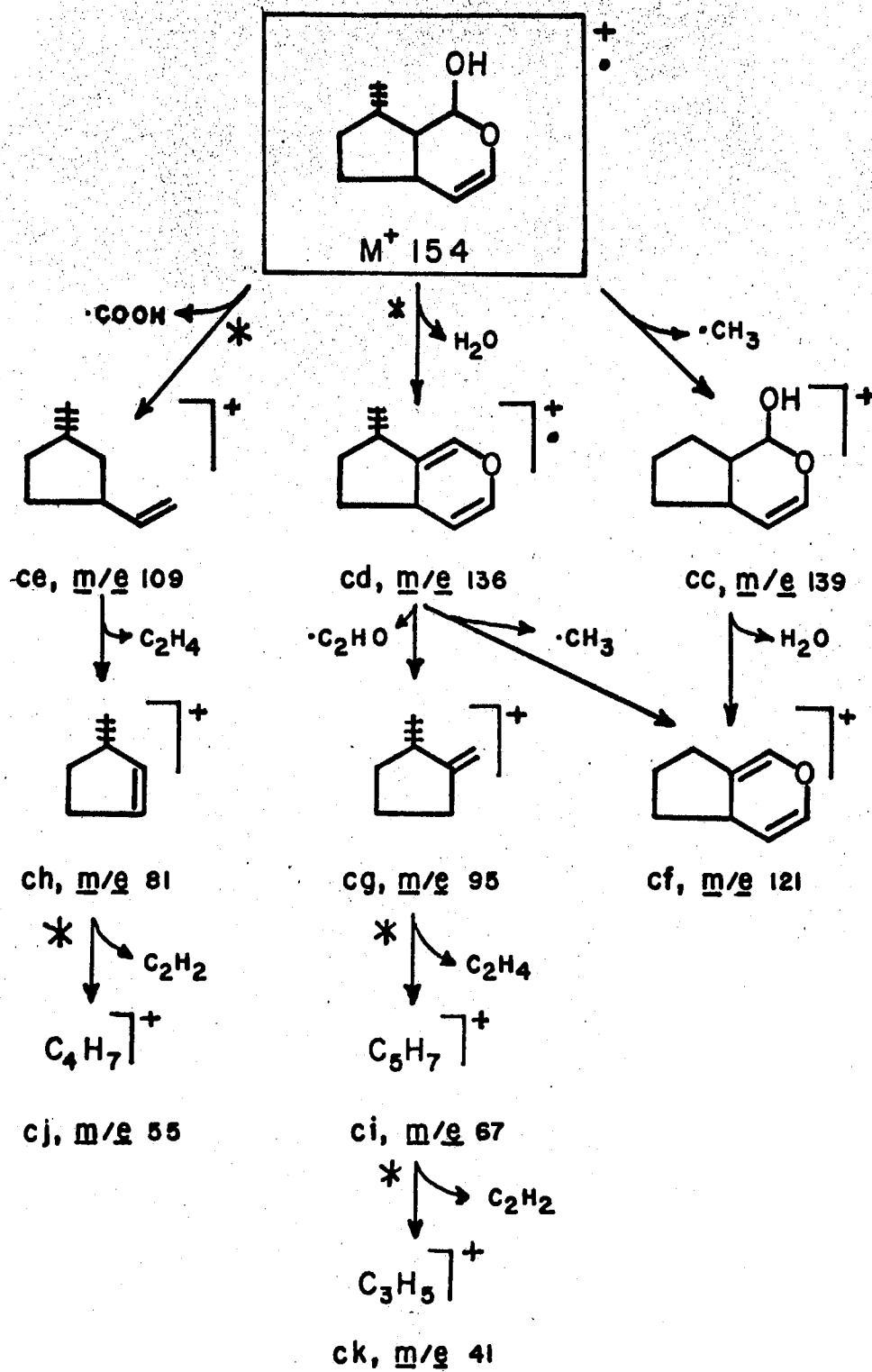
Scheme V. Proposed Partial Fragmentation of Component A'.

scintillation spectrometry. Table XI shows the incorporation of radio-
activity and specific activities for these compound. The specific
activity of compound A' was found to be 1,003 dpm/mg, which was consid-
erably less than the specific activity of administered dihydronepetal-
actone-G-^{14}C (18,400 dpm/mg). The specific activities of B' and C' were
found to be 624 and 450 dpm/mg, respectively. Based on these data it
was concluded that upon treatment with 2N HCl, dihydronepetalactone was
either released from a bound non-steam-volatile form or chemically syn-
thesized from some non-steam-volatile component left in the residue.
The 30- to 40-fold dilution of the specific activities of B' and C'
indicated an unlabeled pool of dihydronepetalactone was either present
(endogenous) or formed by acid catalysis. Acid catalysis would most
likely result in hydrolysis of a glucosidic linkage, isomerization of
the naturally occurring isomer of dihydronepetalactone and/or release
of protein-bound dihydronepetalactone. Compound A' may also have been
formed or released by acid catalysis, since its specific activity was
similar to those of B' and C'.

The average amount of dihydronepetalactone found in the steam-
volatile fraction from N. cataria plants is about 0.002 mg/gm fresh
weight. This can be contrasted to the concentration of nepetalactone,
the major component of the crude oil which is 1-2 mg/gm fresh weight
(19). The weights of the plants used in these experiments were about
200 grams, therefore their crude oils contained about 0.4 mg of di-
hydronepetalactone each. From 11 to 15 mg of labeled dihydronepetalac-
tone was administered, however, more than 15 mg were isolated from the
crude oil of the acid treated residue. Since 1-2 mg of dihydronepetal-
actone was recovered by steam distillation from each of the plants used

TABLE XI

MAJOR COMPOUNDS OF THE CRUDE OIL OBTAINED
FROM THE HCL-HYDROLYSIS OF THE RESIDUE
REMAINING FROM DIHYDRONEPETALACTONE-
G-^{14}C-METABOLISM (EXP. II)

Compounds	Quantity	Radioactivity	
		Total	Sp. Act.
	mg	dpm	dpm/mg
A'	1.4	1,425	1,003
B'	11.1	6,950	624
C'	4.1	1,850	450

in the biosynthesis experiments, the total recovered dihydronepetalactone was about 17-18 mg. Preparative gas chromatography was used to purify dihydronepetalactone before determination of the amount present, and since it results in the loss of approximately 50% of material, the actual total amount of dihydronepetalactone was calculated to be in excess of 30 mg. This led to the conclusion that there must be a large amount of dihydronepetalactone stored in the plant in a non-steam-volatile form and it was released or formed by acid treatment.

Compound A', which was postulated to have a methylcyclopentane monoterpenoid structure, having only 9 carbon atoms, with a methyl group at position 8 missing. This compound may be classified as a degenerate monoterpenoid, and is likely a catabolite of dihydronepetalactone, released from the plant residue by the acid treatment. The catabolism of nepetalactone-G-^{14}C to $^{14}CO_2$ has been initially shown in this laboratory. Thus degradation of these types of compounds could proceed through a degenerate monoterpenoid to CO_2.

A suggestion for further study would be to steam distill N. cataria plants, then hydrolyze the residue with 2N HCl, repeat the steam distillation step, isolate the crude oil and analyze this oil for major components. A comparison of this analysis to a similar one for plants treated with dihydronepetalactone could provide valuable data concerning the natural occurrence of A', B' and C', thus yielding useful information on the biosynthesis of methylcyclopentane monoterpenoids in N. cataria.

2. Nepetadiol-G-^{14}C Metabolism

Two nepetadiol-6-^{14}C biosynthesis experiments were conducted. In experiment I, 5.7 mg (150,000 dpm) of nepetadiol-G-^{14}C (specific activity of 26,316 dpm/mg) were administered to a twelve-week old N. cataria plant. The plant was allowed to metabolize for 10 hours, then the plant was analyzed as described previously. In experiment II, 12.5 mg (150,000 dpm) of nepetadiol-G-^{14}C (specific activity of 12,000 dpm/mg) were administered to a sixteen-week old N. cataria plant. After 18 hours the plant was analyzed as before. In experiment I a methanol extraction was conducted on the plant residue following steam distillation, then the residue from this extraction was treated with 2N HCl for 2 hours at 90-100°C and then steam distilled again. In experiment II the residue from the steam distillation was hydrolyzed with 2N HCl for 2 hours at 90-100°C, then steam distilled again. Table XII shows the distribution of radioactivity in the fractions from these plants. In both cases only a small amount of the label was found in the initial steam-volatile crude oils (3,200 and 1,100 dpm, respectively). Since nepetadiol-G-^{14}C was not steam-volatile, any unreacted nepetadiol-G-^{14}C would not be found in this fraction. In the methanol extraction of the residue from experiment I, 88,889 dpm were found. The residue from this extract was found to contain 55,300 dpm, thus 98.2% of the total radioactivity administered was recovered. When this methanol-extracted residue was treated with 2N HCl and steam distilled again, only a negligible amount of label (560 dpm) was obtained in the volatile fraction. In experiment II, the steam-volatile fraction obtained from the HCl-treated residue contained 12,400 dpm while the residue contained 128,000 dpm. This amounted to a 94.3% recovery of the administered radioactivity.

TABLE XII

RADIOACTIVITY DISTRIBUTION IN <u>NEPETA</u> <u>CATARIA</u>
PLANTS FED NEPETADIOL-G-^{14}C

Exp.	Crude Oil	Residue	MeOH Ext.	Residue	HCl Hydrolysis	Residue
	dpm	dpm	dpm	dpm	dpm	dpm
I	3,200	118,000	88,889	55,330	560	45,000
II	11,000	--	71,520	15,100*	12,400	128,000*

150,000 dpm of nepetadiol-G-^{14}C were injected into each plant.

*In experiment I the methanol extraction was conducted first, then treated with HCl, however, in experiment II, this procedure was reversed, so 128,000 dpm is the amount of radioactivity present in the residue after HCl hydrolysis, while 15,100 dpm is the amount of label in the residue after methanol extraction and HCl hydrolysis.

Analysis of the crude oils from the initial steam distillation yielded purified cis-trans nepetalactone and trans-cis nepetalactone fractions with negligible incorporation of label. Table XIII shows the results of the preparative gas chromatography analysis of these crude oils. The incorporation into cis-trans nepetalactone was 0.08% in experiment I and 0.25% in experiment II, while the incorporation into trans-cis nepetalactone was 0.03% in experiment I and 0.12% in experiment II. These values were small, about 25% of the comparable incorporation values from dihydronepetalactone-G-^{14}C. Compound III-D was not present in the nepetadiol-treated plants.

The methanol extract of the steam distillation residue from experiment I, containing 88,889 dpm, was analyzed by thin-layer chromatography. The results indicated almost all of the radioactivity was present in the lower half of the plate. This plate was divided into one centimeter bands and bands 2 through 5 were shown to contain approximately 40,000 dpm while bands 6 plus 7 also contained approximately 40,000 dpm. The bands above band 7 contained no significant amounts of radioactivity. Analysis of bands 2, 3, 4 and 5 by gas chromatography-mass spectrometry yielded almost no volatile material. Bands 6 plus 7 contained several volatile components. Figure 16 shows the total ion current tracing of the GC-MS analysis of TLC bands 6 plus 7 from nepetadiol-G-^{14}C biosynthesis experiment I. Peak I was identified as cis-trans nepetalactone, while peaks II and III were identified as dihydronepetalactone diastereoisomers. No nepetadiol was recovered from any of the fractions. The remainder of the methanol extract was steam distilled, however, no significant amounts of label were found in the steam volatile fraction while approximately 46,000

TABLE XIII

RADIOACTIVITY DISTRIBUTION AMONG THE PREPARATIVE
GAS CHROMATOGRAPHY FRACTIONS FROM THE
NEPETADIOL-G-^{14}C METABOLISM EXPERIMENTS

Fraction	Amt.	Radioactiv-ity	Specific Activ-ity	Incorp.
	mg	dpm	dpm/mg	%
Exp. I				
cis-trans Nepetalactone	7.1	120	17	0.08
trans-cis Nepetalactone	0.8	48	60	0.03
Exp. II				
cis-trans Nepetalactone	4.0	248	62	0.25
trans-cis Nepetalactone	0.2	182	828	0.12

10 Ft. x 1/4 In. Glass Column
25% Apiezon L On Anakrom ABS
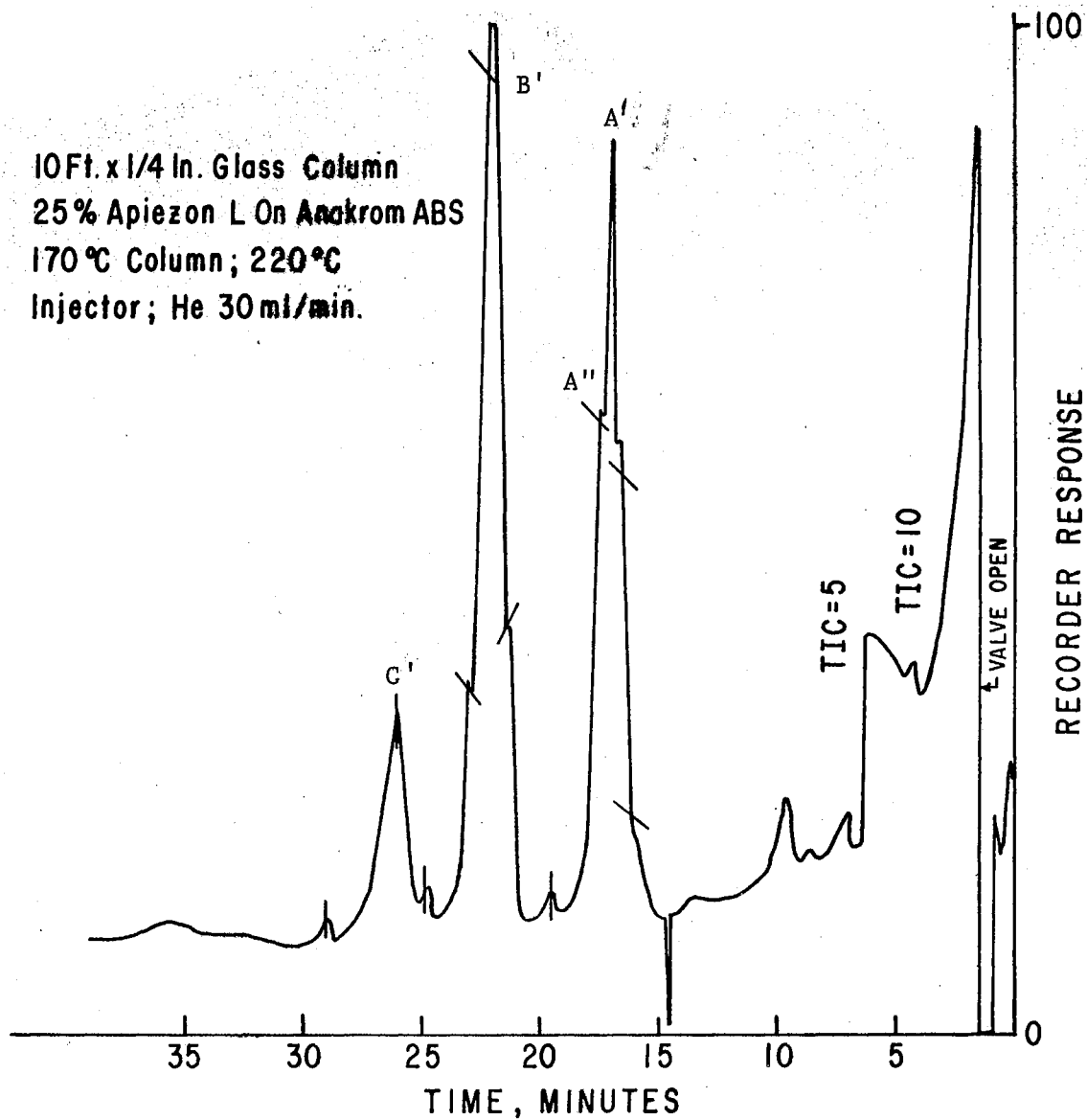170°C Column; 220°C
Injector; He 30 ml/min.

Figure 16.   Total Ion Current Tracing of the GC-MS Analysis of TLC
            Band 6-7.

dpm was found in the residue. Since no radioactivity was present in the volatile fraction GC-MS analysis was not done.
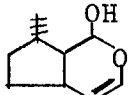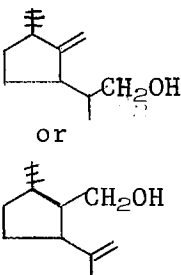
In experiment II, the residue from the initial steam distillation was treated with 2N HCl for 2 hours at 100°C then steam distilled. Analysis of this steam volatile fraction, (12,400 dpm) by gas chromatography-mass spectrometry showed the occurrence of several peaks. Preparative gas chromatography was used to purify these fractions, which correspond to those obtained from the steam-volatile fraction of the HCl-hydrolyzed residue of the dihydronepetalactone-G-^{14}C experiments. Two dihydronepetalactone isomers and compound A' were again identified, however, another component (A") which could not be completely resolved from A', was found. A" was not present in the dihydronepetalactone-G-^{14}C fractions. This mixture of A' plus A" contained most of the radioactivity (7,400 dpm) originally found in the steam volatile fraction from the HCl-treated residue. The approximate relative amounts of A' and A" were 75% and 25%, respectively. Table XIV shows the relative intensities of selected fragment ions from the mass spectra, as well as a tracing of the gas chromatographic separation of A' and A". Mass spectrum 6 corresponds to A', spectrum 8 to A" and spectrum 7 to a mixture of the two. The base peak in all cases was $\underline{m/e}$ 81. The molecular ion was at $\underline{m/e}$ 154 for both compounds. Table XV shows the transitions denoted in the mass spectra of A' and A" while the tentative structures of A' and A" are shown below. The spectra of these two components are similar but several important differences allowed the assignment of tentative structures. The explanation of the mass spectrum of A' and the criteria for assignment of a tentative structure have been discussed in the dihydronepetalactone-G-^{14}C metabolism section. The reasons for

TABLE XIV

RELATIVE INTENSITIES OF SELECTED FRAGMENT
IONS FROM THE MASS SPECTRA OF
COMPOUNDS A' AND A"

7 6 (A')

(A") 8

9   5

10

TIME
MINUTES
(MS No. 2658)
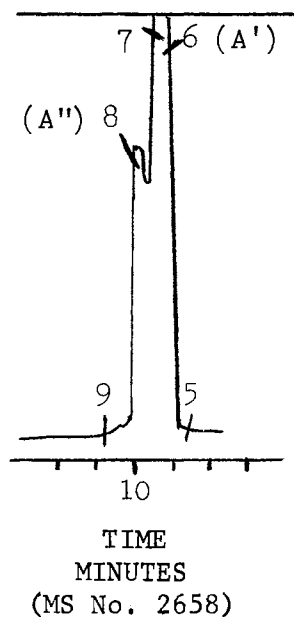
m/e	Relative Intensities		
	A' (6)	A' + A" (7)	A" (8)
	%	%	%
154	7.0	5.7	16.2
139	2.2	2.2	2.9
136	10.2	9.0	15.6
123	–	1.7	28.4
121	10.7	8.9	22.0
111	11.9	15.0	4.1
109	31.8	33.4	22.6
107	8.5	9.0	30.2
95	6.0	10.4	55.5
94	9.8	9.0	46.5
93	17.4	17.5	29.0
91	10.9	8.1	–
82	58.5	58.8	27.8
81	100.0	100.0	100.0

TABLE XV

TRANSITIONS DENOTED IN THE MASS SPECTRA OF
PEAKS A' AND A"

Distribution	Transition Denoted	Probable Neutral Product	Metastable Ion Observed
Common to A' and A"	$(154)^{+\cdot} \longrightarrow (139)^+ + 15$	$\cdot CH_3$	
	$(154)^{+\cdot} \longrightarrow (136)^{+\cdot} + 18$	H_2O	
	$(136)^{+\cdot} \longrightarrow (121)^+ + 15$	$\cdot CH_3$	
(A')	$(139)^+ \longrightarrow (121)^+ + 18$	H_2O	
	$(154)^{+\cdot} \longrightarrow (111)^+ + 43$	$\cdot C_2H_3O$	
	$(136)^{+\cdot} \longrightarrow (95)^+ \quad 41$	$\cdot C_2HO$	
	$(109)^{+\cdot} \longrightarrow (81)^+ + 28$	C_2H_4	
	$(95)^{+\cdot} \longrightarrow (93)^+ + 2$	H_2	
(A") or	$(93)^{+\cdot} \longrightarrow (91)^+ + 2$	H_2	89.2
	$(109)^+ \longrightarrow (82)^{+\cdot} + 27$	$\cdot C_2H_3$	
	$(121)^{+\cdot} \longrightarrow (94)^+ + 27$	$\cdot C_2H_3$	
A" only	$(154)^{+\cdot} \longrightarrow (123)^+ + 31$	$\cdot CH_2OH$	
	$(154)^{+\cdot} \longrightarrow (95)^+ + 59$	C_3H_7O	
	$(154)^{+\cdot} \longrightarrow (109)^+ + 45$	$\cdot C_2H_5O$	77.2
A' only	$(154)^{+\cdot} \longrightarrow (109)^+ + 45$	$\cdot COOH$	77.2
	$(93)^+ \longrightarrow (91)^+ + 2$	H_2	89.2

the assignment of these tentative structures to A" were several-fold.

A number of common transitions were found in the mass spectra of A' and

A", however, the transitions which were not common were more important

in structure elucidation. In A" the transition from m/e 154 to m/e 123

losing a CH_2OH fragment (M^+-31) was found, but was absent in the spec-

trum of A'. The transition, m/e 93 to m/e 91 was present in the mass

spectrum of A' but not in the spectrum of A". Formation of fragment ions

m/e 95, m/e 109 and m/e 121 was found in both spectra, but the pathways

of formation of these ions were postulated to be different. No detailed

fragmentation study will be presented, however, comparison of the two

components mass spectra indicated that the assigned tentative structures

were reasonable. The determination of the amounts of A' + A" was

achieved using analytical gas chromatography and the specific activity

of this A' + A" fraction was found to be 4545 dpm/mg. The postulated

structures of A" were both monodehydrated forms of nepetadiol. Nepeta-

diol-G-^{14}C was not recovered from any fraction in either experiment,

however, radioactivity was found throughout the different fractions.

Repeated analysis failed to isolate nepetadiol-G-^{14}C. Since A' comprises

75% of the mixture of A' plus A", the specific activity of A" could be

higher than 4545 dpm/mg. The specific activity of the administered

nepetadiol-G-^{14}C in experiment II was 12,000 dpm/mg so A" could be

derived directly from injected nepetadiol-G-^{14}C by dehydration, perhaps

as a result of acid treatment. It may also be possible that A' was

formed from nepetadiol-G-^{14}C.

In the methanol extract of the HCl-treated steam distillation

residue from experiment II, 71,520 dpm were found. Analysis of this

extract failed to yield any nepetadiol-G-^{14}C. Further analysis failed

to yield any significant difference from the results of the analysis of the methanol extract from experiment I.

These results have indicated that nepetadiol-G-^{14}C was converted to the nepetalactone isomers only to a minor extent. Compound A' was isolated from the plant after HCl-treatment as well as compound A" which was postulated to be a dehydrated form of nepetadiol-G-^{14}C.

Further analysis of the methanol extracts was not done, however, studies on the metabolism of nepetadiol-G-^{14}C in the future should incorporate different fractionation methods, which allow nepetadiol-G-^{14}C to be recovered.

C. Occurrence of Actinidine

1. Isolation of Actinidine from Valeriana Officinalis

Actinidine was found to be present in the dried roots of Valeriana officinalis. The alkaloid was isolated using the method of Tórssell and Wahlberg (56) combined with gas chromatography, thin-layer chromatography and mass spectrometry. Figure 17 shows a thin-layer chromatogram of the chloroform : methanol (5 : 2) extract of dried V. officinalis roots. Only bands which reacted positively with Dragendorff's reagent are shown on this chromatogram. The band with an R_f value of 0.90 was shown to be actinidine by combination gas chromatography-mass spectrometry on an 8 foot, 3% OV-1 column. Figure 18 shows the recorder tracing of the combination gas chromatography-mass spectrometry analysis of the thin-layer band with an R_f of 0.90. The slash marks indicate where mass spectra were taken. Peak 2 was identified as actinidine by its mass spectrum and by co-chromatography on a 12 foot, 15% Carbowax 20 M column with the column temperature held at 200°C, the injector
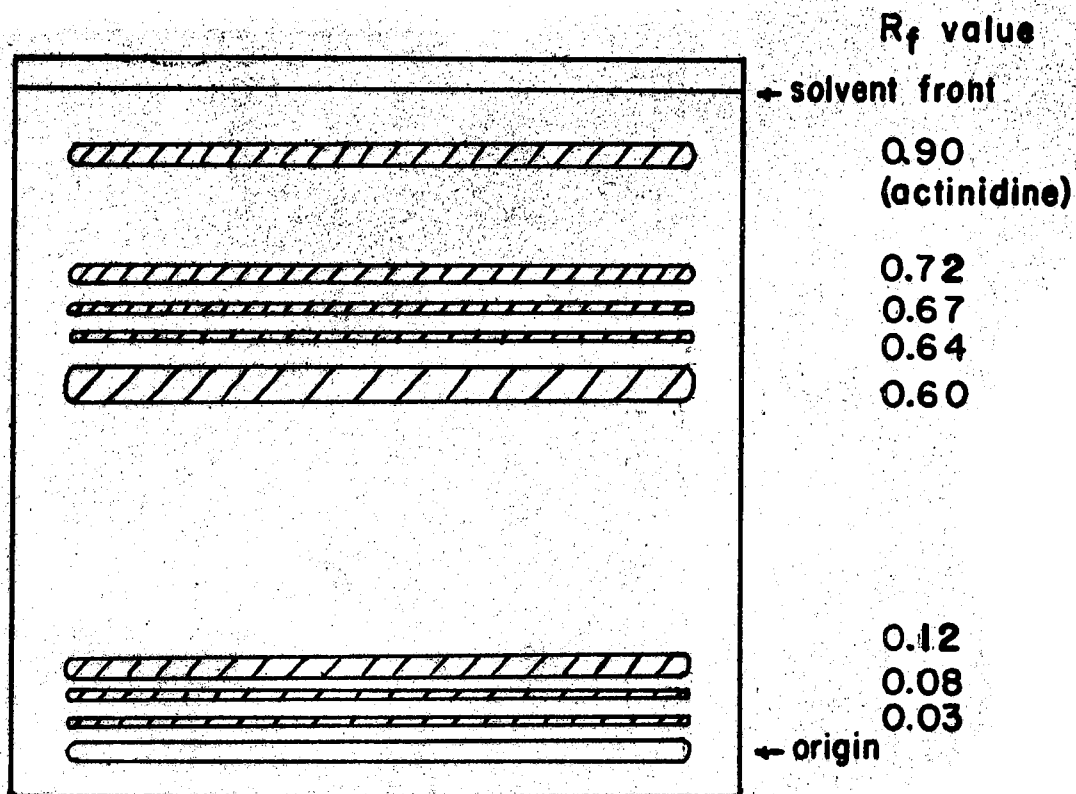
Figure 17.   Thin-Layer Chromatogram of the Chloroform : Methanol
             Extract of Dried <u>Valeriana</u> <u>Officinalis</u> Roots.
             Only bands which reacted positively with Dragen-
             dorff's reagent are shown. The chromatogram was
             developed in ethyl acetate : methanol : ammonium
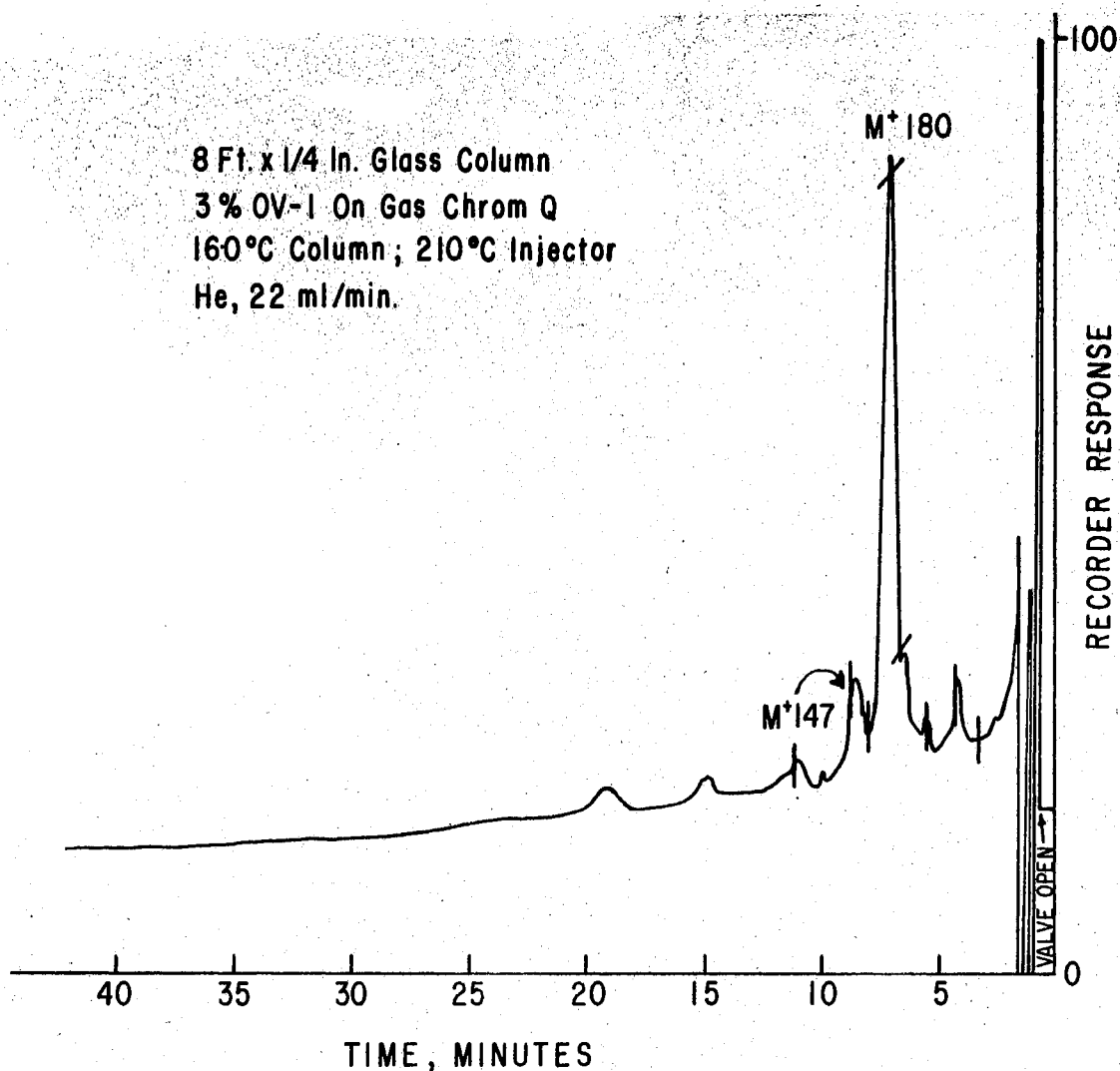   hydroxide (45 : 35 : 20, v/v/v).

Figure 18. Total Ion Current Tracing of the Thin-Layer Purified
Band of R_f = 0.90. The slash marks along the
tracing indicate the point at which mass spectra
were taken. The column, 8 feet x 1/4 inches, was
packed with 3% OV-1 on Gas Chrom Q. The operation-
al parameters were: column temperature of 160°C,
injector temperature, 220°C and He flow rate of 22
ml/min.

temperature held at 225°C and the helium flow rate held at 70 ml/min.
With both standard actinidine and isolated actinidine injected simul-
taneously only one symmetrical peak resulted at a retention time of 13.5
minutes. Analysis of these two samples separately yielded similar
peaks at 13.5 minutes. Mass spectra of the isolated compound were very
similar to that of authentic actinidine previously published (70).
Figure 19 shows the mass spectrum of isolated actinidine. Scheme VI
shows the proposed partial fragmentation of actinidine. The molecular
ion was observed at m/e 147. This ion can undergo loss of one of two
methyl groups to form ion aa, m/e 132 and ion ab, m/e 132. This tran-
ition was verified by a metastable ion at m/e 118.2. Ions aa, m/e 132
and ab, m/e 132 can undergo loss of the remaining methyl group to yield
ion ac, m/e 117. This transition was verified by a metastable ion at
m/e 103.7. Ion aa, m/e 132 and ion ab, m/e 132 and ion ab, m/e 132 may
also undergo loss of C_2H_5N to form ion ad, m/e 91 and C_2H_7N to yield
ion ae, m/e 89. Ion ac, m/e 117 can lose C_2H_3N to yield ion af, m/e
77, while ion ad, m/e 91 can lose C_2H_2 to form ion ag, m/e 65. Ion ae,
m/e 89 can undergo loss of C_2H_2 to yield ion ah, m/e 63.

These data confirmed the identification of actinidine as a com-
ponent of the dried roots of V. officinalis, and were published recently
(32).

2. Variation in the Composition of the Steam-Volatile Distillate of Actinidia Polygama Miq. With Respect To Time.

Actinidine has been found to be present in the steam-volatile
fraction of Japanese A. polygama plants (24) and in A. polygama plants
grown at this institution (71). These plants were first grown at this
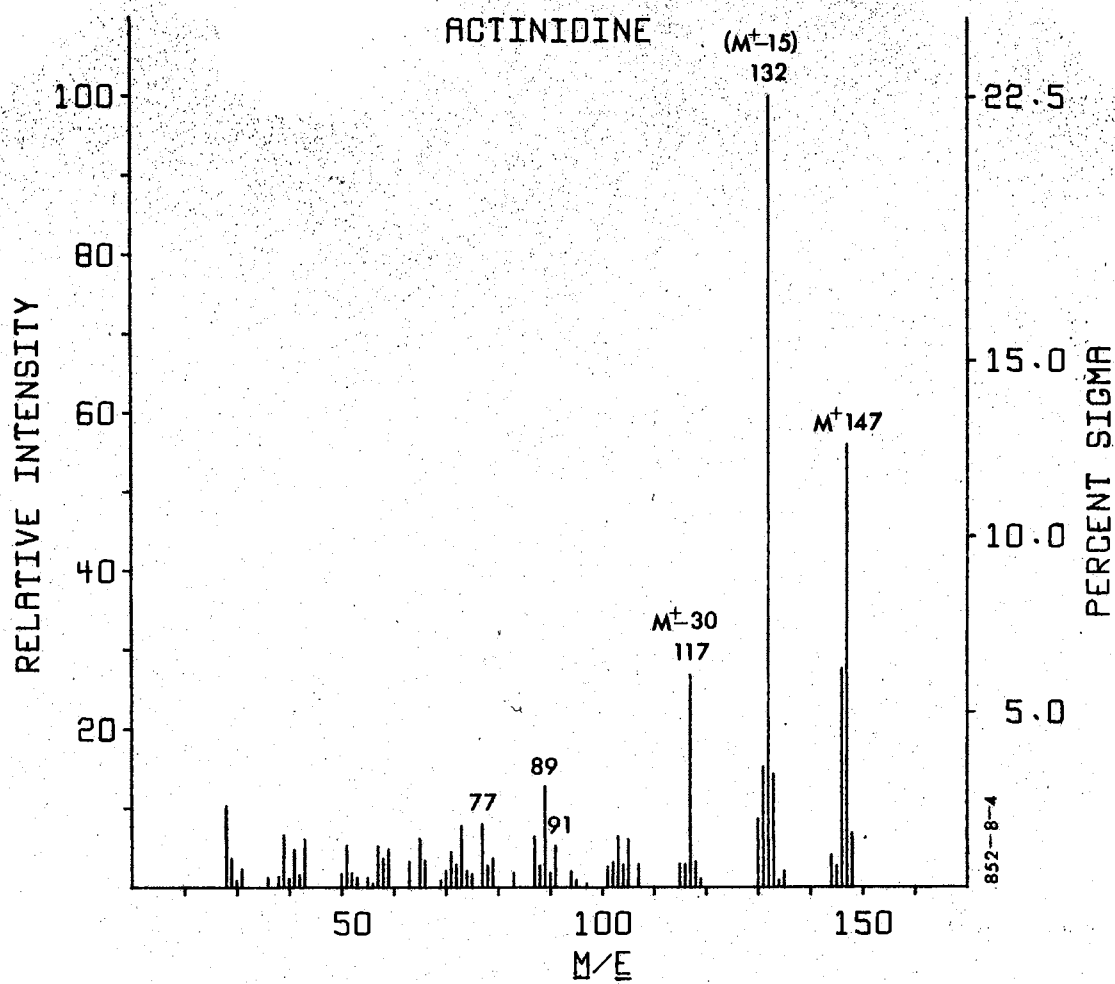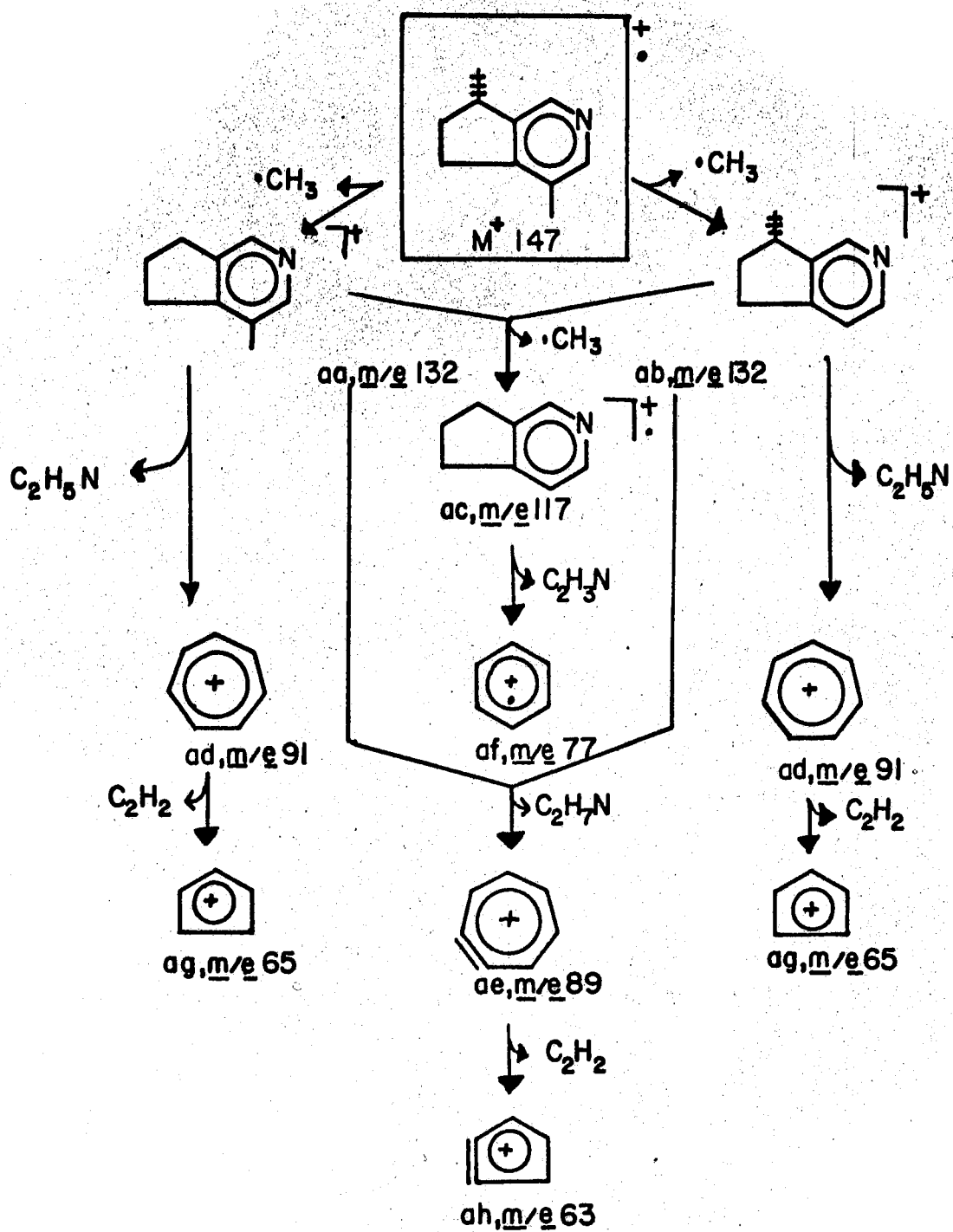
Figure 19. Mass Spectrum of Actinidine.

Scheme VI. Proposed Partial Fragmentation of Actinidine.

institution in 1965 and actinidine was always found to be one of the

major constituents of the steam-volatile distillate. However, during

the winter months (October through March), the plants were into dormancy

and no actinidine was found in the distillate of these dormant plants.

These plants could no longer grow tendrils, and the leaves became

larger and darker in color, however, no other physical signs of dormancy

were observed . Production of actinidine in the plants occurred soon

after the breaking of dormancy; however the relative amount of actini-

dine was observed to decrease each summer from 1965-1968. Finally, in

1969, the plants no longer produced detectable amounts of actinidine.

In Figure 20 the gas-liquid chromatography tracings of the steam-

volatile distillates from plants grown and harvested in Japan in 1967

and from plants grown in Stillwater and harvested in August of 1969 are

shown. Analysis of a similar distillate obtained from Stillwater-

grown plants in 1965 and 1966 may be found in reference (71). In the

Japanese steam-volatile distillate tracing, the large peak at a reten-

tion time of 20 minutes was shown to be actinidine by mass spectrometry.

In the tracing of the August, 1969 steam-volatile distillate essentially

no actinidine was present. From 1969 to the present, no actinidine

was detected in the distillate from A. polygama plants. Table XVI shows

the decrease in the amount of actinidine in the steam-volatile distil-

lates of A. polygama plants with time.

From these data it can be concluded that actinidine was no longer

produced by A. polygama plants in significant amounts after August 1968.

The probable cause for this change in metabolism was the change in en-

vironment the plants underwent when brought to this institution from

Japan, where they grow only above 2,000 feet. Such factors as soil
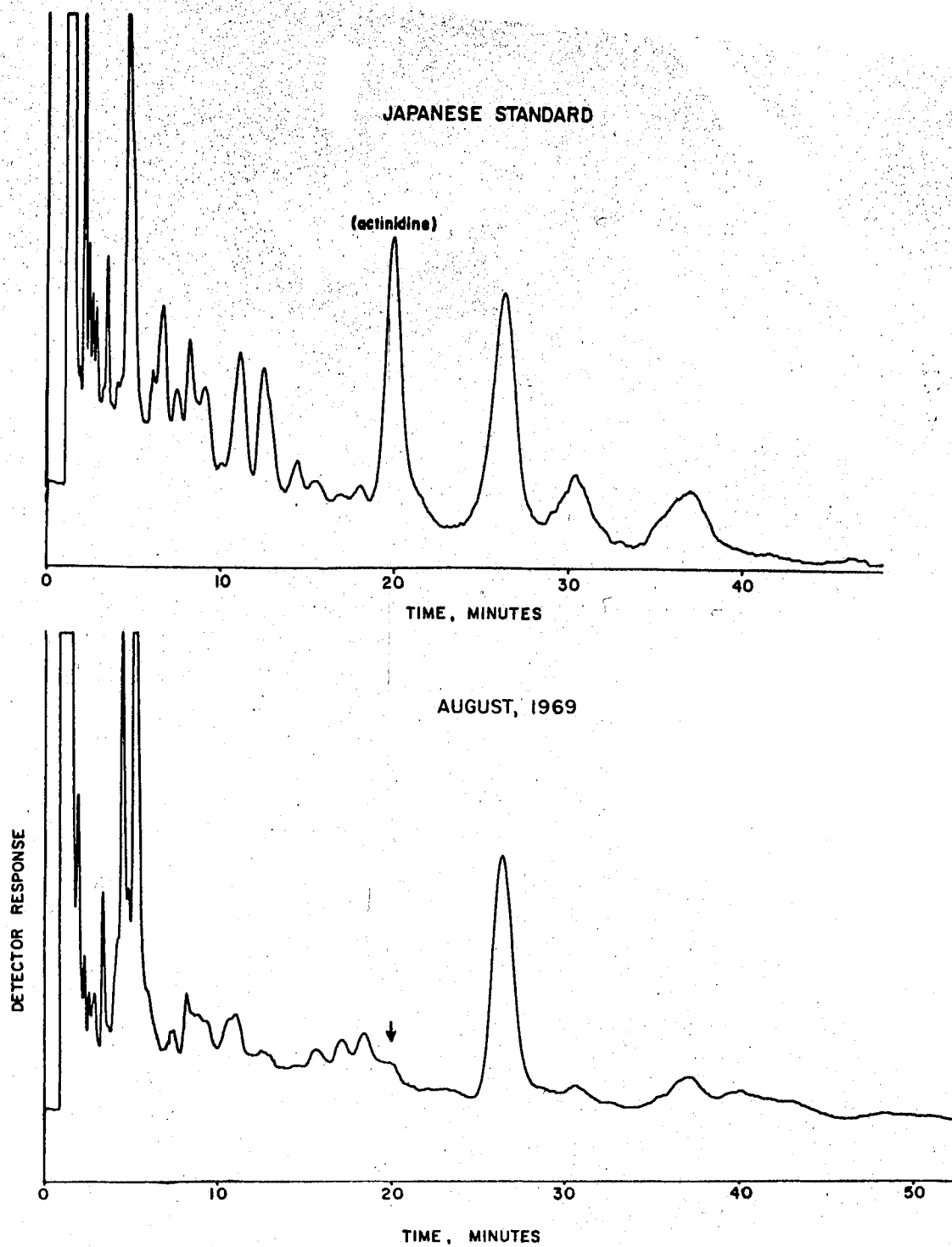
Figure 20. Gas Chromatography Tracing of the Steam-Volatile Fractions from Japanese and Locally-Grown <u>Actinidia polygama</u> Plants.

TABLE XVI

VARIATION IN THE AMOUNT OF ACTINIDINE IN THE
STEAM-VOLATILE DISTILLATE FROM ACTINIDIA
POLYGAMA MIQ. PLANTS WITH TIME

Steam-Volatile Distillate	Harvest Date	Amount of Actinidine
OSU Reference Plants (71)	Summer of 1965	++
	April-Oct.1966	++
	July 1967	++
Japanese Reference Plants		
No. 1	August 1967	++
No. 2	August 1967	++
OSU Plants	August 1968	++
OSU Plants	February 1969	-
OSU Plants	August 1969	-
OSU Plants	May 1970	-
OSU Plants	July 1970	-
OSU Plants	May 1971	-

++ = Major Component

- = Not Detectable

conditions, altitude, day, length, temperature and humidity may have been responsible for this severe metabolic change. It was of interest to note that no outward physical changes in these plants were observed when the production of actinidine ceased.

CHAPTER IX

SUMMARY

The purpose of the research described in part I was to determine the relationship between the pyridine nucleotide cycle and ricinine biosynthesis in Ricinus communis L. The approach used in this study was to compare the incorporation of radioactivity from several precursors into ricinine and into the pyridine nucleotide cycle intermediates in the absence and presence of several inhibitors, some of which have been shown to inhibit the pyridine nucleotide cycle in animals. The purpose of the work in part II was to develop a rapid and easy synthesis of dihydronepetalactone-G-^{14}C and nepetadiol-G-^{14}C for metabolism studies in Nepeta cataria and to study the occurrence of actinidine in Actinidia polygama Miq. and Valeriana officinalis. Modern microanalytical instruments were used for structure determination and identification.

The biosynthesis of ricinine from quinolinic acid through the pyridine nucleotide cycle was confirmed. Pyridine nucleotide cycle inhibitors were used to confirm the obligatory role of the pyridine nucleotide cycle in the biosynthesis of ricinine. A metabolic grid was proposed to account for the similarity in incorporation levels of the pyridine nucleotide cycle intermediates and quinolinic acid into ricinine. Quinolinic acid decarboxylase, which converts quinolinic acid and phosphoribosyl pyrophosphate to nicotinic acid mononucleotide, was postulated as the site of inhibition of azaleucine. This compound has

not previously been shown to be an inhibitor of the pyridine nucleotide cycle. Nicotinamide adenine dinucleotide synthetase, which converts nicotinic acid adenine dinucleotide to nicotinamide adenine dinucleotide, was postulated as the site of inhibition of azaserine. This is the first report of the inhibition of the pyridine nucleotide cycle in plants and of the inhibition of alkaloid biosynthesis in plants.

Rapid, easy synthesis procedures for dihydronepetalactone-G-^{14}C and nepetadiol-G-^{14}C were developed. Upon admimistration of dihydro-nepetalactone-G-^{14}C to Nepeta cataria plants, incorporation of label into cis-trans nepetalactone, trans-cis nepetalactone and a new methyl-cyclopentane monoterpenoid found only in plants administered large doses of dihydronepetalactone, was shown. A structure for this unknown compound was postulated. Incorporation of label into another unknown compound, which was postulated to be a degenerate C_9 methylcyclopentane monoterpenoid, was also shown. Incorporation of label into these compounds from nepetadiol-G-^{14}C was not found.

Actinidine was isolated and identified as a component of Valeriana officinalis roots. The disappearance of actinidine, a major component in the steam-volatile fraction of Actinidia polygama Miq. plants, was observed in locally-grown field and greenhouse-plants during the winter of 1968, when the plants went into dormancy. This severe metabolic change might be explained by the environmental changes to which the plants were exposed. Their native habitat is Japan where they grow at an elevation above 2000 feet. Cuttings from specimen plants introduced in Stillwater in 1965 were used in this study.

A SELECTED BIBLIOGRAPHY

(1) Plouvier, V. and Favre-Bonvin, J., Phytochem., 10, 1697 (1971).

(2) Sakan, T., Isoe, S., Hyeon, S. B., Ono, T. and Takagi, I., Bull.
      Chem. Soc. Japan, 37 (12), 1888 (1964).

(3) Cavill, G. W. K., Ford, D. L. and Locksley, H. D., Australian J.
      Chem., 9, 288 (1956).

(4) Cavill, G. W. K. and Hinterberger, H., Australian J. Chem., 13,
      514 (1960); Chem. Abstr., 55, 9695 (1961); Chem. Abstr., 57,
      11679 (1962); Chem. Abstr., 58, 8258 (1963).

(5) Trave, R. and Pavan, M., Chem. and Ind., 38, 1015 (1956).

(6) Clark, K. J., Fray, G. I., Jaeger, R. H. and Robinson, R., Tetra-
      hedron, 6, 217 (1959).

(7) Meinwald, J., Chadha, M. S., Hurst, J. J. and Eisner, T., Tetra-
      hedron Letters, 29 (1962).

(8) Cavill, G. W. K. and Whitfield, F. B., Australian J. Chem., 17,
      1245, 1260 (1964).

(9) McElvain, S. M., Bright, R. D. and Johnson, P. R., J. Am. Chem.
      Soc., 63, 1558 (1941).

(10) Bates, R. B., Eisenbraun, E. J. and McElvain, S. M., J. Am. Chem.
      Soc., 80, 3420 (1958).

(11) Bates, R. B. and Sigel, C. W., Experientia, 19, 564 (1963).

(12) Sakan, T., Isoe, S., Hyeon, S. B., Katsumura, R., Maeda, T.,
      Wolinsky, J., Dickerson, D., Slabaugh, M. and Nelson, D.,
      Tetrahedron Letters, 4097 (1965).

(13) McGurk, D. J., Degradation Studies and Structure Proof of cis-cis
      Nepetalactone, Ph.D. Thesis, Oklahoma State University, July,
      1968.

(14) Purohit, R. M. and Nigem, S. S., J. Univ. Saugar, Pt. II, Sect. A,
      8, 46 (1959); Chem. Abstr., 57, 2353 (1962).

(15) Regnier, F. E., Waller, G. R. and Eisenbraun, E. J., Phytochem.,
      6, 1281 (1967).

(16) Meinwald, J., _J. Am. Chem. Soc._, _76_, 4571 (1954).

(17) Sakan, T., Fujino, A., Murai, F., Suzui, A. and Butsugan, Y., _Bull. Chem. Soc. Japan_, _33_, 1737 (1960).

(18) Trave, R., Marchesini, A. and Garanti, L., _Gazz. Chim. Ital._, _98_, 1132 (1968).

(19) Regnier, F. E., Eisenbraun, F. J. and Waller, G. R., _Phytochem._, _6_, 1271 (1967).

(20) Cavill, G. W. K. and Clark, D. V., _J. Insect. Physiol._, _13_, 131 (1967).

(21) Wolinsky, J. and Nelson, D., _Tetrahedron_, _25_, 3767 (1969).

(22) Hyeon, S. B., Isoe, S. and Sakan, T., _Tetrahedron Letters_, 5325 (1968).

(23) Sutherland, M. D. and Park, R. J., _Terpenoids Plant Proceedings_, Aberystwyth, p. 147 (1966); _Chem. Abstr._, _68_, 47024 (1968).

(24) Sakan, T., Fujino, A., Murai, F., Butsugan, Y. and Suzui, A., _Bull. Chem. Soc. Japan_, _32_, 315 (1959).

(25) Murai, F., _Nippon Kagaku Zasshi_, _81_, 1322 (1960).

(26) Pavan, M., _Ricerca Sci._, _19_, 1011 (1949).

(27) Minato, H., _Chem. Pharm. Bull. Tokyo_, _9_, 625 (1961).

(28) Arthur, H. R., Johns, S. R., Lamberton, J. A. and Loo, S. N., _Australian J. Chem._, _20_, 2505 (1967).

(29) Sakan, T., Fujino, A., Murai, F., Suzui, A. and Butsugan, Y., _Bull. Chem. Soc. Japan_, _32_(10), 1157 (1959).

(30) Sakan, T., Fujino, A., Murai, F., Suzui, A., Butsugan, Y. and Terashima, Y., _Bull. Chem. Soc. Japan_, _33_(5), 712 (1960).

(31) Gross, D., Edner, G. and Schutte, H. R., _Arch. Pharmaz._, _304_, 19 (1971).

(32) Johnson, R. D. and Waller, G. R., _Phytochem._, _10_, 3338 (1971).

(33) Franck, B., _Abh. dtsch. Akad. Wiss Berlin_, 1970 (in press).

(34) Sakan, T., Murai, F., Hayashi, Y., Honda, Y., Shono, T., Nakajima, M. and Kato, M., _Tetrahedron_, _23_, 4635 (1967).

(35) Danilova, A. V. and Konovalova, R. A., _Zhurn. Obschei. Khimii_ (USSR), 22, 2237 (1952); _Chem. Abstr._, _48_, 691a (1954).

(36) Danilova, A. V. and Konovalova, R. A., Zhurn. Obschei. Khimii
(USSR), 26, 2069 (1956); Chem. Abstr., 51, 5098 (1957).

(37) Ubaev, K., Yuldashev, P. K. and Yunusov, S. Y., Uzbeksk. Khim.
Zhurn., 7(3), 33 (1963); Chem. Abstr., 59, 15602a (1963).

(38) Abdusamatov, A., Khakimdzhanov, S. and Yunosov, S. Y., Khim. Prir.
Soedin., 4(3), 195 (1968); Chem. Abstr., 69, 57450a (1968).

(39) Lutfullin, K. L., Yuldashev, P. X. and Yunasov, S. Y., Khim. Prir.
Soedin., 1(5), 365 (1965); Chem. Abstr., 64, 3620c (1966).

(40) Abdusamatov, A., Yagudaev, M. R. and Yunusov, S. Y., Khim. Prir.
Soedin., 4(4), 265 (1968); Chem. Abstr., 70, 68580g (1969).

(41) Torssell, K., Acta Chem. Scand., 22, 2715 (1968).

(42) Dickinson, E. M. and Jones, G., Tetrahedron (London), 25, 1523
(1969).

(43) Arthur, H. R. and Loo, S. N., Phytochem., 5, 977 (1966).

(44) Arthur, H. R., Johns, S. R., Lamberton, J. A. and Loo, S. N.,
Australian J. Chem., 20, 2505 (1967).

(45) Ray, A. B. and Chatterjee, A., Tetrahedron Letters (London), 445
(1966).

(46) Hart, N. K., Johns, S. R. and Lamberton, J. A., Australian J.
Chem., 22, 1283 (1969).

(47) Hammouda, Y. and LeMen, J., Bull. Soc. Chim. France, 2901 (1961).

(48) Hammouda, Y., Plat, M. and LeMen, J., Ann. Pharm. France, 21, 699
(1963).

(49) Hammouda, Y. and Motawi, M. M., Egypt. Pharm. Bull., 41, 73 (1959);
Chem. Abstr., 54, 21646 (1960).

(50) Jones, G., Fales, H. M. and Wildman, W. C., Tetrahedron Letters,
397 (1963).

(51) Djerassi, C., Kutney, J. P., Shamma, M., Schoolery, J. N. and
Johnson, L. F., Chem. and Ind., 210 (1961).

(52) Casinovi, C. G., Garbarino, J. A. and Marini-Bettolo, G. B.,
Chem. and Ind., 253 (1961).

(53) Appel, H. H. and Muller, B., Scientia, 115, 3 (1961).

(54) Eisenbraun, E. J., Bright, A. and Appel, H. H., Chem. and Ind.,
1242 (1962).

(55) Casinovi, C. G., Delle Monache, F., Grandolinie, G., Marini-Bettolo, G. B. and Appel, H. H., Chem. and Ind., 984 (1963).

(56) Torssell, K. and Wahlberg, K., Tetrahedron Letters, 445 (1966).

(57) Torssell, K. and Wahlberg, K., Acta Chem. Scand., 21, 53 (1967).

(58) Todd, N. B., "The Catnip Response", Unpublished Ph.D. Thesis, Harvard University, Cambridge, Mass.

(59) Eisner, J., Science, 148, 1218 (1965).

(60) Hamasaki, T., Tottori Nogakkaiho, 13, 84 (1961); Chem. Abstr., 59, 7902 (1963).

(61) Pavan, M., Ricerca Sci., 20, 1853 (1950); Mem. Soc. Entomol. Ital., 30, 107 (1951); Chem. and Ind., 37, 625, 714 (1955).

(62) Sakan, T., Kagaku no Ryoika, 14, 237 (1960).

(63) Appel, H. H., Scientia, 130, 1 (1966).

(64) Gatti, G. and Marotta, M., Ann. Inst. Super. di Sanita, 2, 29 (1966).

(65) Hammouda, H. and Amer. M. S., J. Pharm. Sci., 55(12), 1452 (1966).

(66) Waller, G. R., Progr. Chem. Fats and Other Lipids, 10, 170 (1971).

(67) Casinovi, E. G., Giovannozzi-Sermanni, G. and Marini-Bettolo, G. B., Gazz. Chim. Ital., 94, 1356 (1964).

(68) Casinovi, C. G. and Marini-Bettolo, G. B., IUPAC Meeting, London Abstract AB-3, p. 285 (1963).

(69) Auda, H., Juneja, H. R., Eisenbraun, E. J., Waller, G. R., Kays, W. R. and Appel, H. H., J. Am. Chem. Soc., 89, 2476 (1967).

(70) Regnier, F. E., Waller, G. R., Eisenbraun, E. J. and Auda, H., Photochem., 7, 221 (1968).

(71) Auda, H., Waller, G. R. and Eisenbraun, E. J., J. Biol. Chem., 242, 4157 (1967).

(72) Meinwald, J., Happ, G. M., Labows, J. and Eisner, T., Science, 151, 79 (1966).

(73) Battersby, A. R., Pure Appl. Chem., 14, 117 (1967).

(74) Eisenbraun, E. J., Waller, G. R. and Appel, H. H., (unpublished results).

(75) Huni, J. E. S., Hiltebrand, H., Schmid, H., Groger, D., Johne, S. and Mothes, K., Experientia, 22, 656 (1966).

(76)   Horodysky, A. G., Waller, G. R. and Eisenbraun, E. J., *J*. *Biol*. *Chem*., 244, 12, 3110-3116 (1969).

(77)   Bate-Smith, E. C. and Swain, T., *Comparative Phytochemistry*, T. Swain, ed., Academic Press, New York, 1966, p. 159.

(78)   Gross, D., *Adv*. *Bot*., 32, 93 (1970).

(79)   Bjoerndal, H., Hellerquist, C. G., Lindberg, B., and Svenson, S., *Angew*. *Chem*. *Internat*. *Ed*., 9, 610 (1970).

(80)   Waller, G. R., *Proc*. *Okla*. *Acad*. *Sci*., 47, 271 (1968).

VITA

Ronald Doyle Johnson

Candidate for the Degree of

Doctor of Philosophy

Thesis: I. THE RELATIONSHIP OF THE PYRIDINE NUCLEOTIDE CYCLE TO
             RICININE BIOSYNTHESIS IN RICINUS COMMUNIS L.
         II. BIOCHEMISTRY OF METHYLCYCLOPENTANE MONOTERPENOIDS

Major Field: Biochemistry

Biographical:

    Personal Data: Born in Collinsville, Oklahoma, February 9, 1945,
        the son of Mr. and Mrs. Ralph Doyle Johnson.

    Education: Attended the public schools of Collinsville, Oklahoma;
        and graduated from Collinsville High School; received the
        Bachelor of Science degree from Oklahoma State University,
        1967, with a major in Biochemistry; completed the requirements
        for Doctor of Philosophy degree in May, 1972.

    Professional Experience: Part-time laboratory research assistant,
        Department of Biochemistry, Oklahoma State University, January
        1964 to May 1967; N.S.F. Summer Research Trainee, Department
        of Biochemistry, Oklahoma State University, May 1967 to
        September 1967; Graduate research assistant, Department of
        Biochemistry, Oklahoma State University, September 1967 to
        September 1968; NDEA Fellow, September 1968 to September 1971.

    Professional and Honorary Societies: Phi Lambda Upsilon, Sigma Xi
        and American Chemical Society.